ASSESSMENT OF THE LONG-TERM WASTE MANAGEMENT AND PROLIFERATION RESISTANCE OF DIFFERENT FUEL CYCLES FOR THE GENERATION-IV CANADIAN CONCEPT OF SUPER-CRITICAL WATER REACTOR

ASSESSMENT OF THE LONG-TERM WASTE MANAGEMENT AND PROLIFERATION RESISTANCE OF DIFFERENT FUEL CYCLES FOR THE GENERATION-IV CANADIAN CONCEPT OF SUPER-CRITICAL WATER REACTOR

BY REMON IBRAHIM, B.SC, M.SC

A Thesis
Submitted to the School of Graduate Studies
in Partial Fulfillment of the Requirements for the Degree
Doctor of Philosophy

McMaster University

DOCTOR OF PHILOSOPHY (2022) McMaster University

(Department of Engineering Physics) Hamilton, Ontario

AUTHOR : ASSESSMENT OF THE LONG-TERM WASTE MANAGEMENT AND PROLIFERATION RESISTANCE OF DIFFERENT FUEL CYCLES FOR THE GENERATION-IV CANADIAN CONCEPT OF SUPER-CRITICAL WATER REACTOR

AUTHOR : Remon Ibrahim

B.Sc. (University of Ain Shames)

M.Sc. (University of Ain Shames)

SUPERVISOR : Professor Dr. Adriaan Buijs – Professor Dr. John Luxat

NUMBER OF PAGES : xiv,189

Abstract

The Canadian concept of Super Critical Water Reactor uses a mixture of reactor-grade plutonium and thorium (Pu/Th) as a fuel, in a once-through cycle. The implications of using Pu/Th on long-term waste management and proliferation resistance were investigated in this study. Other fuels were investigated as well. These fuels are Low-Enriched Uranium (LEU), a mixture of LEU and thorium (LEU/Th), re-enriched reprocessed uranium (RepU), and a mixture of Pu/Th and natural uranium (Pu/Th/U).

A quantitative estimation of the size of the deep geological repository (DGR) was done, and it was found that Pu/Th fuel would require three to four times larger DGR compared with uranium fuels. Criticality safety was investigated, and it was found that, even in the most reactive conditions, criticality safety is not hazardous.

Assessment of the occupational dose to the workers in DGR from handling and storage of Pu/Th fuel showed a higher dose, around 8%, compared with LEU. The peak dose rate to the public, in case of an accident after the closure of DGR, was 75% higher in the case of Pu/Th compared with uranium, but it is still less than the regulatory limit.

The attractiveness of the various fuel cycle for weapons were estimated using the Figure-of-Merit method. A numerical ranking system was proposed to facilitate the comparison between the different fuels from the proliferation point of view. It was found that RepU is the most proliferation-resistant fuel, while Pu/Th is the least one among all the studied fuels. Investigation of the reactivity coefficients of the studied fuel cycles showed that all fuels have the same sign of reactivity feedback. Regarding coolant void reactivity (CVR), the Pu/Th/U will have the most negative value which will help to bring the core to a safe state faster in case of an accident.

Acknowledgement

Words cannot express my gratitude to my supervisor Dr. Buijs for his invaluable patience, help and support. Dr. Buijs encouraged me to learn, search and try new things without being afraid. His believe in me, mentorship, knowledge, and expertise really impacted and inspired me.

When I face difficulties during my research, Dr. Buijs was always here to answer my questions. During my hard times, when I feel I want to give up, he pushed me up. Dr. Buijs taught me many times, academically and personally. I need a separate book to mention everything Dr. Buijs did for me.

Also, I cannot, and I would never forget the help of Dr. Luxat. Without Dr. Luxat, I would not be able to start my PhD program and I would never reach to this point. Dr. Luxat was always generous in time, knowledge, and feedback. I owe Dr. Luxat a lot of things he taught me. I wish I have more time to learn more things from him, but every journey must come to an end.

I'm very grateful to my colleague, at this time, David Hummel, He is the most helpful colleague I ever met. I cannot remember how many times I asked him questions about my research. He never said no or showed any signs of tiredness. I'd like also to thank all my fellow graduate students for their help, either in my research or in getting adapted in a new country. Thanks go to Darryl McClure, Shlomi Schneider, Edilson Jacinto, Memgmeng Lou, Jason Sharpe, and Frederic Salaun.

Lastly, I would like to thank my family for supporting me during my journey. It was hard for them to let me go to another country, but they did sacrifice for giving me a better future. Their belief in me has kept my spirits and motivation high during the hard times in my research. I wish my dad was still here with me. He was always dreaming to call me Dr. Remon, but unfortunately, he passed away before I could fulfil his dream.

Table of Contents

List of Figures

List of Tables

List of List of Acronyms

ABWR	Advanced Boiling Water reactor
ACR	Advanced CANDU Reactor
AECL	Atomic Energy of Canada, Limited
AGR	Advanced Gas-cooled Reactor
APM	Adaptive Phased Management
CANDU	CANada Deuterium Uranium reactor
CDF	Core Damage Frequency
CS	Canister Spacing
CVR	Coolant Void Reactivity
DBF	Dense Backfill
DGR	Deep Geological Repository
DU	Depleted Uranium
DUF_6	Depleted-Uranium Hexafluoride
ENDF	Evaluated Nuclear Data Library
EPR	European Pressurized Reactor
FOM	Figure-of-Merit
FPPs	Fossil Power Plants
GFR	Gas-cooled Fast Reactor
GIF	Generation IV International Forum
GWd	Giga-Watt-Day
HCB	High-Compact Bentonite

HRW	High-Radioactive Waste
HWR	Heavy Water Reactor
IAEA	International Atomic Energy Agency
INS	Innovative Nuclear energy Systems
KE	Kinetic Energy
LBF	Light Backfill
LEU	Low Enriched Uranium
LFR	Lead-cooled Fast Reactor
LWR	Light Water Reactor
MeV	Mega Electron Volt
MOX	Mixed-Oxide Fuel
MPa	Mega Pascal
MSR	Molten Salt Reactor
MTHM	Metric Ton of Heavy Metals
Nat-U	Natural Uranium
NES	Nuclear Energy System
NPPs	Nuclear Power Plants
PR	Proliferation Resistance
PT-SCWR	Pressure-Tube SuperCritical Water-cooled Reactor
RepU	Reprocessed Uranium
SCWR	SuperCritical Water-cooled Reactor
SFR	Sodium-cooled Fast Reactor

SNF	Spent Nuclear Fuel
SQ	Significant Quantity
TS	Tunnel Spacing
UFCs	Used Fuel Containers
UFPP	Used Fuel Packaging Plant
UOX	Uranium Oxide
VHTR	Very High Temperature Reactor

List of Symbols

a	Area [m^2]
C	Dancoff factor
D	Diffusion coefficient [cm]
E	Neutron energy [ev]
I	Intensity [neutrons.cm^{-2}.s^{-1}]
J	Neutron current [neutrons.cm^{-2}.s^{-1}]
k	Neutron multiplication factor
N	Number of nuclei per unit volume [atoms.cm^{-3}]
n	Neutron density [neutrons.cm^{-3}]
r	Position/location [cm]
S	Neuron source [neutrons/cm^{-3}.s^{-1}]
T	Temperature [°C; K]
t	Time [s]
v	Neutron's velocity [m.s^{-1}]
V	Volume [cm^3]
W_R	Radiation weighting factor
W_T	Tissue weighting factor
σ_0	Background cross-section
σ_e	Escape probability
γ_{ji}	Yield of nuclide i from fission of nuclide j

Greek Letters

$\vec{\Omega}$	Direction [sr]
f	Thermal utilization
p	Resonance escape probability
ε	Fast fission factor
η	Number of neutrons released per absorption

μ	Scattering angle [rad]
σ	Microscopic cross section [barn = 10^{-24} cm^2]
Σ	Macroscopic cross section [cm^{-1}]
ϕ	Scaler total flux [neutrons.cm^{-2}.s^{-1}]
Φ	Angular neutron flux [neutrons.cm^{-2}.s^{-1}]
λ	Decay constant [s^{-1}]
ν	Number of neutrons released per fission
$\chi(E)$	Energy spectrum of neutrons released from fission

Subscripts and Superscripts

a	Absorption
eff	Effective
F	Fission
g	Energy group
s	Scattering
t	Total
tr	Transport
∞	infinite

Declaration of Academic Achievement

This work was done by the author since 2016 under the supervision of Professor Adriaan Buijs and Professor John Luxat.

The ideas of the papers were chosen by the author and with the guidance of his supervisors and his supervisory committee, which include Dr. Jeremy Pencer, who left in 2021 when Dr. Shinya Nagasaki joined the supervisory committee

All the work was performed mainly by the author, with close guidance from his supervisors. All the models, simulations, analysis of the results, and writing the papers were done by the author. The discussions and recommendations drawn by supervisors and the supervisory committee were very helpful, especially during the peer review of the publications.

The thesis consists of three journal papers, which are all accepted and published in high-rank journals in the field of nuclear engineering. These journals are Annals of Nuclear energy, Progress in Nuclear Energy, and Nuclear Engineering and Technology.

Chapter 1

Introduction

1.1 Historical Background

Nuclear power is the largest contribution to the world's electricity after fossil power. Nowadays, there are over 440 commercial nuclear power plants (NPPs) operable in 31 countries, with over 390,000 MWe of total capacity. About 60 more reactors are under construction. They provide over 11% of the world's electricity as continuous, reliable power, without carbon dioxide emissions [1]. Since electricity was generated for the first time by a nuclear reactor on December 20, 1951, at the EBR-I experimental station near Arco, Idaho, the nuclear power reactors have evolved drastically. The stages of this development are called "generations". Figure 1.1 shows the different generations of nuclear reactors.

The first generation (Gen-I) refers to the prototype and early power reactors which were developed in the 1950s and 60s. These reactors were the first power plants to provide electricity for the grid on a commercial scale. Examples of Gen-I reactors include Dresden-1 (1960-1978) in Illinois and Shippingport (1957-1982) in Pennsylvania. The last commercial reactor from Gen-I was the Wylfa Nuclear Power Plant. It was a Magnox reactor which was operated for nearly 45 years in the UK. This reactor was closed on 2015 [2].

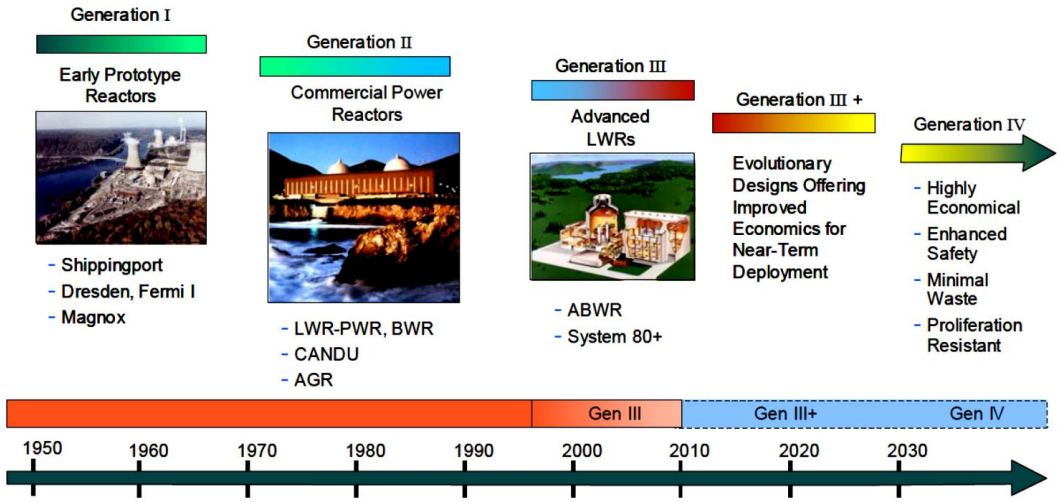

Figure 1.1: Generations of nuclear reactors

Generation II (Gen-II) refers to a type of commercial reactors that are designed to be cost-effective and reliable. Gen-II reactors began operations in the late 1960s. Initially, they were designed to operate for 40 years, but many Gen-II reactors got a life extension to 50 or 60 years. The US-NRC approved the extension of 74 of the 100 operating reactors in the USA by 20 years, allowing these reactors to run for a total of 60 years. The common feature of these reactor systems is the usage of active safety features (which need electrical power to be initiated). The majority of Gen-II reactors are cooled and moderated by light water, thus known as light-water reactors (LWRs). Other examples include CANada Deuterium Uranium reactors (CANDU), which are moderated and cooled by heavy water instead of light water, and the advanced gas-cooled graphite-moderated reactors (AGR) [2].

Generation III began in the early 1990s. It is an evolution of Gen-II reactors with improvements in safety and economics. The characteristics of Gen-III include standardized design, which helps in the reduction of capital costs and construction time, a significant reduction of the core damage frequencies (CDF), and better utilization of fuel (by increasing the burnup and thermal efficiency).

Longer operational lifetimes – typically 60 years, but potentially much longer was one of the Gen III technical advancements. Examples of Gen-III reactors include the Advanced Boiling Water Reactor (ABWR) and the Enhanced CANDU-6. Only four reactors of Gen-III are operating, all of them are ABWRs.

Gen-III+ designs are an evolutionary development of Gen-III reactors with significant improvement in safety, especially, the incorporation of passive safety features, which rely on natural phenomena like gravity and natural circulation. Examples of Gen-III+ reactors are Advanced CANDU Reactor (ACR-1000) and European Pressurized Reactor (EPR) [3].

1.2 Generation IV reactors

To advance nuclear energy to meet future energy needs, nine countries in 2001, have set out a framework, known as Generation IV International Forum (GIF), for international cooperation in the development of a future generation of nuclear energy systems [4]. These countries are Canada, the Republic of Korea, Argentina, France, South Africa, Brazil, the United Kingdom, Japan, and the United States. Currently, there are 14 members of GIF including, in addition to the founding members: Switzerland, Euratom, China, Russia, and Australia.

The goals of Gen-IV energy nuclear systems cover four broad areas: sustainability, economics, safety and reliability, and proliferation resistance and physical protection [4]. A brief description of each area is given below:

1. Sustainability

Sustainably means the ability to produce energy without affecting the ability of future generations to produce their energy needs. Accordingly, the energy generation should not be harmful to the environment or deplete natural resources. Increasing fuel utilization and minimizing waste are two ways to produce nuclear energy sustainably.

2. Economics

Gen-IV should be designed in a way to be economically attractive. Therefore, the life cycle cost (construction costs, production costs, and construction duration) should be minimized. Also, the financial risk associated with Gen-IV designs should be comparable to that of other energy sources.

3. Safety and reliability

The safety of nuclear power plants has continually improved since the deployment of the first power plant. This is reflected in the reduction of the CDF. Gen-IV systems should achieve an even higher level of safety and reliability by further reduction of CDF and eliminating the need for off-site emergency response.

4. Proliferation resistance and physical protection

Generation IV nuclear energy systems should improve the assurance that they are extremely undesirable, and the least preferred path for the diversion of weapons-usable materials. Also, they should provide more robust physical security against terrorist attacks.

All goals are equally important; therefore, a proposed design should not weaken one goal to strengthen another one [4]. This is particularly important when comparing different design options.

The GIF consortium chose six candidate reactor types that have the potential for meeting the Gen-IV goals. These reactor types are Very High-Temperature Reactor (VHTR), Sodium-cooled Fast Reactor (SFR), Gas-cooled Fast Reactor (GFR), Molten Salt Reactor (MSR), Lead-cooled Fast Reactor (LFR), and Supercritical-Water-cooled Reactor (SCWR).

1.3 Super-Critical Water reactor (SCWR)

The Supercritical-Water-Cooled Reactor system (SCWR) is a class of reactors which are cooled with supercritical water. The supercritical phase of water is achieved when the pressure and temperature of the water are increased beyond its critical point, which is at 22.1 MPa and 374°C, respectively (Figure 1.2) [5]. Beyond this point, it is not longer possible to differentiate between liquid and gas phases, instead the water reaches a new phase called supercritical fluid phase.

There is no change of phase in the supercritical water, therefore, the temperature of water can increase without boiling. Cooling with supercritical water will allow the NPPs to operate at temperatures that were not possible using subcritical water.

As the thermal efficiency increases by increasing the temperature difference between the heat source and heat sink, increasing the temperature of the coolant will increase the thermal efficiency. SCWR's efficiency can reach 44% or more compared to 34-36% for existing reactors [6]. This high thermal efficiency is beneficial not only for reducing the cost of energy but also in terms of minimising the quantity of spent fuel per watt-hour of energy generated.

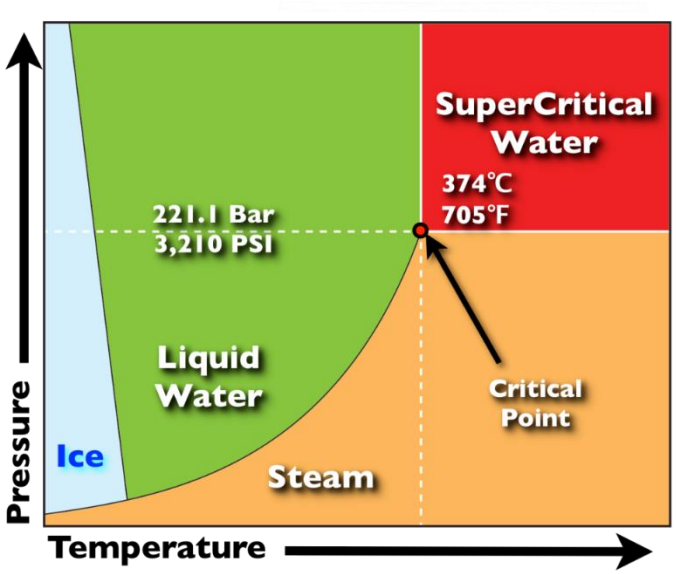

Figure 1.2: Phases of water [5]

In addition to the higher thermal efficiency, supercritical coolant will simplify the plant design by omitting the steam generators in PWR and steam separators and dryers in BWR. Figure 1.3 shows a schematic view of SCWR [4]. The main coolant pump pressurises the water coolant to supercritical pressure. The coolant is pumped through the core to the turbines. All the above-mentioned features help SCWR to reduce the cost of generation of electricity compared with current NPPs.

SCWRs are built based on two proven technologies; the LWRs, which are the most widely used nuclear power reactors in the world, and supercritical water which is used nowadays in supercritical fossil power plants (FPPs). In fact, there are more supercritical FPPs worldwide than NPPs [6].

Several conceptual designs have been proposed. These designs fall into two categories: pressure vessel design and pressure tube design. USA (lately USA stopped developing SCWR), Japan, China, and EU were concerned with pressure vessel design while Canada developed the pressure tube one.

In the pressure vessel design, the reactor is cooled and moderated by supercritical water. While in the pressure tube version, it is cooled by supercritical light water while moderated by low-pressure heavy water.

1.4 Canadian Concept of SCWR

The Canadian concept of SCWR is a direct-cycle, pressure-tube reactor which is moderated by low-pressure heavy water and cooled by supercritical light water. It was developed by Atomic Energy of Canada Limited (AECL), and several Canadian universities. The design targets of the Canadian SCWR design, known as Pressure-Tube SCWR (PT-SCWR), are the generation of 2540 MW of thermal power and about 1200 MW of electric power (assuming a 48% thermodynamic cycle efficiency of the plant), and negative Coolant Void Reactivity (CVR).

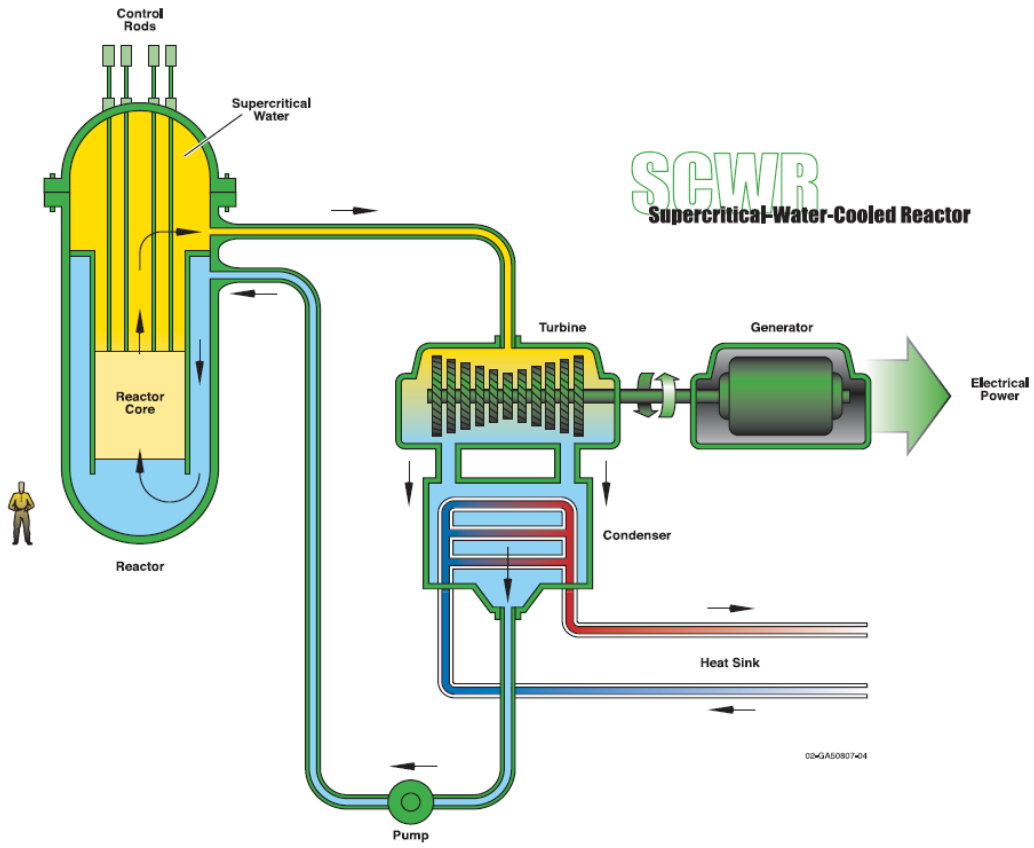

Figure 1.3: A Schematic diagram of the concept of a supercritical water reactor [4]

1.4.1 Core concept of Canadian SCWR

Figure 1.4 is a 2D view of the Canadian core concept of SCWR [7], while Figure 1.5 shows the 3D model [8]. It consists of 336 pressure tubes (fuel channels) immersed in low-pressure heavy water, which acts as a moderator. The pressure tubes, which contain the fuel assembly and the high-temperature/high-pressure light water coolant, are attached to a common inlet plenum where the coolant enters through inlet nozzles. The pressure and temperature of the inlet coolant are 25 MPa and 350 °C respectively. These conditions correspond to subcritical conditions of the water.

The subcritical water is directed to the lower end of each fuel assembly through a central channel (see Figure 1.5 (b)). During its travel to the lower end, the coolant participates in the moderation of neutrons. At the bottom of the fuel assembly, the coolant is forced to move upwards through the fuel pins (Figure 1.5 (c)). Due to heat transfer from the fuel pins, the coolant gradually becomes supercritical. The supercritical water from the different channels is collected in the outlet header and exits from the reactor through one of the four exit pipes at a temperature of 625 °C [8]. This temperature was chosen to match the turbines used in the supercritical FPPs.

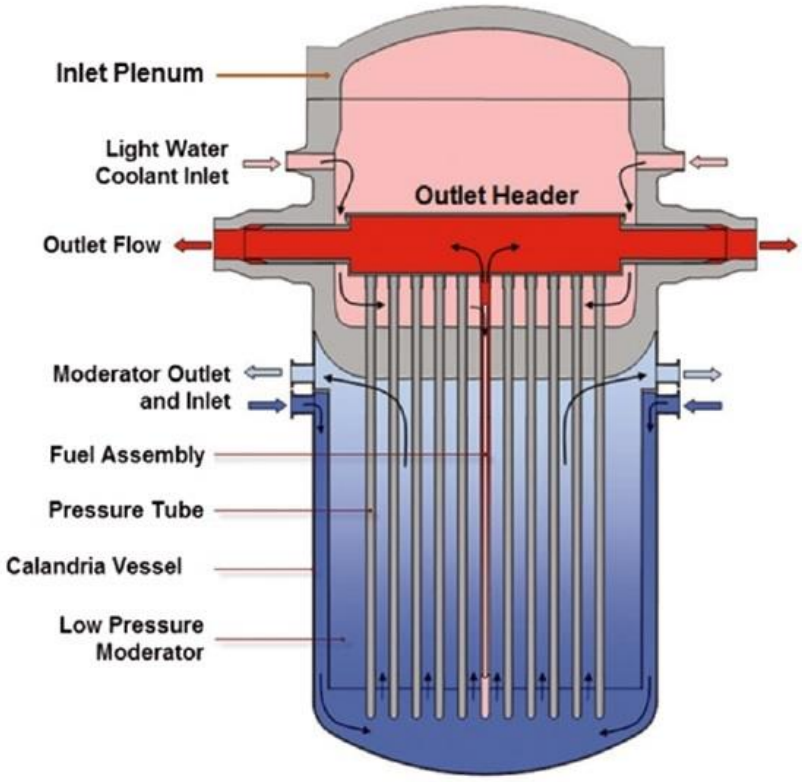

Figure 1.4: Cross-sectional view of the Canadian concept of SCWR [7]

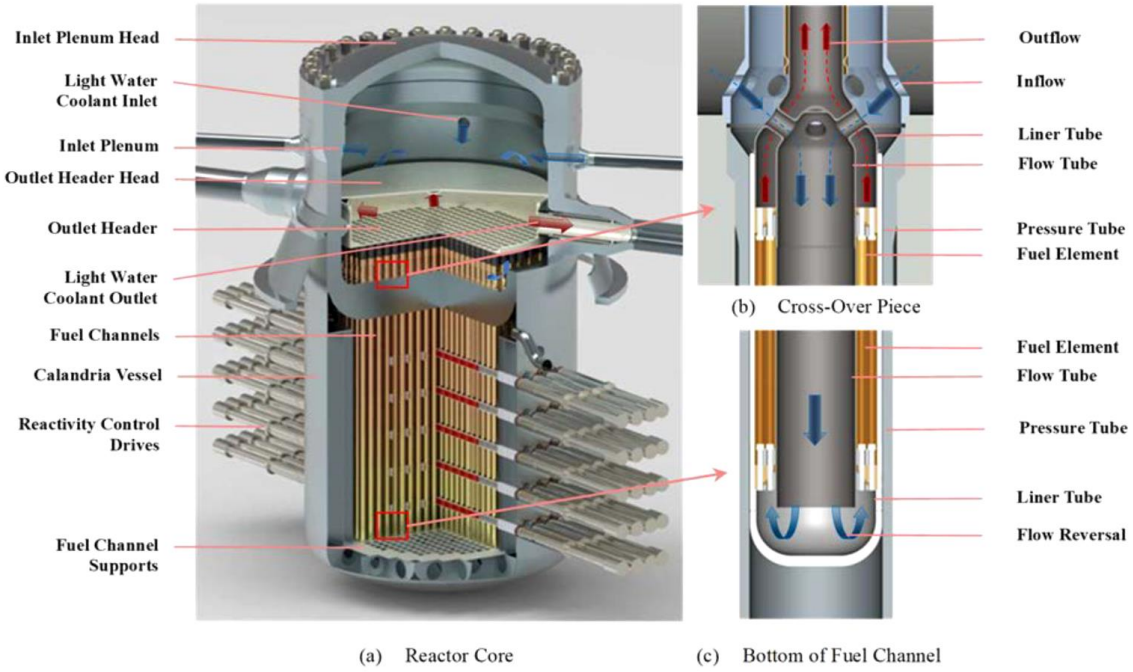

Figure 1.5: 3D model of Canadian concept of SCWR [8]

The heavy water moderator, fuel channels, reactivity control mechanisms, and emergency shutdown devices are all contained in the calandria vessel, which is at low pressure. The moderator works at subcooled temperatures by using an active recirculation system, but in the case of station blackout, the decay heat is removed from the core by flashing-driven natural circulation loop [9] (Figure 1.6).

The PT-SCWR shares some features with the well-known CANDU reactors. The shared features include using the pressure tubes rather than pressure vessel, and the separation of coolant and moderator. Separation of moderator from coolant has the advantage of leaving the moderator as a backup heat sink capability, which makes the pressure-tube type inherently safe.

Also, this separation helps in avoiding the lack of moderation that occurs when supercritical water is the moderator. Supercritical water has a lower density than subcritical water which reduces the neutron's thermalization. Hence, an extra moderator is needed in this case. This issue is encountered in the pressure-vessel designs, which use a solid moderator to overcome this problem.

Although the PT-SCWR shares some features with CANDU, it is different from CANDU as it uses offline instead of online refuelling. Also, in the case of PT-SCWR, the core is oriented vertically while the core is horizontal in CANDU.

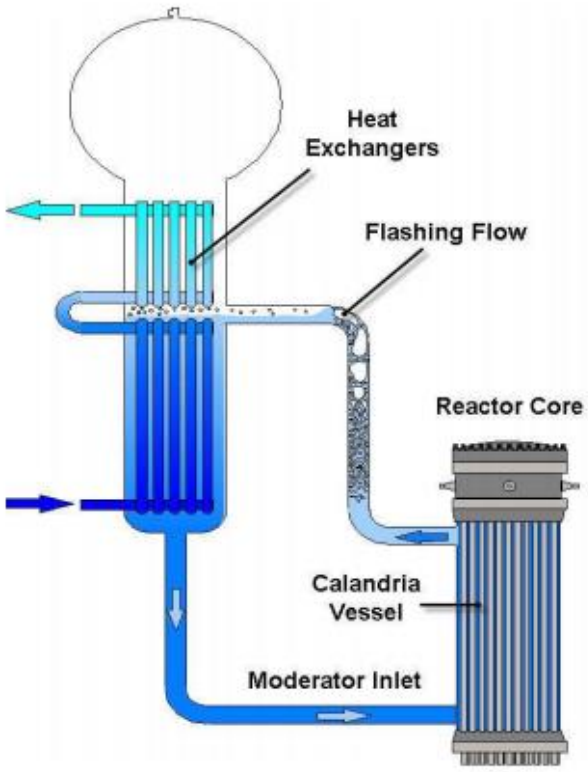

Figure 1.6: Schematic Diagram of the Passive Moderator Cooling System [9].

1.4.2 The fuel assembly

Figure 1.7 shows a 2D representation of the fuel assembly of the PT-SCWR. Different conceptual designs of the fuel assembly have been investigated. The fuel assembly in the current concept consists of 64 fuel elements in two concentric rings around the flow tube, which directs the coolant downwards. At the end of the fuel channel, the coolant's direction is reversed upwards cooling the fuel pins. An insulator, made from yttria-stabilized zirconia, and encapsulated by an inner and outer liner, exists between the upward coolant and the pressure tube. This insulator separates the high temperate coolant from the pressure tube (which is in contact with the low-temperature heavy water moderator).

The fuel elements are arranged into two concentric rings. The radii of the pins in the inner and outer rings are 0.415 and 0.44 cm respectively. The active length of the fuel element is five meters.

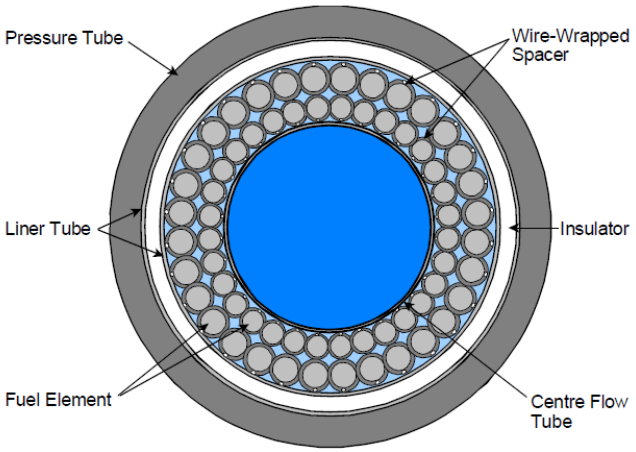

Figure 1.7: 2D view of 64-element fuel assembly inside the pressure tube [8].

The fuel is a mixture of reactor grade plutonium oxide, reprocessed from spent fuel of LWRs, and thorium oxide. The weight percentage of PuO_2 to ThO_2 is 15% and 12% for inner and outer rings respectively. As the heavy water moderator provides an excellent neutron economy, other fuel mixes can be used [10].

The motivation behind using plutonium as fissile material was to preserve the uranium resources. Mixed-Oxide fuel (MOX) was proposed first for PT-SCWR, but it does not entirely eliminate the dependence on uranium, as MOX is a Pu/U oxide mixture. On the other hand, thorium is three times more abundant than uranium. Accordingly, using thorium with plutonium in a Pu/Th mixture will eliminate the dependence on uranium and hence enhanced the sustainability comparing with MOX fuel.

1.5 Motivation and objectives

As mentioned before, Pu/Th fuel will enhance the sustainability of nuclear energy. The other goal, which also falls under the umbrella of sustainability, is that the GEN-IV systems should minimize their waste and reduce the burden of long-term waste management on the next generations [4].

For Canada, the plan for the long-term management of spent fuel is to store the spent nuclear fuel in a deep geological repository (DGR), with the ability to retrieve it if needed [11]. As PT-SCWR is a once-though concept, the spent Pu/Th will be eventually disposed in the DGR. Therefore, the implications of using Pu/Th on the design and safety of the DGR must be assessed.

In addition to sustainability, another goal of GEN-IV designs is to increase its proliferation resistance. As mentioned before, all goals are equally important, and enhancing one goal should not result in weakening another one. Therefore, the assessment of the current design of PT-SCWR against proliferation resistance should be evaluated as well.

The objectives of this thesis are to evaluate the implication of using the Pu/Th fuel on the size and safety of the Canadian design of the DGR, and on the proliferation risk as well. A comparison between Pu/Th and other fuels, namely Low-Enriched-Uranium (LEU), LEU/Th, and Re-enriched Reprocessed Uranium (RepU) was performed as well. The results of this work may help the decision-makers, among other investigations, to choose the optimal fuel cycle for PT-SCWR.

1.6 Outline of this thesis

This is a sandwich thesis which consists of seven chapters (including this introductory chapter).

Chapter 2 outlines the necessary theoretical aspects related to the work done in this thesis. This chapter is divided into several sections, covering one topic each. The topics include the interaction of radiation with matter, reactor theory, and radiological dose units.

Chapter 3 summarizes the nuclear fuel cycle, management of the spent fuel, and the principles of proliferation resistance.

Chapter 4 is the first journal article, published in *Annals of Nuclear Energy*. In this article, the size of the Canadian concept of DGR, needed to store the spent Pu/Th fuel from PT-SCWR, was estimated. The size of DGR, if uranium oxide fuel (UOX) were used instead of Pu/Th, was calculated as well. The criticality safety of both Pu/Th and UOX was investigated in this article.

Chapter 5 is the second journal article, published in *Progress of Nuclear Energy*. In this article, the radiological occupational dose incurred by workers in the DGR was estimated for Pu/Th and for various fuel cycles which include LEU, LEU/Th, and UOX. The peak dose rate to the public after the closure of the DGR was estimated as well.

Chapter 6 represents the third journal paper which was published in *Nuclear Engineering and Technology*. In this study, the attractiveness of different fuels, which can be used in PT-SCWR for obtaining weapons-usable materials was calculated using the Figure-of-Merit (FOM) method [12]. The optimal amount of natural uranium needed to denature Pu/Th fuel was estimated, and a numerical system was proposed to easily compare different fuels. The proposed numerical system considers the proliferation risk of fresh fuel as well as spent fuel. Finally, the reactivity feedback coefficients for all proposed fuels were calculated.

Chapter 7 presents the conclusions and recommendations drawn upon these analyses and suggestions for future study.

Chapter 2 Theoretical Background

In this chapter, the theoretical background, which is relevant to this thesis, is presented. Interaction of radiation with matter, reactor theory, and radiation dosimetry are presented here. The fuel cycle and waste management will be discussed in the next chapter.

2.1 Interaction of radiation with matter

The word "*radiation*" was used in the beginning to describe electromagnetic waves. Nowadays, especially after the de Broglie theory of duality of matter (which says that each matter can be acted as a wave or as a particle), the distinction between waves and particles is no longer valid and the term radiation is used to describe the electromagnetic waves as well as all atomic and subatomic particles (electrons, neutrons, protons, etc.) [13].

Radiation is divided into two categories, ionizing and non-ionizing depending on its kinetic energy. Ionizing radiation has enough energy to ionize the medium as it traverses through, while non-ionizing radiation can only increase the vibrational motions of the atoms (and hence, its temperature).

Ionizing radiation includes electromagnetic waves with wavelengths of 10 nm or shorter, all atomic and subatomic particles. This is the type of radiation that causes harmful effects on humans and the environment and must be protected against. The term *radiation* mentioned hereafter will refer only to ionizing radiation.

As the radiation cannot be sensed, it can be only detected through its interaction with the medium it travels through. Therefore, knowing the methods of interaction of radiation with matter is essential for radiation detection and measurements. Radiation can be further divided, according to the mechanisms of interaction with matter, into three categories: charged particles, photons, and neutrons.

2.1.1 Interaction of charged particles with matter

Charged particles, like alpha, beta, and heavy ions, loss their kinetic energy when moving through matter in two main ways: Coulomb interactions with electrons or nuclei, and through the emission of electromagnetic radiation.

A) Coulomb interactions

Coulomb forces are that forces that are acted between two charged particles. As a charged particle incidents on a matter, it interacts with the negatively orbital electrons or nuclei. Given that the radius of atoms is much larger than that of the nucleus (10^{-10} m vs. 10^{-14} m), it is expected that the number of interactions with the atomic electrons is much larger than that with nuclei. Therefore, incident-charged particles will transfer their kinetic energy to the bound atomic electrons of the medium. This will result in either ionization or excitation.

Ionization happens when the incident particles have enough energy to liberate an electron out of its orbit and becomes a free particle. The free electron acts as another charged particle, which can cause another ionization or excitation.

Excitation occurs when the energy transferred to the orbital electron is not enough to free the bound electron. In this case, the bound electron will gain energy to move to a higher energy state but still be bound to the atom, which will be excited. Within a timeframe of about 10^{-8} s, the excited electron will go back to its lower energy state. This is accompanied by the emission of photons with kinetic energy equal to the difference in energy between the two energy states [14].

B) Emission of electromagnetic radiation

Another mechanism of losing the energy of charged particles is the emission of electromagnetic waves. These waves are known as *bremsstrahlung* or breaking radiation. It is the radiation that is emitted when charged particles are accelerated or deaccelerated when deflected by another charged particle, typically deceleration of electrons by an atomic nucleus (Figure 2.1).

This mechanism of energy loss is only significant for light particles, like electrons, and for medium with high atomic number (this is the reason that shielding against beta particles is made from low atomic number materials like aluminum).

The bremsstrahlung radiation is not monoenergetic but rather has a continuous energy spectrum, with maximum energy equal to the kinetic energy of the incident particles.

Another type of emitted electromagnetic radiation is Cerenkov radiation. It is visible radiation that is emitted when the speed of a charged particle in a certain medium is greater than the speed of light in the same medium. Cerenkov emission constitutes a very small fraction of energy loss, and it can be neglected in most practical applications.

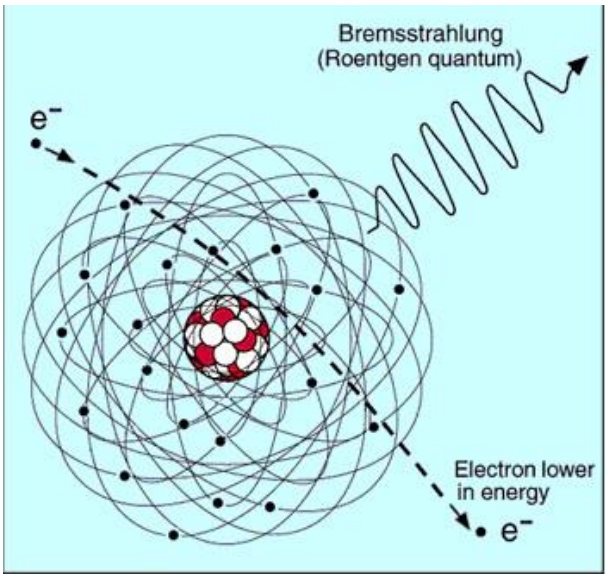

Figure 2.1: Bremsstrahlung radiation [15]

2.1.2 Interaction of photons with matter

Electromagnetic waves, like X-ray or gamma rays, behave during interaction with matters as particles called *photons*, which have zero mass and travel with the speed of light. The three most important reactions are 1) the photoelectric effect; 2) Compton scattering; and3) pair production (Figure 2.2).

1) The photoelectric effect

In this reaction, the energy of the incident photon is transferred completely to an orbital electron ejecting it from its atom. The incident photon disappears, and the ejected electron moves with kinetic energy equal to the difference between the kinetic energy of the photon and the binding energy of the electron.

The atom is left with a vacancy in its inner shell, this vacancy is filled with another electron from a higher energy shell. The difference in energy between the outer and inner shells is released as X-rays or it can be transferred to another electron expelling it from its orbit. The expelled electrons are known as Auger electrons.

2) Compton scattering

It is the scattering of a photon with a free electron (Figure 2.2). Although the electrons in the atom are bounded, the outermost electrons can be considered free electrons compared with photon's energy.

In this scattering, the electron and photons are moved in different directions with part of the photon's energy transferred to the electron. The kinetic energy of the photon is reduced but the photon still exists and moves through the medium. The scattered photon will either be absorbed by a photoelectric effect or undergoes another Compton scattering.

3) Pair production

In this process, the photon's energy is transferred to an electron-positron pair. The minimum energy of the photon should be equal to the rest masses of the electron-positron pair which is 1.02 MeV (for photons with higher energy, the excess energy will be carried away as kinetic energies of the electron and positron in an equal manner).

For the conversation of momentum, pair production can only happen in the vicinity of the nucleus. The positrons will be eventually captured by electrons causing the annihilation of the two particles, and the emission of two photons each with an energy of 0.51 MeV. These two photons can lose their energy through Compton scattering or the photoelectric effect.

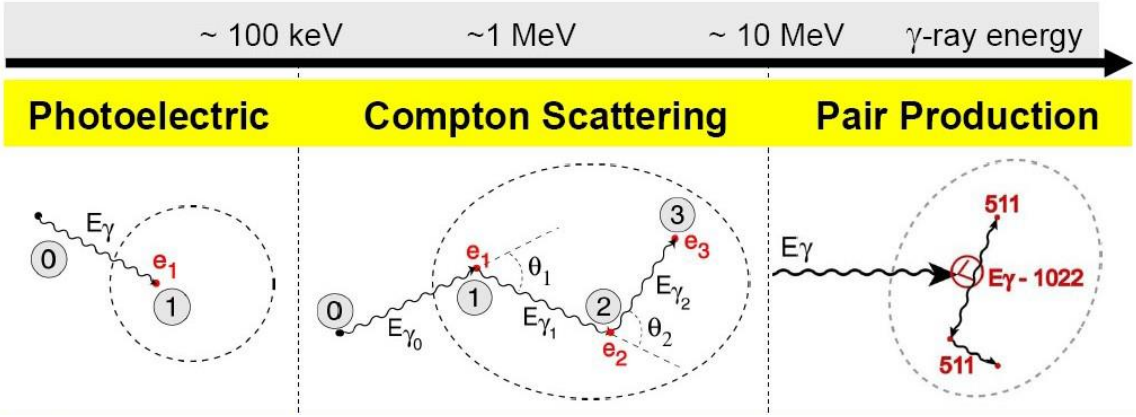

Figure 2.2: Mechanisms of interaction of photons with matter [16]

4) Photodisintegration reactions

This type of reaction occurs when high-energy photons are absorbed by the nucleus. This causes excitation of the nucleus, which immediately decays by the emission of a subatomic particle (neutron, proton, or alpha).

As the photon's energy must be higher than the binding energy of the emitted subatomic particles, this reaction is only possible with very high gamma energy. Such high energies are not usually encountered in reactor applications with some exceptions. The main exception to this rule is the emission of neutrons by the interaction of photons with the nuclei of deuterium and beryllium (Photoneutrons). The energy threshold for this reaction is 2.22 MeV and 1.67 MeV respectively. Other materials need much higher gamma energy which is not encountered in reactors (for example carbon-12 needs gamma with energy equal to 18.72 MeV) [17].

Photoneutrons should be considered especially for reactors that have heavy water, like CANDU, or that use beryllium as a neutron reflector.

The probability of a certain mechanism depends on the photon's energy as well as the atomic number of the medium it travels through. Figure 2.3 shows this relationship. As can be seen, for low Z materials and low photon energy (below 0.5 MeV), the photoelectric effect is the dominant one, while for intermediate energy, the Compton scattering is dominant. For photon's energy higher than 1.02 MeV, the pair production mechanism predominates.

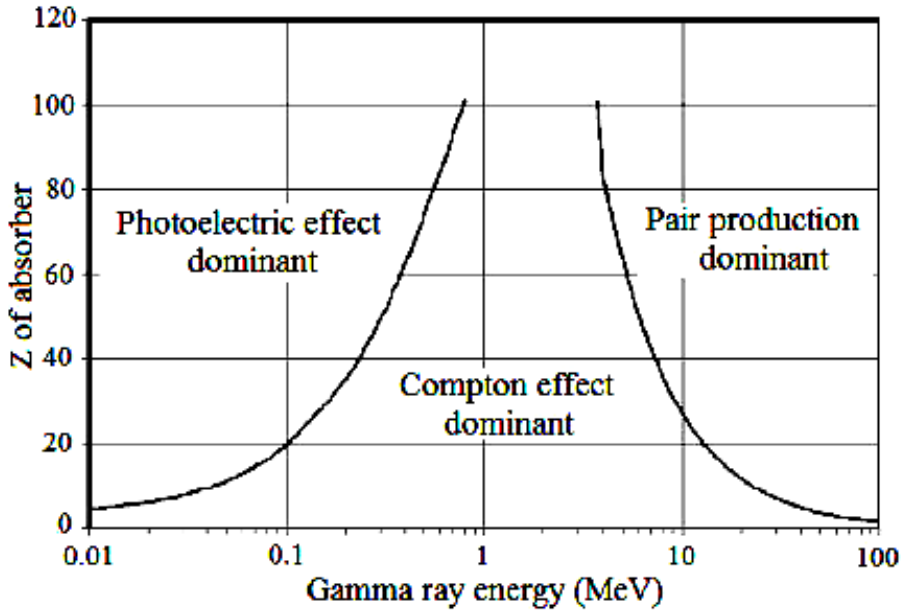

Figure 2.3: Relative importance of the three major types of gamma-ray interaction [14]

2.1.3 Interaction of neutrons with matter

Neutrons are uncharged particles; therefore, they do not interact with the electrons, but with the nuclei of the atoms. The neutron-nucleus interaction can be done through the formation of a compound nucleus or potential scattering as explained below.

2.1.3.1 Formation of the compound nucleus

The incident neutron can be absorbed by the nucleus to form a "compound" nucleus. According to the shell model of the atomic nucleus, the nucleus can only be in quantized (discrete) energy states (like the energy states of electrons). The absorbed neutron will add extra energy to the nucleus (equal to the kinetic energy (KE) of the incident neutron plus the neutron's binding energy). As the nucleus can be only in certain energy states, the compound nucleus can only be formed if this added energy matches one of the energy states of the nucleus.

This exited compound nucleus is very unstable and must be de-excited, which can be done through the emission of one or more nucleons, photons, or fission (as shown in Figure 2.4).

a) Resonant scattering

The compound nucleus can reach stability by emission of neutrons, if the energy of the emitted neutron is the same as the incident one, this reaction is called *elastic scattering*. In this case, the residual nucleus (the nucleus after the emission of the neutron) will be in its ground (stable) state.

On the other hand, if the residual nucleus was left in one of its excited states the reaction is called *inelastic scattering*. The KE of the emitted neutron will be less than that of incident neutrons. The residual nucleus will reach its ground energy state by the emission of photons. Scatting which involves the formation of a compound nucleus is called *resonant scattering*.

b) Radiative capture

The compound nucleus can also be de-excited by the emission of gamma photons instead of neutrons. In this case, the reaction is called radiative capture.

c) Transmutation

The compound nucleus can also emit protons or alpha particles. This will result in a residual nucleus with different atomic number and hence different element.

d) Fission

Fission occurs when the compound nucleus splits into two heavy fragments with the release of more than one neutron. The released neutrons can start another fission reaction causing a chain reaction. This is what is employed in fission reactors, and therefore, it will be explained in more detail in the next section.

2.1.3.2 Potential scattering

Potential scattering is an elastic scattering where the neutrons are bounced off by the nuclei of the target material, in the same way as two billiard balls collide. No absorption of the neutrons is needed in this type of reaction. The forces acting on the neutron in the vicinity of the target nucleus determine the potential scattering, and these forces are dependent on the nucleus' size and shape [19].

The resonant scattering requires that the KE of the incident neutron and its binding energy corresponds to one of the energy states of the nucleus, on the other hand, the potential scattering can occur at any energy of incident neutrons.

2.2 Nuclear Fission

For fission to occur, there is a potential barrier that must be overcome. The size of this fission barrier is typically 6 – 9 MeV in most nuclei of interest. For some nuclei, the binding energy of the captured neutron is sufficient to overcome this fission barrier, regardless of the energy of the incident neutrons. These nuclides are called *fissile* nuclides.

Fissile nuclides can be induced to fission even with neutrons of zero energy. These nuclides include ^{233}U, ^{235}U, ^{239}Pu, and ^{241}Pu.

For other nuclides, the potential barrier is higher than the neutron's binding energy. In this case, minimum kinetic energy (threshold) of the incident neutrons would be required to induce fission. In this case, these nuclides are called *fissionable* nuclides. Examples are ^{238}U, ^{240}Pu, and ^{232}Th.

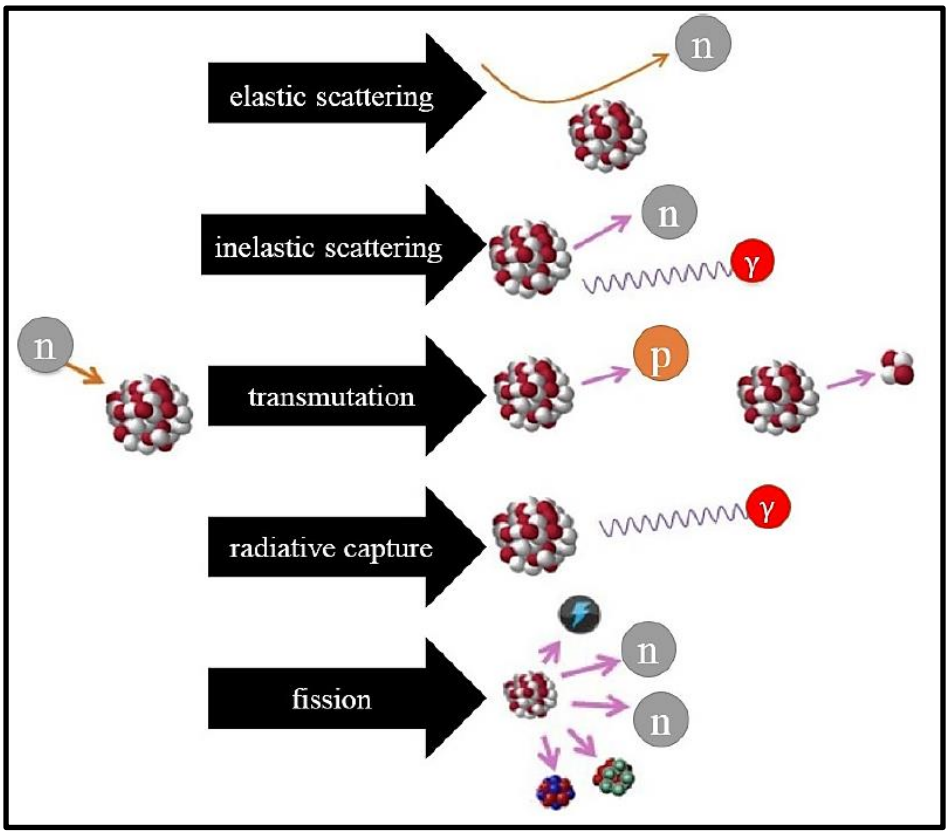

Figure 2.4: Different pathways of de-excitation of the compound nucleus [18]

The fission yield, which is defined as the average number of nuclei obtained per fission, is shown in Figure 2.5 as a function of the fission products' mass number. As can be seen, the fission products are not of equal masses. The two peaks, which are shown in Figure 2.5, account for the most probable mass numbers of fission products [20]. As the fissile nuclide gets heavier, the left peak of the fission yield moves towards nuclides with higher atomic numbers.

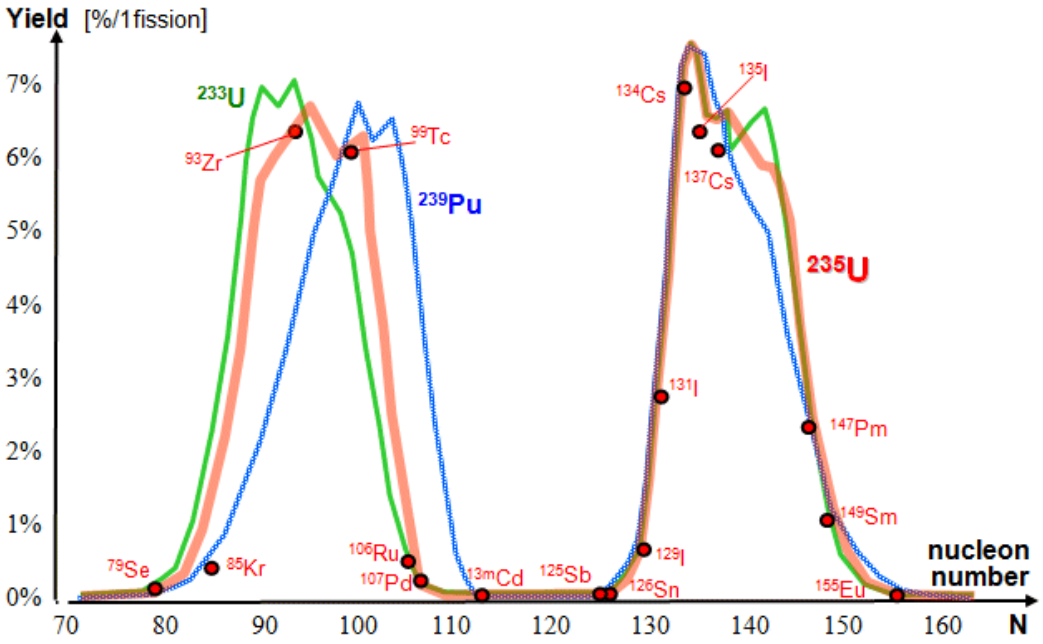

Figure 2.5: Fission Yield Curves for U-235, U-233, and Pu-239 [20]

Not all the energy released per fission, which is about 200 MeV, can be recovered as heat inside the reactor. Table 2-1 shows the breakdown of the fission energy for thermal fission of ^{235}U [21]. Most fission energy appears as kinetic energy of the fission fragments (80%). Fission fragments are heavy charged ions that have a very small range of travel as described in section 2.1. Therefore, their kinetic energy is absorbed, and appears as heat, inside the fuel pellets.

The neutrons from fissions lose their kinetic energy in the moderator. There are between two to three neutrons born per fission, one of them is used to sustain the chain reaction. The other neutrons are absorbed in radiative capture, which produces gamma rays. These gammas, alongside other gammas from the decay of fission fragments, or prompt gammas from fission, are absorbed within the reactor or in the shield. The antineutrinos escape completely from the reactor, but this lost energy is compensated by the kinetic energy of gammas from radiative capture [21].

Table 2.1: Breakdown of fission energy [21]

Form of released energy	Energy released in fission (MeV)	Recoverable energy (MeV)
KE of fission fragments	168	168
Prompt gamma-ray	7	7
Prompt neutrons	5	5
Gamma decay	7	7
Beta decay	8	8
Anti-neutrinos	12	-
Gamma emitted by neutron capture	-	3 – 12
Total	207	198 - 207

The number of neutrons produced per fission is expressed by (v). It depends on the fissile material and neutrons' energy. It is between two to three neutrons per fission. As not every neutron's capture will lead to fission, another useful parameter is the number of neutrons emitted per absorption. It is donated by (η).

The neutrons emitted in fission have a continuous energy spectrum, as shown in Figure 2.6. The average emitted neutron's energy is around 2 MeV, with the most probable energy equal to 0.73 MeV [22].

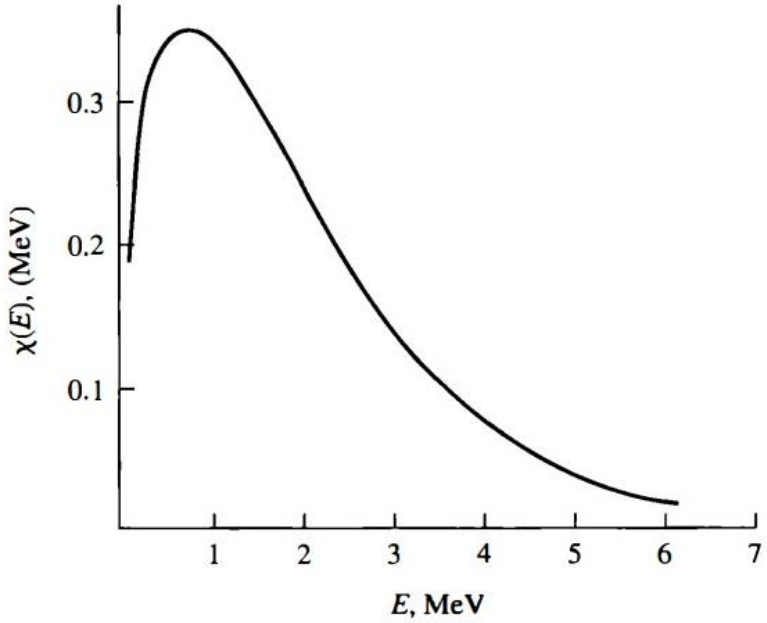

Figure 2.6: Energy spectrum of emitted neutrons from thermal fission in ^{235}U [22]

2.3 Nuclear cross-sections

As mentioned in the previous section, the interaction of neutrons with matter can be done in different ways. The probability of a certain reaction can be evaluated by using the concept of the *nuclear cross-section.* Which can be explained as follows:

Consider a parallel beam of neutrons with an intensity I [neutrons.cm^{-2}.s^{-1}], with the same energy, hitting a thin target of thickness t (as shown in Figure 2.7). The number of reactions per second, R, taking place in this target may be written as [13]:

R (reactions/s) = (neutrons per m^2 per s hitting the target) x (number of nuclides exposed to the beam) x (probability of interactions per m^2 per nucleus)

$$R = I\ a\ t\ N\ \sigma = I\ a\ t\ \Sigma \tag{2.1}$$

where *I*, *N*, and *a* are: the neutron intensity, number of nuclei per volume, and the area of the target hit by the neutrons (as shown in Figure 2.7) respectively. While σ is the probability, per nucleus, per unit area that a neutron will interact with. It is called a *microscopic cross-section*. The unit of the cross section is the area unit (m^2). Due to the small values of σ, it is expressed in the unit of *barn* ($b = 10^{-28}\ m^2$).

On the other hand, Σ is called the macroscopic cross-section, it is the multiplication of the microscopic cross-section (σ) with the number of nuclei per unit volume (*N*).

The definition given above for the cross section is the same for any reaction. To distinguish between the cross sections of different reactions, a subscript is written to indicate the type of reaction. For example, σ_a, *and* σ_s represent the microscopic absorption and scattering cross section respectively. The total microscopic cross section (σ_t) is the summation of the cross sections of all possible reactions.

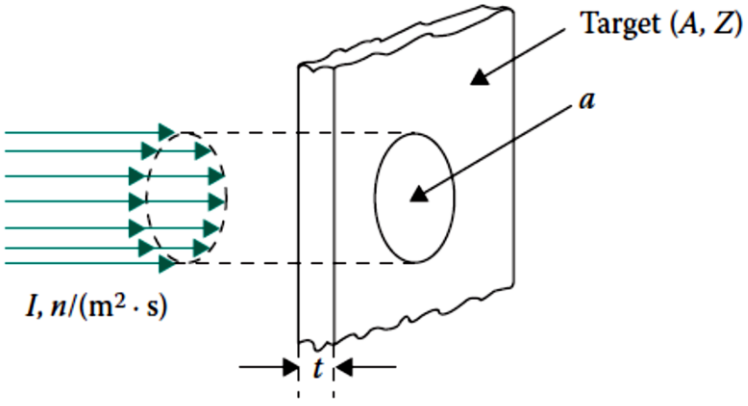

Figure 2.7: A parallel neutron beam hitting a thin target [13]

The *mean free path of neutrons (λ)* is defined as the average distance travelled by neutrons between collisions [9]. It is related to the total macroscopic cross section by the following:

$$\lambda = \frac{1}{\Sigma_t} \tag{2.2}$$

The cross section depends strongly on the neutrons' energy, which can be varied between hundreds of MeV down to fractions of an eV. Figure 2.8 shows the radiative capture cross section for ^{238}U [23]. This figure can be characterized by three regions.

At low energy, the cross-section is inversely varying with the neutron's velocity (1/v region). This occurs because the nuclear force between the target nucleus and the neutron has a longer time to interact when the neutrons are slow [24].

The intermediate region is the resonance region. In this region, the energy added by the incident neutrons matches one of the energy states of the compound nucleus as described before. The energy states of heavy materials are closely displaced; therefore, it is very probable that the incident neutron, will find an available energy state in the compound nucleus.

In heavy materials, the space between different energy states is getting smaller with increasing the energy of the energy states. For high energy states, the gap between energy states is very narrow, so it is hard to be observed. In this case, the cross-section will show a continuous and smooth behavior (unresolved resonance region) [19].

In the last region (fast neutron region), the cross-section decreases. This can be explained by the de Broglie wavelength of the incident neutrons. For high-energy neutrons, the wavelength will be short. According to Ramsauer Model, the cross-section is proportional to the effective radius of the neutrons which is proportional to its wavelength. As the wavelength is small in this region, the cross-section (likelihood of interaction) decreases as well [25].

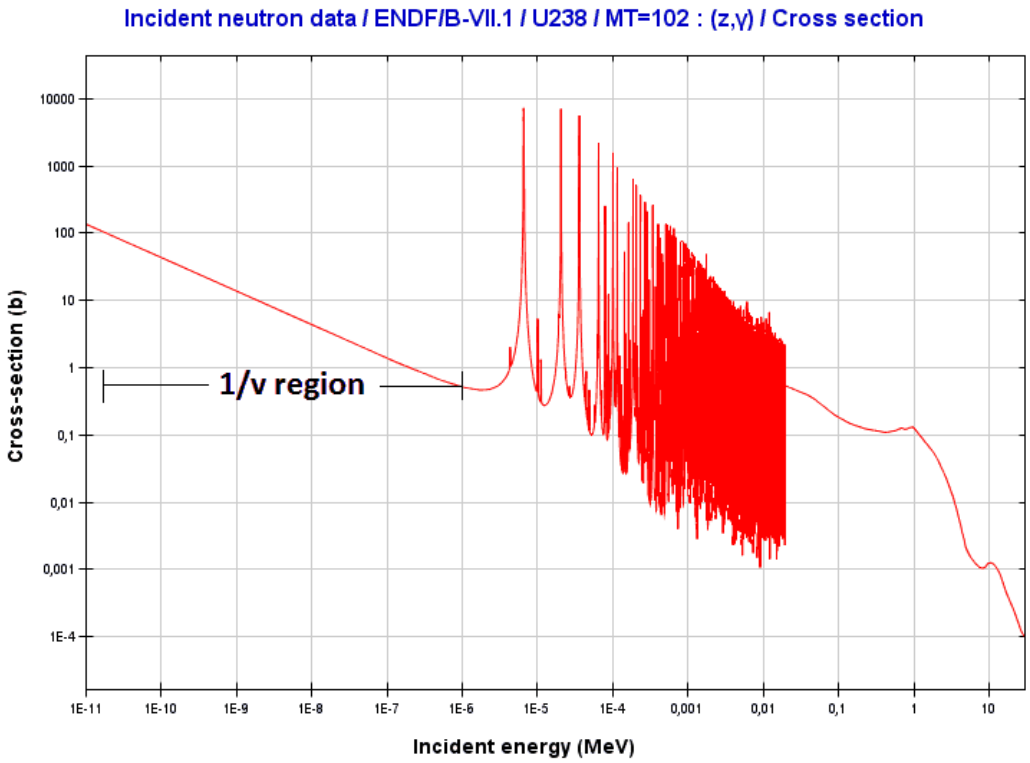

Figure 2.8: Radiative capture cross section of ^{238}U [23]

2.3.1 Doppler broadening

The cross sections depend on the relative speed between the incident neutrons and the nucleus of the target material. In most situations, the speed of neutrons is much higher than that of nuclei, and therefore, the nuclei can be considered stationary relative to neutrons.

In reality, the target nuclei are in continuous thermal motions. Therefore, the neutrons appear to the target nuclei as having a continuous distribution of energy. Thus, the relative speed could be greater or lower than the incident neutron energy.

As a result, the range of neutron energies that may be absorbed in the resonance is essentially expanded. Compared to when the nuclei are at rest, the resonance is now shorter and broader.

Figure 2.9 shows the variations in the capture cross-section of ^{238}U with increasing temperature. This phenomenon is called *Doppler broadening*. Because of the widened resonances, more neutrons would be absorbed with the increasing temperature of the nuclear fuel.

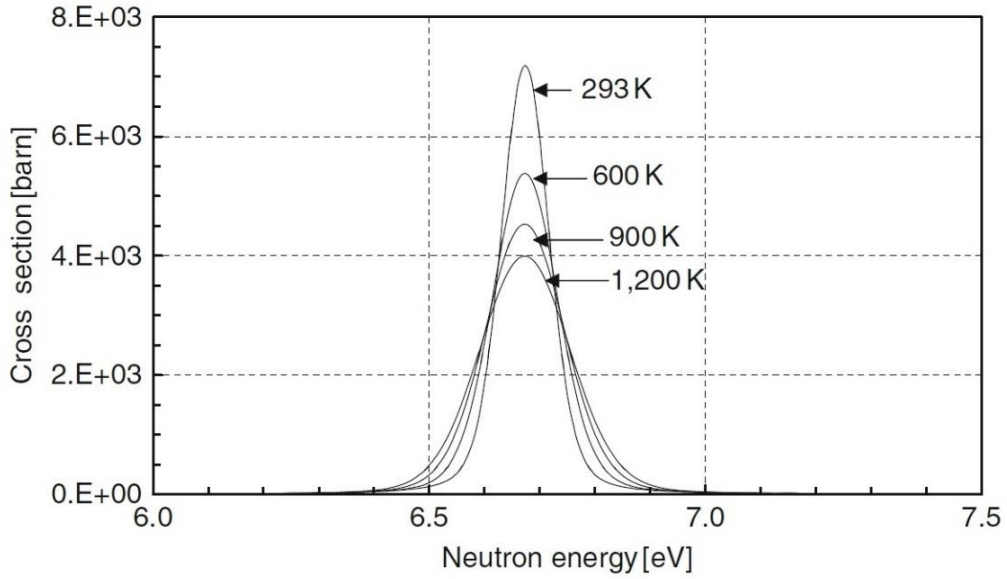

Figure 2.9: Doppler effect on the capture cross section of ^{238}U [26]

2.3.2 Neutron life cycle

The fission cross section increases with decreasing the neutron's energy. This is the feature employed in thermal reactors. Neutrons born in fission have an average energy of 2.0 MeV. This energy can be decreased by scattering reactions with materials with low-mass number like water (light or heavy) and graphite.

During the slowing down of neutrons, some neutrons will have energies (after scattering) corresponding to the capture resonance energies. These neutrons would be absorbed in a radiative capture reaction (parasitic absorption). Some neutrons escape from the core during slowing down.

The remaining neutrons will be absorbed in fuel which will cause more fissions. Figure 2.10 shows a typical life cycle of neutrons in a thermal reactor.

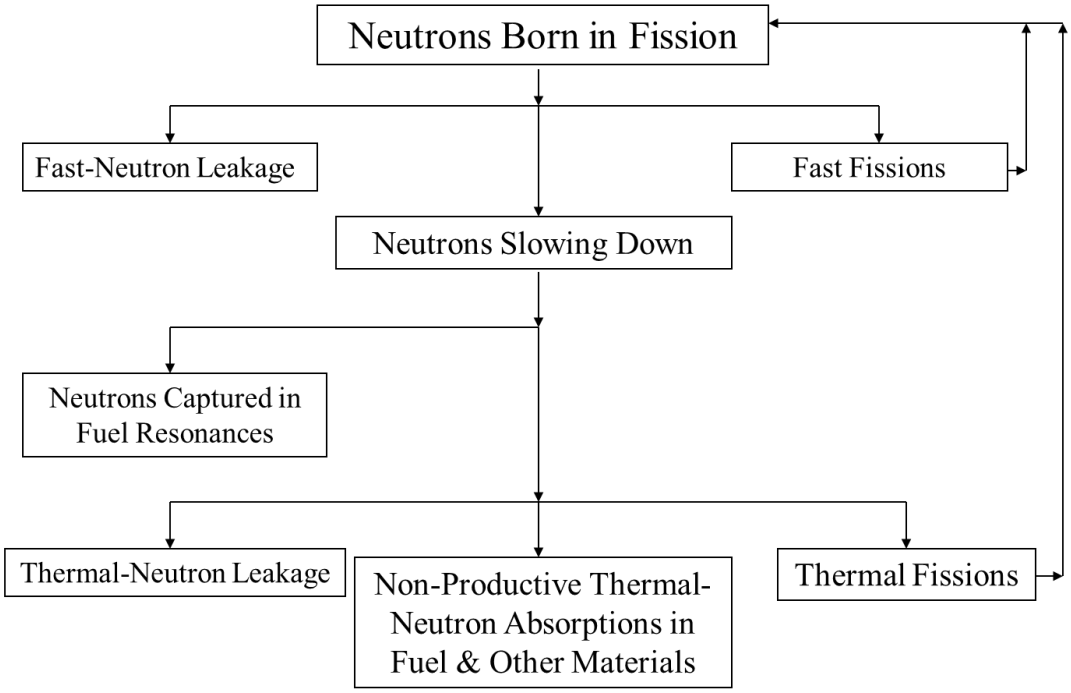

Figure 2.10: Neutron's life cycle in thermal reactors [27]

The ratio between the number of neutrons produced to that absorbed is known as the *multiplication factor* (k). If $k > 1$, more neutrons are produced than absorbed and the reactor would be in a supercritical state. If $k < 1$, more neutrons are absorbed than produced. In this case, the chain reaction cannot be sustained, and the reactor is in a subcritical state. For a critical, self- sustained reactor, k should be equal to one.

2.3.3 Four-factor formula

Refereeing the previous discussion about the neutron life cycle inside a reactor, the multiplication factor can be expressed in the following way:

For an infinite medium (no leakage), *N* neutrons were born in one generation of thermal fission. Although these neutrons are fast, some of them can cause fission. This is accounted for by introducing parameter (ε), which is called the *fast fission factor*. It is the total number of neutrons born by thermal and fast fissions to that born by thermal fission only. Therefore, the number of neutrons in the new generation is $N\,\varepsilon$.

During slowing down, some neutrons are absorbed in the resonance. If *p* is the *resonance escape probability*, which is the probability that a neutron will escape from resonance absorption, then the number of neutrons slowed down is $N\,\varepsilon\,p$.

Not all these neutrons will be absorbed in the fuel, some of them will absorb in other components like structural materials. If *f*, which is called *thermal utilization*, is defined as the fraction of neutrons absorbed in the fuel, then the number of neutrons absorbed in fuel is $N\,\varepsilon\,p\,f$.

As η is the number of neutrons produced per absorption, then the number of neutrons born in the new generation will be $N\,\varepsilon\,p\,f\,\eta$. Accordingly, the multiplication factor is defined as:

$$k_{inf} = \frac{N\epsilon pf\eta}{N} = \epsilon pf\eta \tag{2.3}$$

This is called the four-factor formula for infinite multiplication factor (k_{inf}). The word infinite means that there is no leakage.

When leakage is considered, the multiplication factor is called the *effective multiplication factor* (k_{eff}) and it is given with six-factor formula as given by:

$$k_{eff} = \epsilon pf\eta P_F P_T \tag{2.4}$$

Where P_F is the non-escape probability of fast neutrons. It is the ratio of the number of fast neutrons which did not escape from the reactor to the total number of fast neutrons produced by fission. P_T is the non-escape probability of thermal neutrons; it is defined in the same way as P_F [22].

2.4 Neutron density and reaction rate

The fission induced by neutrons can produce around 200 MeV of energy as well as more neutrons, which can be used for inducing other fission. This feature is the main principle of the nuclear reactor. To calculate the amount of energy produced in a certain reactor, the number of fissions per unit volume, and per unit time must be determined.

The reaction rate given in Equation (2.1) is for a monoenergetic parallel beam of neutrons. In reality, neutrons can have different energies and can move in different directions.

For a volume d^3r, as shown in Figure 2.11, the $n(r,\vec{\Omega},E,t)\,d^3r d^2\vec{\Omega}dE$ is defined as the *angular density of neutrons*. It is the number of neutrons in the volume d^3r around point *r*, with energy between *E* and *E+dE* and moving in the direction $\vec{\Omega}$ inside the solid angle $d^2\Omega$.

The *angular neutron flux* is the multiplication of neutron density with neutron speed, and it is given by:

$$\Phi(r,\vec{\Omega},E,t) = vn(r,\vec{\Omega},E,t) \tag{2.5}$$

When the neutrons interact with nuclei, the nuclei do not "care" from which direction the neutrons came. Therefore, for reaction rate, the angle-integrated flux is the important parameter. It is given by:

$$\phi(r,E,t) = \int_{4\pi} \Phi(r,\vec{\Omega},E,t)d\vec{\Omega} \tag{2.6}$$

where $\phi(r,E,t)$ is the angle-integrated flux.

Integrating the angle-integrate flux with respect to all possible energies will give the *total flux* at a certain point *r* at time *t*.

$$\phi(r,t) = \int_0^\infty \Phi(r,E,t)dE = vn(r,t) \tag{2.7}$$

where $n(r,t)$ is the total neutron density.

The total flux is a scalar quantity, its unit is (neutrons.cm^2.s^{-1}). It represents the total number of neutrons passing through a unit area per unit time regardless of the direction (from left to right or right to left).

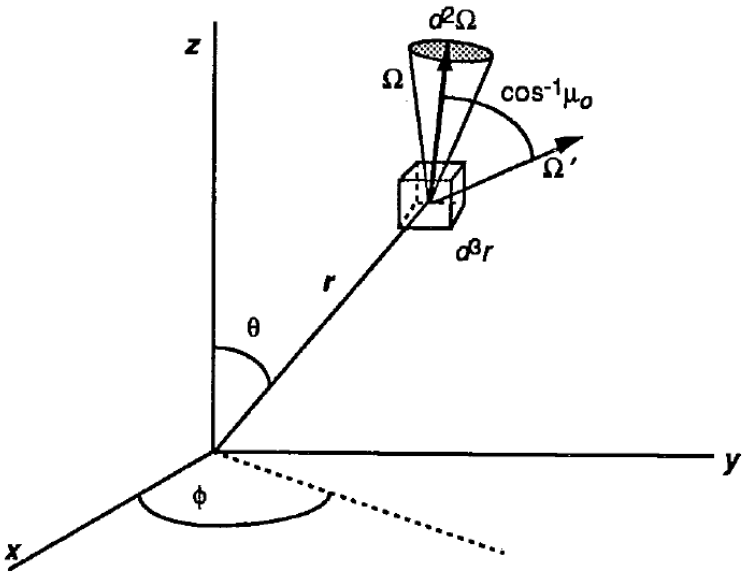

Figure 2.11: Representation of neutron's position and direction [28]

As the speed is the distance traveled by neutrons in one second, v is the distance travelled by neutrons in one sec. Therefore, flux can also be interpreted as the total path length traversed by all neutrons in unit volume per second.

The total reaction rate, at point (r) and at time (t) is given by:

$$F(r,t) = \Sigma_t(r,E)\phi(r,t) \tag{2.8}$$

Another important concept in reactor physics is the *angular current density*, denoted by $\vec{J}(r,\vec{\Omega},E,t)$ defined by:

$$\vec{J}(r,\vec{\Omega},E,t) = \vec{\Omega}\Phi(r,\vec{\Omega},E,t) \tag{2.9}$$

It is a vector quantity, and its magnitude is the angular flux.

The total current can be obtained, in the same way as flux by integrating over all energies and directions.

$$\vec{J}(r,t) = \int_0^\infty dE \int_{4\pi} \vec{J}(r,\vec{\Omega},E,t)d\vec{\Omega} \tag{2.10}$$

Although the current and flux have the same units, but the current is a vector quantity. Therefore, the total current is the *net rate* of neutrons crossing a surface (the difference between neutrons crossing a surface from left to right and from right to left). While the flux is the total rate at which neutrons cross a unit area, regardless of the direction. Therefore, the current is suitable to describe the leakage through surface, while flux is suitable to describe the reaction rate (where the direction of interaction is not important).

2.5 Neutron transport equation

As can be seen from the previous section, to calculate the reaction rate, the total flux is needed at each point, at each time in the reactor. The equation that describes the neutron behavior is called the *neutron transport equation, or the Boltzmann equation.* The derivative of this equation is explained below.

For a volume, like the one shown in Figure 2.11, the rate of change of neutrons' density inside this volume is given by:

$$\frac{\partial n(r,\vec{\Omega},E,t)}{\partial t} = Production\ rate - Loss\ rate \tag{2.11}$$

The production of neutrons inside the volume can occur from the following sources:

1. Neutrons are produced from fission, on average 2 – 3 neutrons are produced per fission,
2. Neutrons scattered from outside the volume to the inside of the volume under consideration, and
3. Other sources like spontaneous fission or external source.

The losses of neutrons are:

1. Absorption by the nuclei inside this volume,
2. Leakage of the neutrons outside the volume, and
3. Scattering out of the volume.

Each term of the above-mentioned terms is expressed using the reaction rate. This results in the *neutron transport equation* and is given by Equation (2.12) [19].

$$\frac{\delta}{\delta t}n(r,\vec{\Omega},E,t)=\frac{1}{v}\frac{\delta}{\delta t}\Phi(r,\vec{\Omega},E,t)= \\ =\frac{\chi(E)}{4\pi}\int_0^{4\pi}\int_0^{\infty}\bar{\nu}\,\Sigma_f(r,E',t)\Phi(r,\overrightarrow{\Omega'},E',t)dE'd^2\overrightarrow{\Omega'} \\ +\int_0^{4\pi}\int_0^{\infty}\Sigma_s\left(r,E'\rightarrow E,\overrightarrow{\Omega'}\rightarrow\Omega\right)\Phi(r,\overrightarrow{\Omega'},E',t)dE'd\overrightarrow{\Omega'} \\ -\Sigma_t(r,E,t)\Phi(r,\vec{\Omega},E,t)-\vec{\Omega}\cdot\vec{\nabla}\Phi(r,\vec{\Omega},E,t) \\ +S(r,E,t) \qquad (2.12)$$

The explanation of each term of the previous equation is given below:

1. The first term represents the fission source. It is the rate at which neutrons, with energy between E and $E+dE$, are born due to fission. $\Sigma_f,\bar{\nu}$ are the macroscopic fission cross-section and average neutrons produced per fission respectively,
2. The second term is the production rate of neutrons at a certain energy E and direction $\vec{\Omega}$ due to scattering from energy E' and $\overrightarrow{\Omega'}$,
3. The third term is the rate of neutrons' loss of due to absorption and scattering to other energy,
4. The fourth term is the leakage of neutrons of energy E out of the differential volume d^3r at r in the direction $\vec{\Omega}$, and
5. The final term is the external sources.

Unfortunately, the transport equation is much easier to derive than to solve. It involves both derivatives and integrals of the flux; it also involves 7 independent variables: 3 for space (*r*), one for energy (*E*), one for time (*t*), and two for direction (Ω).

2.5.1 Diffusion approximation

However, the fission process does not depend on the direction, so it would be easier if we can eliminate the direction-dependent variable from Equation (2.12). This can be done by integration with respect to ($\vec{\Omega}$). This will result in what is called the *neutron continuity equation* is given by Equation (2.13).

$$\begin{aligned}\frac{\delta}{\delta t}n(r,E,t) &= \frac{1}{v}\frac{\delta}{\delta t}\phi(r,E,t)\\ &= \chi(\mathrm{E})\int_0^\infty \bar{\nu}\,\Sigma_f(r,E',t)\phi(r,E',t)dE'\\ &+ \int_0^\infty \Sigma_s(r,E'\rightarrow E,t)\phi(r,E',t)dE'\\ &- \Sigma_t(r,E,t)\phi(r,E,t) - \vec{\nabla}.\vec{J}(r,E,t) + S(r,E,t) \qquad (2.13)\end{aligned}$$

As can be seen, this equation is a function of two unknowns (the angular-integrated current and angular-integrating flux), while the transport equation has only one unknown (the angular flux). To solve this equation, a relationship between them is needed. There is no direct relation between these two terms which hinders the simplification of the transport equation. But an approximate relationship is given by *Fick's law,* which is expressed as:

$$\vec{J}(r,E,t) = -D(r,E)\vec{\nabla}\phi(r,E,t) \qquad (2.14)$$

where *D(r, E)* is known as the *diffusion coefficient*, and it is given by:

$$D(r,E) = \frac{1}{3\Sigma_{tr}} = \frac{1}{3(\Sigma_t(r,E) - \bar{\mu}_0\Sigma_s(r,E))} \qquad (2.15)$$

where $\Sigma_{tr} = \Sigma_t - \bar{\mu}_0\Sigma_s$ is defined as *macroscopic transport cross-section*, and $\bar{\mu}_0$ is the average of the cosine of the angle between the directions of neutron before and after scattering (Figure 2.11).

This relation states that neutrons are moving "diffusely" from places of high density of neutrons to that of low density. Although it is a simple relation it is not always valid. It is not valid in regions with strong absorptions (like fuel) or near boundaries between regions with large differences in properties (like reflectors).

Substituting Equation (2.14) into equation (2.13) gives the time-dependent, energy-dependent diffusion equation given by:

$$\begin{aligned}\frac{\delta}{\delta t}n(r,E,t) &= \frac{1}{v}\frac{\delta}{\delta t}\phi(r,E,t)\\ &= \chi(\mathrm{E})\int_0^\infty \bar{\nu}\,\Sigma_f(r,E',t)\phi(r,E',t)dE'\\ &+ \int_0^\infty \Sigma_s(r,E'\to E,t)\phi(r,E',t)dE'\\ &- \Sigma_t(r,E,t)\phi(r,E,t) + \vec{\nabla}.D(r,E)\vec{\nabla}\phi(r,E,t)\\ &+ S(r,E,t)\end{aligned} \tag{2.16}$$

2.5.2 Steady state

If there is no change in the number of neutrons inside the considered volume, the transport equation is reduced to a steady-state transport equation, which is given by:

$$\begin{aligned}\frac{\delta}{\delta t}n\left(r,\vec{\Omega},E,t\right) &= \frac{1}{v}\frac{\delta}{\delta t}\Phi\left(r,\vec{\Omega},E,t\right) = 0\\ &= \frac{\chi(E)}{4\pi k}\int_0^{4\pi}\int_0^\infty \bar{\nu}\,\Sigma_f(r,E')\Phi\left(r,\overrightarrow{\Omega'},E'\right)dE'd^2\overrightarrow{\Omega'}\\ &+ \int_0^{4\pi}\int_0^\infty \Sigma_s\left(r,E'\to E,\overrightarrow{\Omega'}\to\Omega\right)\Phi\left(r,\overrightarrow{\Omega'},E'\right)dE'd\overrightarrow{\Omega'}\\ &- \Sigma_t(r,E)\Phi\left(r,\vec{\Omega},E\right) - \vec{\Omega}\cdot\vec{\nabla}\Phi\left(r,\vec{\Omega},E\right)\end{aligned} \tag{2.17}$$

In the steady state transport equation, the external source has been eliminated, also the multiplication factor (*k*), which is defined in Section 2.3.3, is included.

The reason for including (*k)* in the steady state equation is that: for given material composition and geometry, it is highly unlikely to get the produced neutrons equal to lost neutrons from the first guess, therefore the term (*k*) will be used to adjust the composition (or geometry) to get critical reactor. Using diffusion approximation in the steady state will give the following equation:

$$\Sigma_t(r,E)\phi(r,E) - \vec{\nabla}.D(r,E)\vec{\nabla}\phi(r,E) = \frac{1}{k}\,\chi(\mathrm{E})\int_0^\infty \bar{\nu}\,\Sigma_f(r,E')\phi(r,E')dE' + \int_0^\infty \Sigma_s(r,E'\rightarrow E)\phi(r,E')dE' \quad (2.18)$$

2.5.3 Solution of the transport equation

The transport equation can be solved, either using deterministic methods (where the angular flux is calculated as a deterministic value) or Monte Carlo methods (where the stochastic nature of neutron-nucleus interactions is considered). In this section, a brief description of both methods is given. Both methods were used in this thesis.

2.5.3.1 Deterministic methods

Deterministic methods involve discretization of the independent variables in Equation (2.17), with the replacement of differential and integral operators with subtraction and summation respectively.

For angular variables, two methods are usually employed to deal with them. The first method is P_N method, where the angular flux is expanded in terms of spherical harmonics. In the other method, the discrete ordinate method (S_N method), the transport equation is solved in a finite *N* number of distinct directions.

Regarding the energy variable, the energy spectrum is discretized into *G* energy groups (around 200 groups). Discretizing the angular and energy variables will transform the transport equation into *N*G* algebraic equations. In addition to that, the spatial variable *(r)* is decomposed into an appropriate mesh. Ideally, the mesh size should be less than the mean free path of neutrons in the material.

Due to it is complexity, it is very difficult or time-consuming to solve this equation for the 3D full core. At the same time, the diffusion equation is not valid for certain situations.

So, the most common methodology used in reactor analysis is to divide the 3D core into certain numbers of repeating units (called lattice cells or nodes) and solve the transport equation for this lattice cell using the appropriate boundary conditions. The computer code which solves the transport equation for the unit cell is known as lattice code. Examples of these codes are WIMS [29], DRAGON [30], and CASMO [31].

The resultant angular flux from the transport equation is used to generate *homogenized* (cell-averaged) macroscopic cross sections for this lattice cell. Homogenization means representing the heterogeneous unit cell as a homogenous mixture. In addition to homogenization, the *G* energy groups, used to solve the transport equation, are *condensed* into few-groups (usually between two and eight groups). The resultant few-group homogenized cross sections are used in solving the multi-group diffusion equation for the 3D full core [19]. Examples of such diffusion codes are DONJON [32] and PARCS [33]. This method of core analysis is known as *the nodal method*.

The steady-state diffusion Equation (2.18), when discretized into energy groups, will have the following multi-group diffusion equation:

$$-\nabla D_g(r)\nabla\phi_g(r) + \Sigma_{t,g}(r)\phi_g(r) = \sum_{g'=1}^{h} \Sigma_s^{g'-g}(r)\phi_{g'}(r) + \chi_g \sum_{g'=1}^{h} \left(\nu\Sigma_f\right)_{g'}\phi_{g'}(r) \quad (2.19)$$

where D_g is the average diffusion coefficient for group *(g)*given by:

$$D_g(r) = \frac{\int_{E_g}^{E_{g-1}} D(r,E)\nabla\phi(r,E)dE}{\int_{E_g}^{E_{g-1}} \nabla\phi(r,E)dE} \quad (2.20)$$

; and $\Sigma_s^{g'-g}$ is the average group-to-group transfer scattering cross section defined such that the quantity:

$$\int_{E_g}^{E_{g-1}} dE \int_{E_{g'}}^{E_{g'-1}} dE'\Sigma_s(r, E' \to E)\phi(r,E') = \Sigma_s^{g'-g}(r)\phi(r) \quad (2.21)$$

gives the neutrons per unit volume per unit time which are initially in energy group g' and after collision ended-up in group energy g. While $\chi_g$is the fraction of fission neutrons with energy fall in the energy group g.

2.5.3.2 Monte-Carlo method

Deterministic methods discretize the transport equation in each of its variables, which results in very large numbers of algebraic equations which must be solved. On the other hand, stochastic methods depend on the physics of the interactions between neutrons and the nucleus, which has stochastic (random) nature. According to quantum mechanics, knowing the properties of neutrons (like energy, and direction) and the properties of the medium it interacts with, can only give us the probabilities of interaction and the probabilities of outcomes.

In the actual physical process of particle transport, when a large number of neutrons hit a medium, there is a probability (cross section) for each interaction. There is a probability for scattering, radiative capture, fission, etc. As a result, although all the neutrons had the same initial parameters, their outcomes after the collision were different [34].

Due to the inherent uncertainty in neutron-nucleus interaction, the Monte-Carlo method is used to model this interaction. Monte-Carlo method is a mathematical technique invented by John von Neumann and Stanislaw Ulam to improve decisions based on uncertain inputs [35].

In Monte Carlo methods, the same process is simulated using computers, by generating a large number of fictitious Monte Carlo particles. Each of these particles is tracked individually, and the numerous events they take part in (collision, absorption, fission, escape, etc.) are recorded. All the interactions (events), experienced by one particle, constitute its history. At the end of each history, the expected value of the required parameter ($\hat{x}$); flux, for example, can be estimated according to:

$$\hat{x} = \frac{1}{N}\sum_{n=1}^{N} x_n \tag{2.22}$$

where x_n is the tallied (recorded) parameter resulting from each history.

Due to the stochastic nature, the calculated parameter will have statistical uncertainty, which can be reduced by increasing the number of histories. For example, a reduction in the uncertainty by a factor of 10 requires increasing the number of histories by a factor of 100 [36]. This happens at the expense of computational costs.

Monte-Carlo methods can model complex geometries, which cannot be modeled using deterministic methods. In addition to that, energy, space, and angle are all continuously treated, eliminating discretization errors that can arise from the use of multigroup approximation.

On the other hand, deterministic methods are less computationally expensive than the Monte Carlo method, therefore, it is usually used for benchmarking practices.

2.5.4 Cross section libraries

To solve the Boltzmann equation, the nuclear cross sections must be known at all energies. The cross-sections are obtained either by experiments or by theoretical estimation using nuclear models. These data are stored in a huge database known as *nuclear data file*. Examples of these data files are ENDF/B [37], JEFF [38], and JENDL [39].

The cross sections are given as a function of the neutron's energy in a tabulated form, alongside interpolation schemes that can be used to estimate the cross sections between the tabulated values. Resonance parameters are included in the data files as well, which can be used to construct the cross sections at the resonance part of the energy spectrum.

The nuclear data files contain highly detailed information, but not all of it is needed for transport calculations. Therefore, these data files are processed, using codes like NJOY [40] to construct *cross-section libraries.*

Depending on the method used in the transport calculations, two types of cross section libraries are needed: continuous energy or multi-group library.

The continuous energy library, which is used in Monte Carlo codes like MCNP, contains the cross sections at all energies. Given the complicated behavior of cross sections around resonances, the number of energy points in the continuous energy library can reach several hundred thousand.

Deterministic transport codes, on the other hand, solve the Boltzmann equation by discretizing the energy variable. Therefore, a multi-group library is more suitable for deterministic transport codes. Some Monte Carlo codes can be run in a multi-group mode as well.

In the multi-group library, the energy spectrum is divided into different energy groups. The number of energy groups needed, and their boundaries depend on the specific application. The library suitable for thermal reactors is different from that for fast reactors for example

The cross sections in each energy group are averaged according to the following equation:

$$\sigma_x^g = \frac{\int_{E_g}^{E_{g-1}} \sigma_x(E)\phi(E)dE}{\int_{E_g}^{E_{g-1}} \phi(E)dE} \tag{2.23}$$

where *x* is a reaction type; *g* is an energy group over the energy interval between *E and E+ΔE;* $\sigma_x(E)$ is the microscopic cross-section at energy *E;* and $\phi(E)$ is the energy-dependent flux.

The transport code uses the group-averaged cross-section for the solution of the Boltzmann equation. Therefore, careful calculation of this cross-section must be done. A contradiction may appear in Equation (2.23) as it contains the flux spectrum, which is the parameter that transport codes are supposed to estimate. Therefore, an approximate flux spectrum must be assumed.

For the fast spectrum, the flux is assumed to have the fission spectrum shown in Figure 2.6, while for thermal neutrons, it is assumed to have Maxwell-Boltzmann distribution. For intermediate energies, it is assumed to be slowing down the spectrum(1/E).

As shown in Figure 2.12, this is not a good approximation due to the depression of the flux near the resonance. This phenomenon is called energetic self-shielding and it must be accounted for during the transport calculations.

The method to account for the self-shielding is to solve the neutron slowing down equation, at a reference temperature of 300 K, in an *infinitely diluted*, *homogeneous medium*.

This medium consists of a homogenous mixture of scatter (material that only scatters neutrons like a moderator) and infinite dilution of resonant material (like fuel, which absorbs neutrons). The dilution of the resonant materials is expressed in terms of *background cross section* (σ_0). It represents the cross-section of all materials other than the resonant one, therefore for infinitely diluted resonant, the background cross section is set to a large value (10^{10} barn).

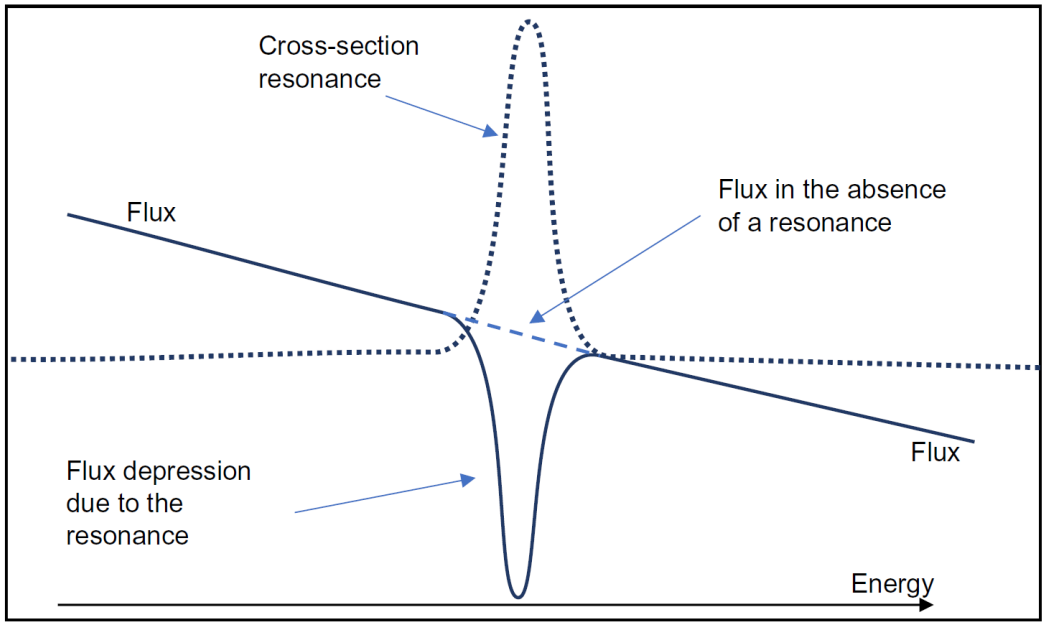

Figure 2.12: Flux depression due to resonance [41]

The calculated flux, at infinite dilution and a certain temperature, is used by NJOY to generate what is called *base cross-section* $\sigma(\sigma_0^{inf}, T_{ref})$ *library*. The same procedure is repeated for different background cross sections (between 10 barns and 10^{10} bars) and for different temperatures (between 300 and 2500 K) to calculate the *self-shielding factor* which is defined by [26]:

$$f(\sigma_0, T) = \frac{\sigma(\sigma_0, T)}{\sigma(\sigma_0^{inf}, T_{ref})} \tag{2.24}$$

Where: $f(\sigma_0, T)$ is the self-shielding factor for temperature T and background cross-section σ_0; $\sigma(\sigma_0, T)$ is the effective cross-section at temperature T and background σ_0; and $\sigma(\sigma_0^{inf}, T_{ref})$ is the base cross-section for infinitely diluted medium and at a reference temperature T_{ref}.

The self-shielding factor is tabulated in the cross-section library as well as the base cross-section. In transport calculation, the temperature of the resonant material (fuel) is usually given, but the background microscopic cross section must be estimated by the transport code. The macroscopic background cross-section (Σ_0) is used to estimate the microscopic background cross section [26].

The macroscopic cross section is estimated as a summation of two components: volume component and surface component as given by $\Sigma_0 = \Sigma_\mathrm{p} + \Sigma_\mathrm{e}$

The volume component, Σ_p is the macroscopic potential scattering cross-section. It represents the neutrons that are scattered into the resonance part of the energy spectrum by the resonant material (not the moderator for example). This scattering is assumed to be potential scattering; therefore, it is energy independent and only depends on the size of the nucleus. This component is given by:

$$\Sigma_p = \sum_{iso} N_{iso}\, \sigma_{p,iso} \tag{2.25}$$

where N_{iso} is the number density of all isotopes and $\sigma_{p,iso}$ is the potential scattering microscopic cross-section.

The surface component Σ_e accounts for the neutrons that escape from the fuel surface and are scattered by the moderator to energies corresponding to resonance energies. These neutrons re-enter the fuel where they got absorbed by the fuel. In estimating the surface components, the heterogeneity of fuel and moderator must be considered.

Several formulas were proposed to estimate the escape probability from the fuel surface depending on the fuel and moderator arrangements. For example, in the isolate fuel approach, the fuel is assumed to be a single pin inside an infinite moderator, so the neutrons will interact with the moderator only. In real life, the fuel pins are tightly packed into an array. In this packed design, the neutrons may suffer their first collision in another fuel pin, rather than the moderator.

The later situation is accounted for by including a correction factor called, *Dancoff factor C*, which represents the probability that the neutrons escape from the fuel will suffer their first collision in another fuel pin, not in the moderator.

Dancoff factor is used to correct the macroscopic escape cross section estimated using the isolated fuel assumption. Therefore, the background macroscopic and microscopic cross-section can be estimated using the following equations:

$$\Sigma_0 = \Sigma_p + D\Sigma_e \tag{2.26}$$

$$\sigma_{0,iso} = \frac{\Sigma_0}{N_{iso}} - \sigma_{p,iso} \tag{2.27}$$

After estimating the background microscopic cross-section, the lattice code searches the multi-group library for the corresponding self-shielding factor. The effective microscopic cross-section is then calculated and used in the transport calculations.

2.6 Burnup calculations

The fuel's composition changes due to fission, radiative capture, and radioactive decay. This change in fuel composition is known as *burnup*. The macroscopic cross sections, which appear in the transport equation, depending on the number of nuclei per unit volume (number density). Therefore, the burnup will change the macroscopic cross sections, which in turn change the calculated flux from the transport equation.

The burnup of the fuel is estimated by knowing that the rate of change in the number density of a certain nuclei equals to production rate of this nucleus minus the loss rate (due to absorption and radioactive decay).

The burnup equation is a first-order differential equation (Bateman equation) given by:

$$\frac{dN_i}{dt} = \sum_j \gamma_{ji}\sigma_{f,j}N_j\phi + \sigma_{c,i-1}N_{i-1}\phi + \sum_k \lambda_{ki}N_k - \sigma_{a,i}N_i\phi - \lambda_i N_i \qquad (2.28)$$

where N_i is the number density of nuclide *i*; γ_{ji} is the yield of nuclide *i* from fission of nuclide *j* ; λ_{ki} is the decay constant of nuclide *k* to nuclei *i* ; $\sigma_{c,i-1}$ is the capture cross-section of nuclei (*i*-1), which is the isotope of nuclei (*i*) with one mass number less; λ_i is the decay constant of nuclei (*i*) and ϕ is the flux [26].

The first and second terms are the production rate of nuclide (*i*) due to fission of all nuclides (*j*) and neutron capture (n,γ) respectively. The third term is the production rate of (*i*) due to the decay of nuclide (*k*) to nuclide (*i*), while the last two terms are the loss rate due to absorption and radioactive decay respectively.

As seen in Equation (2.28) , the number density is a function of the flux, which is also dependent on the number density as indicated in the transport equation. Therefore, the solution of transport and burnup equations should be done in a coupled way. The burnup equation is solved at discrete time steps, where the flux is assumed to be constant for the time interval between each step, which is explained below.

At the beginning of the life of the core, the fuel composition (which is known) is used to calculate the flux. The burnup equation is solved, using this flux, to calculate the fuel composition at the end of the time interval. Which is used to get the flux from the transport equation. This flux is used to solve the burnup equation for the second time interval and so on.

At beginning of life of the core, the burnup steps should be small enough to capture all the changes that occur in the fuel composition (a few hours). By increasing the burnup, the time interval can be increased.

2.7 Radiation units

As described in section 2.1, radiation traverses through the medium deposits energy inside this medium. This energy breaks the chemical bonds in the medium and causes changes in its properties. When this radiation interacts with human cells, it causes harmful effects. In this section, the radiation units, which can be used to quantify the radiation hazards, are briefly described.

2.7.1 Absorbed dose

It is defined as the energy absorbed per unit mass of the matter. The SI unit is *Gray (Gy)* which is the absorption of one joule in one kilogram of the material. Another common unit is *rad* which is equal to 0.01 Gy.

2.7.2 Equivalent dose

The previously stated unit of absorbed dose is sufficient for the quantitative evaluation of the effects of radiation on inanimate items like reactor fuel. However, the biological consequences of radiation exposure, rather than the quantity of energy deposited, are crucial for ensuring human protection. Equally absorbed dosages won't have the same biological consequences, which depends on the type of radiation. For example, one Gy of alpha is more harmful than 1Gy of gamma. This is the reason that a new unit that considers the biological impacts of radiation had to be developed.

This unit is called *equivalent dose*, and it is calculated by multiplying the absorbed dose by a dimensionless factor called radiation weighting factor (W_R), the radiation weighting factor is 1 for photons and electrons; 2 for protons; 20 for alpha and heavy ions, while it is variable for neutrons depending on neutron's energy [42]. The unit for equivalent dose is the sievert (Sv), therefore, the biological effects of one Sv of alpha radiation and 1 Sv of beta radiation are equivalent.

2.7.3 Effective dose

Different organs have different sensitivity to radiation. The head, for instance, is less sensitive than the chest. This effect is considered using the concept of *effective dose*. Effective dose, as shown by Equation (2.29), is calculated by the summation of the multiplication of the equivalent dose to each organ by a tissue weighting factor (W_T).

$$E = \sum_T w_T \sum_R w_R D_{T,R} = \sum_T w_T H_T \tag{2.29}$$

E is the effective dose for the whole body; H_T is the equivalent dose to the tissue or organ (T) from all types of radiation (R); $D_{T,R}$ is the absorbed dose in tissue or organ (T) from radiation (R). The unit of effective dose is the sievert (which is the same as equivalent dose).

2.7.4 Collective dose

Collective dose, S, is defined as the summation of the individual effective doses received by a group of people in a given period.

It can be used to calculate the overall health impact of a process that exposes a population to ionizing radiation. The name of the unit of collective dose is man sievert (man Sv).

The collective dose is mainly used for the optimization of radiation protection by comparing different protection procedures. It should not be utilized in risk projections [42].

Chapter 3 Nuclear Fuel Cycle and Proliferation Resistance

As mentioned in chapter 1, GEN-IV systems should reduce the burden of long-term management of spent nuclear fuel, as well as increase the proliferation resistance. In this chapter, the nuclear fuel cycle, including the current practices for long-term management of nuclear spent fuel, is mentioned in Section 3.1, while proliferation resistance aspects are given in Section 3.2

3.1 Nuclear Fuel Cycle

The uranium fuel cycle, which is the main fuel used in current reactors, is described here. Figure 3.1 depicts the fuel cycle of uranium [43]. Uranium exists in the earth's crust with a concentration of 2.8 g/ton. It is more abundant than gold (which has a concentration of 0.004 g/ton) but less abundant than thorium, copper, and zinc [44].

After geological exploration for uranium, the first step is mining the uranium ore, which means the extraction of the uranium ore from underground. Different methods are employed. There are three methods of uranium mining; namely: open pit, underground mining tunneling, and in-situ leaching. Extracting (or collecting) the uranium from the ore is a process known as milling. In this process, the ore is grinded and then dissolved in nitric acid.

The combined process of mining and milling is known as uranium recovery. The result of this process is a U_3O_8 concentrate known as a yellow cake (due to its yellowish color). The uranium in the yellow cake is natural uranium (Nat-U) with isotopic composition of 0.711 % ^{235}U, 99.284% ^{238}U, and traces of ^{234}U.

The yellow cake is packaged in drums and sent to the conversion plant, where it is converted to uranium hexafluoride UF_6. UF_6 exits the conversion plant as a gas, which is subsequently cooled to a liquid and emptied into 14-ton storage and transportation cylinders. UF_6 changes from a liquid to a solid as it cools over a period of five days. UF_6, in solid white crystalline form, is shipped to either a fuel fabrication plant or to an enrichment plant, depending on the required fuel [45].

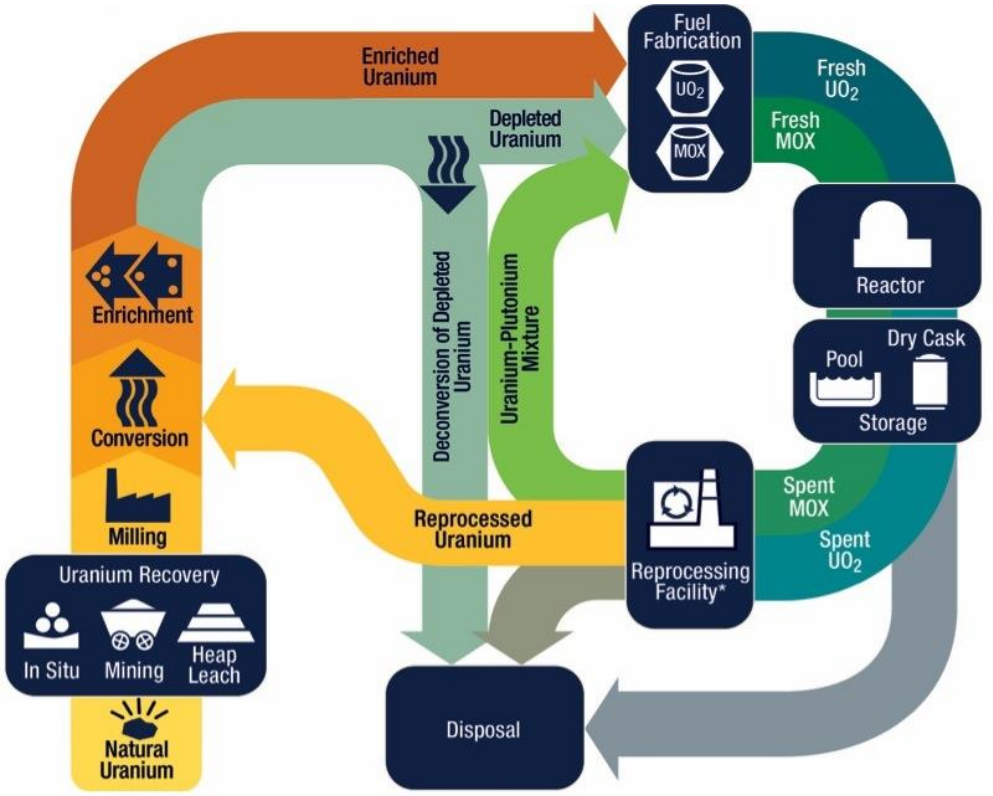

Figure 3.1: Nuclear Fuel Cycle [43]

For light-water reactors (LWRs), the uranium must be enriched before usage, which means increasing the amount of ^{235}U relative to ^{238}U. In this case, UF_6 is shipped to the enrichment plant. Uranium must be in gaseous form for enrichment. Solid UF_6 transitions straight to UF_6 gas (sublimation) under atmospheric pressure, bypassing the liquid phase, when its temperature is raised to 57° C [46].

In addition to the enriched uranium, the enrichment plant produces large quantities of uranium (tails) which contain less ^{235}U than the natural concentration (typically between 0.2-0.3%). This is known as depleted uranium, which exits the enrichment process in the form of depleted-uranium hexafluoride (DUF_6). The tails are stored on-site inside cylinders.

As fluoride poses a chemical hazard, DUF_6 undergoes a process called "deconversion" to convert the DUF_6 to stable depleted uranium oxide. In addition to reducing the chemical hazard of fluoride, the deconversion process has another purpose of recovering the commercially valuable, high-purity fluoride compounds.

For heavy-water reactors, like CANDU, natural uranium is used as a fuel. In this case, UF_6 cylinders are shipped directly to the fuel fabrication plant (sometimes the fuel fabrication plant receives natural uranium in form of UO_3 instead of UF_6 if no enrichment is needed).

Inside the fuel fabrication plant, UF_6 is converted to UO_2 powder using chemical processes, as shown in Figure 3.2. UO_2 powder is formed into fuel pellets and fed into Zircaloy tubes, which act as a sheath for the fuel. These tubes are assembled into fuel assembles/bundles and shipped to the reactor as fresh fuel [47].

The fuel is irradiated inside the reactor core, to produce electricity. During this time, the fuel is depleted reducing the concentration of the fissile material. After a certain time, the fuel cannot be used anymore and must be discharged from the reactor. The amount of energy extracted from the fuel is measured in a unit called burnup, which is the amount of thermal energy produced per unit mass of the heavy metal inside the fuel. A typical unit of burnup is giga-watt-day per metric ton of heavy metals (GWd/MTHM). As the majority of nuclear power plants use uranium, the burnup is expressed in units of GWd per metric ton of uranium (GWd/MTU).

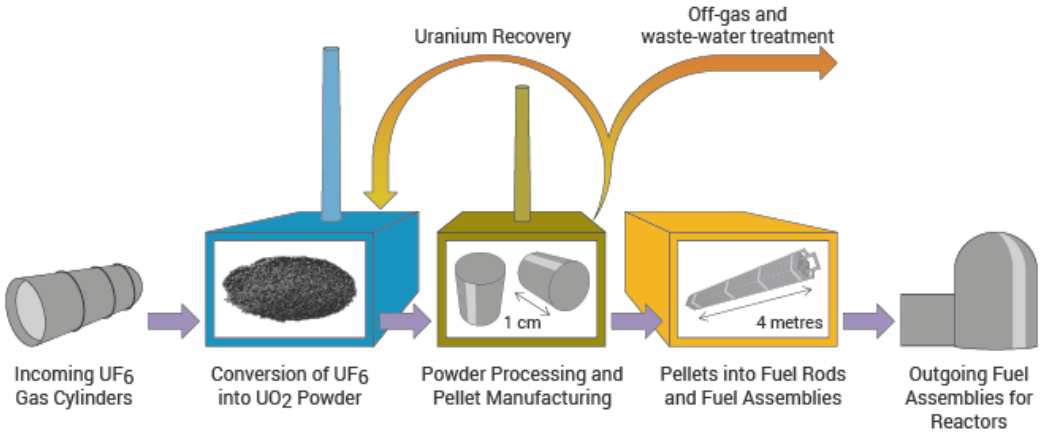

Figure 3.2: Steps of fabrication of fuel pellets inside fuel fabrication plant [47]

The used fuel is discharged from the reactor and treated as High-Radioactive Waste (HRW). The discharged fuels are stored in interim storage on-site. When the fuel is just discharged, it is stored, underwater, in spent fuel pools. As the capacity of the water pools is limited, the spent fuels must be transferred, after about five years, to dry-cask storage. These storage casks are cylinders, made of steel or concrete and cooled with air.

The steps of the fuel cycle before irradiation inside the reactor are called the front-end part, while after discharge from the reactor, they are called the back-end part.

Referring to Figure 3.1, the spent fuel can be sent to a long-term disposal facility or can be reprocessed.

3.1.1 Reprocessing of spent fuel

A typical fuel used in LWR, with exit burnup of 50.0 GWd/MTU, consists of around 93.4% uranium, of which ~ 0.8% is fissile ^{235}U, 5.2 % fission products, 1.2% plutonium and 0.2 % minor actinides (neptunium, americium, and curium) [48]. These materials can be extracted using a chemical process in a reprocessing facility. Different methods of reprocessing are employed worldwide. The most common one is the Purex method, which extracts plutonium and uranium.

The reprocessed uranium (RepU) can be re-enriched and then reused as a fuel inside LWRs (or HWRs). The plutonium can be mixed with depleted or reprocessed uranium in the fuel fabrication plant, to form Mixed-Oxide fuel (MOX).

MOX fuel was used inside some existing reactors instead of enriched uranium to preserve the uranium resources. MOX fuel may be used for the whole core, but due to the small yield of delayed neutrons from plutonium, only one-third of the core is usually filled with MOX while the rest is uranium [49].

If the fuel cycle involves reprocessing of the spent fuel it is called a closed cycle, if the spent fuel is sent directly to the disposal facility without reprocessing it is called an open or direct cycle.

3.1.2 Long-term management of spent nuclear fuel

The long-term management of spent nuclear fuel (SNF) is a major challenge in the nuclear industry. The current approach is to dispose the SNF inside a deep geological repository (DGR) hosted in a suitable rock formation like crystalline or sedimentary rock. Sweden, Finland, and Korea proposed conceptual designs for their DGRs [50-51].

3.1.3 Canadian concept of DGR

The Canadian plan for the long-term management of spent nuclear fuel is known as Adaptive Phased Management (APM). According to this plan, the SNF, after being packaged into Used Fuel Containers (UFCs), will be placed into a deep geological repository, with the ability to retrieve the spent nuclear fuel, if needed [11].

Since the adaptation of the APM by the Canadian federal government in 2007, different conceptual designs of the Canadian DGR were proposed. There are two reference concepts for the Canadian DGR. In the first concept, the UFCs are placed inside in-floor boreholes drilled vertically, while in the second concept the UFCs are placed in a horizontal configuration [52-53].

Figure 3.3 shows a schematic representation of the in-floor borehole Canadian concept of DGR. It consists of surface facilities and an underground disposal area.

The underground disposal area consists of eight panels excavated (as shown in Figure 3.4), at a depth of 500 meters, inside the gneiss rock. Each panel consists of several placement rooms (tunnels) where the boreholes are drilled vertically.

There are 124 tunnels in the conceptual design, each tunnel has 89 holes. The tunnel spacing is 40 meters while the canister spacing is 4.2 meters and, hence, the length of each tunnel (only the boreholes section) is 369.6 meters. There are segments of eight meters at the end of each tunnel and 16 meters at the entrance (Figure 3.5). Therefore, the overall length of each tunnel is 395.6 meters. The entrance to the tunnel is an elliptical arch which has base and height of 5.5 meters. The overall dimension of the DGR is 1565 m × 2001 m [53].

As can be seen in Figure 3.5, the UFCs are placed inside the boreholes and are surrounded by blocks of high-compact bentonite (HCB), which acts as a buffer between the UFCs and the rocks. There are two gaps between the UFCs and the bentonite and between bentonite and the rocks. These gaps are filled with bentonite pellets.

After placement of the containers, the floors of the tunnels are leveled with 25 cm of light backfill (LBF); blocks of dense backfill (DBF) will be used to close the tunnel. The space between the blocks of the dense backfill will be filled with light backfill [53].

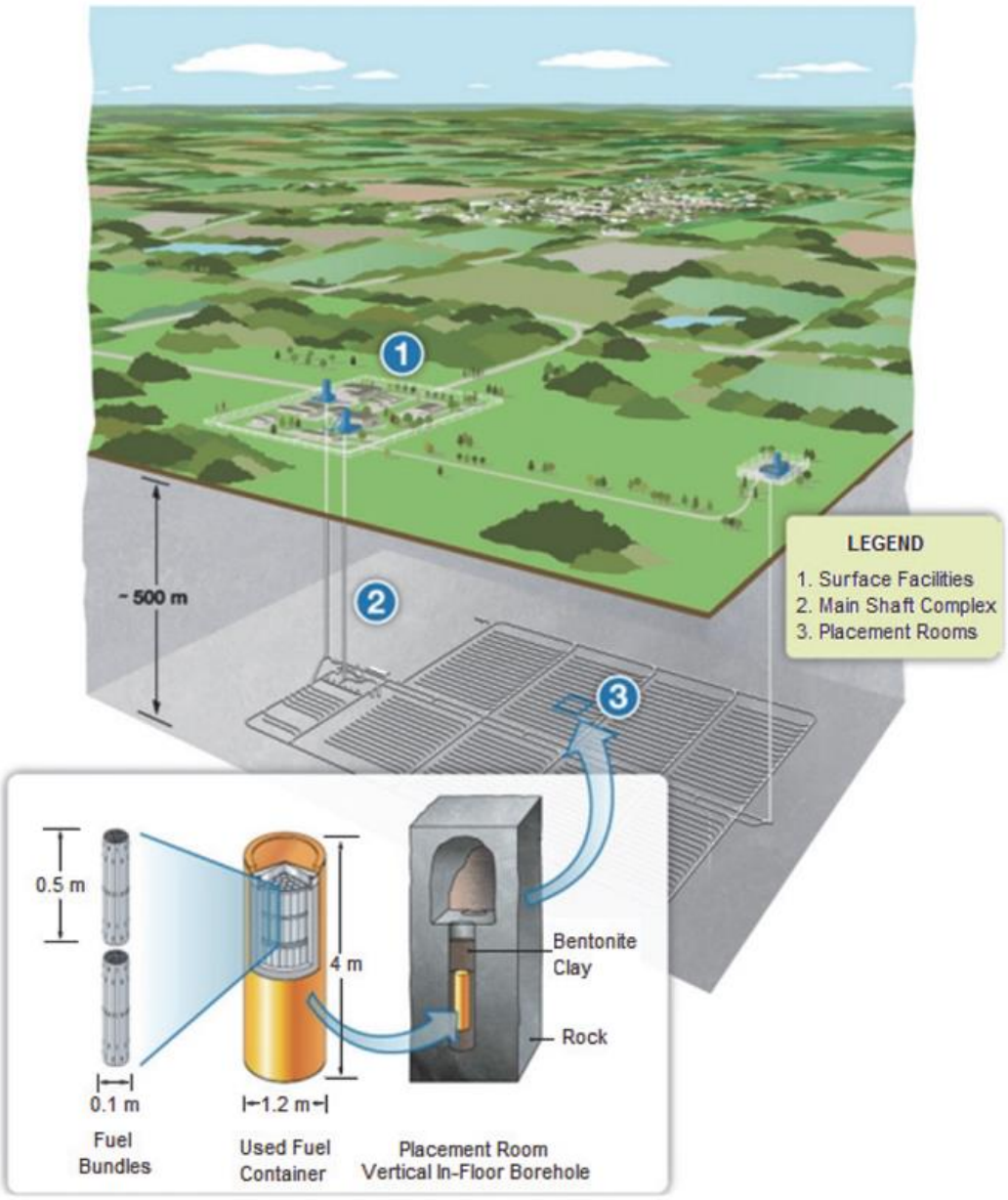

Figure 3.3: Schematic view of in-floor borehole Canadian DGR [53]

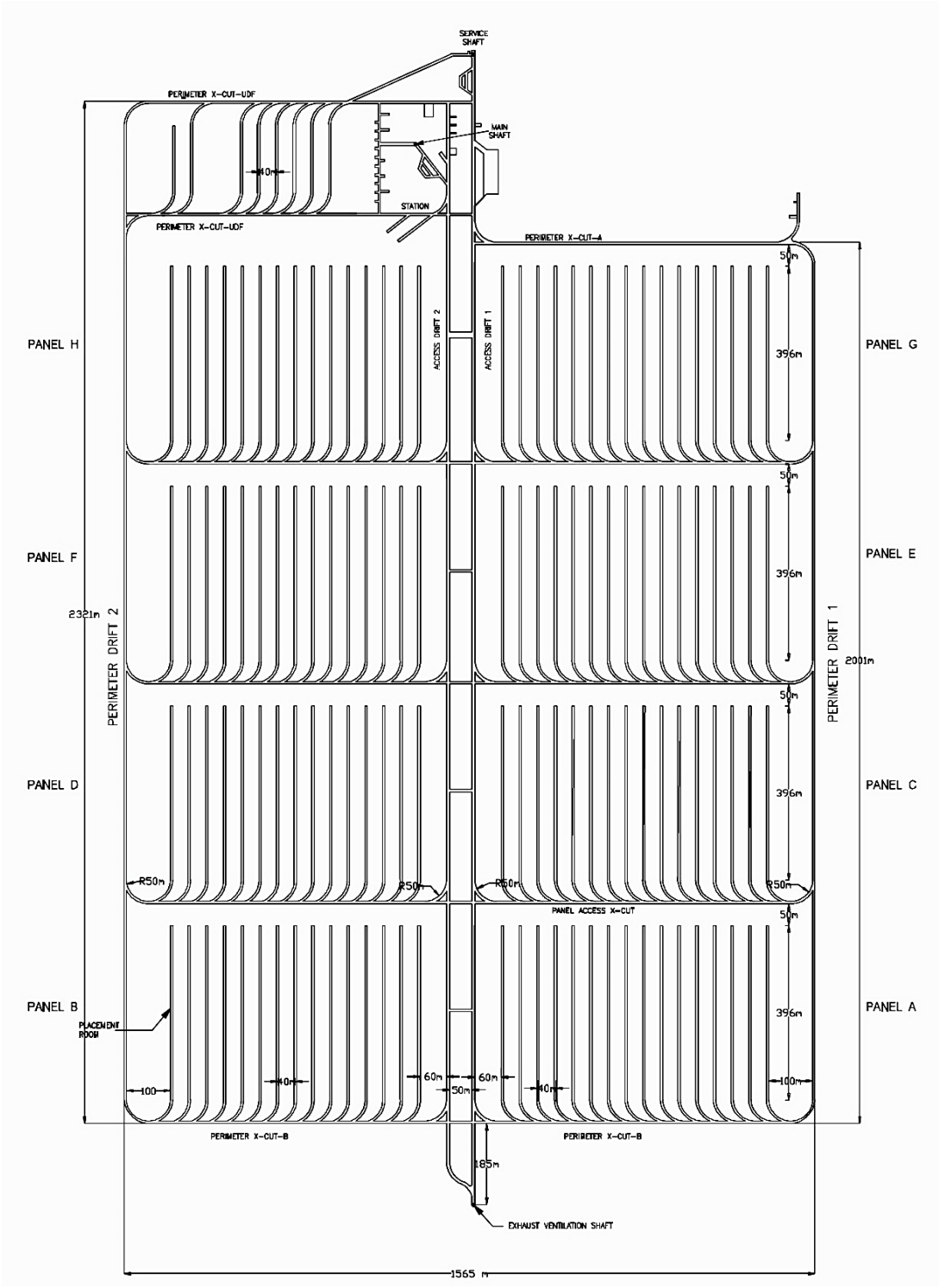

Figure 3.4: Layout of the underground repository [53]

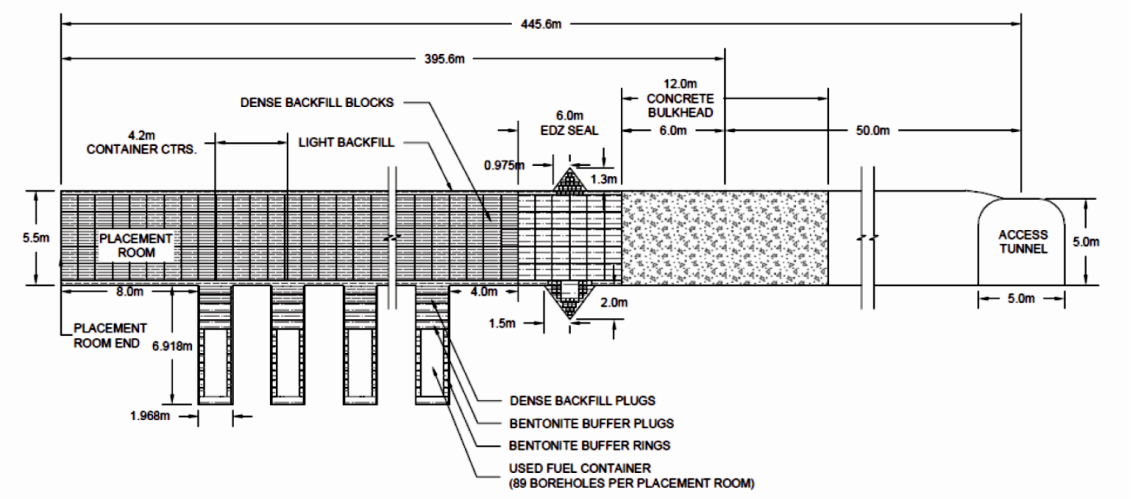

Figure 3.5 Section of the one tunnel in the in-floor borehole Canadian DGR

3.1.3.1 Thermal criteria

Due to the decay heat of the SNF, a single canister inside a borehole is treated as a heat source. This heat is transferred by conduction to the pellets, the bentonite, and eventually to the rocks. To keep the integrity of the bentonite, the maximum temperature of the bentonite, in contact with the canister's surface, must be below 100 °C [54]. This is the thermal criterion used to design the layout of any repository.

The temperature of bentonite, in contact with a certain canister, is raised not only due to the heat transfer from this canister, but also due to the heat transferred from other canisters in the same tunnel and adjacent tunnels. Accordingly, the temperature at the canister/bentonite interface depends on the distance between the different canisters, the distance between tunnels, the power of the canister at the time of deposition, the rate of the power decay, and the thermal properties of the bentonite and rock.

Therefore, the thermal requirement of the repository can be fulfilled by changing: the distance between the adjacent canisters (canister spacing (CS)); the distance between adjacent tunnels (tunnel spacing (TS)); and/or the initial power of the UCFs (which is a function of the cooling time after discharge from the reactor).

The canister spacing and tunnel spacing determine the layout and the area of the repository. As all the spent fuels in Canada are coming from CANDU, the Canadian concept of the DGR was based only on the disposal of CANDU fuel bundles. Due to the low burnup and hence, low decay heat of CANDU bundles, the canister spacing was found to be 4.2 m when the tunnel spacing was 40 m.

3.1.3.2 Surface facilities

In addition to the underground disposal rooms, the DGR contains surface facilities (above the ground). The main surface facility is the Used Fuel Packaging Plant (UFPP), where SNFs are received and transferred to the UFCs for final disposal [55].

There are storage areas inside the UFPP to store the filled UFCs before discharge to the underground repository.

In addition to UFPP, the surface facilities also include a sealing plant, where the concrete and sealing materials (HCB, LBF, bentonite pellets, and DBF) are produced, quality control offices, and labs.

3.1.4 Phases of the DGR

The development of the geological disposal facility is expected to take decades. It can be divided into three phases: pre-operational, operational, and post-operational (post-closure) phase (shown in Figure 3.6). The pre-operational phase involves site selection, licensing, and construction of the DGR. The operational phase starts when the waste is received at the facility for the first time, while the post-closure phase begins when all access paths from the surface to the underground are sealed and the surface facilities are disassembled [56].

The safety of the DGR is ensured by different means during the different phases:

1. The pre-operational phase

   No safety measures with respect to nuclear materials are required.

2. The operational phase

   The safety of DGR in this phase is ensured by active control measures, which are performed in the same way as other facilities handling radioactive materials. Examples of these measures include monitoring of the environment and inspections performed by the regulatory authorities.

3. The post-closure period

   During this period, no human control is assumed to exist and the safety of the DGR relies only on the passive safety features incorporated in the design.

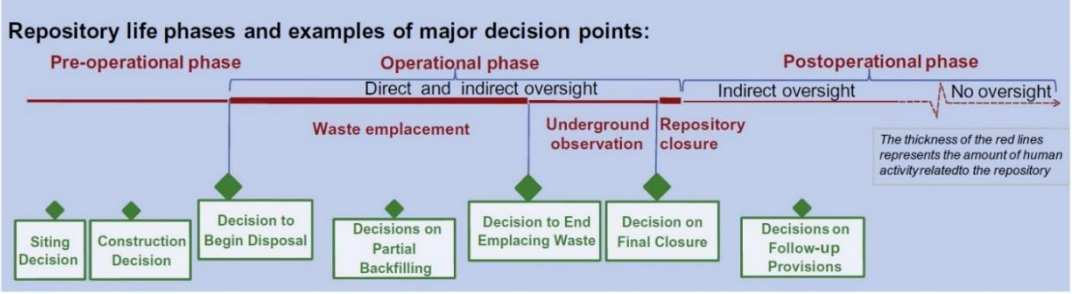

Figure 3.6: Phases of DGR [56]

For some time after the closure, it can be assumed that some passive institutional controls still exist. Examples of these measures include monitoring the environmental conditions, keeping records of the facility, and using warning signs to inform future generations about the existence of the repository. But, as the post-closure period is very long (can be hundreds of thousands of years), there is no guarantee that the memory of the site will not be lost. Therefore, the design of the DGR must include all possible passive provisions to ensure the safety of the humans and the environment after the closure of the repository [57].

The post-closure safety of the DGR was studied before for the Canadian DGR [58-59]. Assessment of the post-closure safety for different types of fuels proposed for PT-SCWR was performed as part of this thesis and is presented in Chapter 5.

3.2 Proliferation Resistance

One of the challenges associated with nuclear energy is the potential usage of nuclear materials to construct nuclear weapons. One stated goal of the GEN-IV program is to increase the proliferation resistance of the nuclear energy systems (NES). The definition of proliferation resistance (PR) and the different methodologies to assess the PR of a nuclear system are briefly given in this section.

The proliferation resistance is defined as: "*that characteristic of a nuclear system that impedes the diversion or undeclared production of nuclear material, or misuse of technology, by States in order to acquire nuclear weapons or other nuclear explosive devices*" [60].

The PR can be enhanced using a combination of intrinsic features and extrinsic measures. The intrinsic features are the inherent properties of the NES that hinder the diversion of nuclear materials, i.e., unattractive material types, while the extrinsic measures are the international safeguards applied by the International Atomic Energy Agency (IAEA) to verify that all nuclear materials are used according to their declared purposes.

Extrinsic measures will always be needed regardless of the level of the intrinsic PR features, but by designing the facility in a way to increase the time and cost needed for diversion, the safeguards measures and, hence the resources needed by IAEA to perform its inspections, will be reduced. This is very important now given that many countries show interest in nuclear energy. Hence, increasing the intrinsic PR is encouraged in Gen-IV designs to help the application of efficient safeguards.

3.2.1 Methodologies for assessment of PR

An evaluation of the proliferation resistance at the earliest stage of the design is recommended. This will help in detecting any vulnerabilities of a proposed design and changing it accordingly. Using a different fuel cycle or changing the layout to implement the safeguards more easily, are examples of the possible changes in design to increase its proliferation resistance.

There are different methodologies proposed for assessing the PR of NES. Examples of these methodologies are Technological Opportunities to Increase the Proliferation Resistance of Global Civilian Nuclear Power Systems (TOPS) [61], developed by the US Department of Energy; the Proliferation Resistance and Physical Protection (PR&PP), developed by the Gen-IV forum [62]; and PR of The International Project on Innovative Nuclear Reactors and Fuel Cycles (INPRO) developed by IAEA [63]. A brief explanation of each one is given below.

3.2.1.1 TOPS

In this methodology, a set of barriers against proliferation were identified; The flowchart of this methodology is shown in Figure 3.7 [64]. These barriers are categorised into material, technical and institutional barriers. The material and technical barriers are intrinsic features (related to the inherent properties of the facility/fuel cycle), while the institutional barrier is extrinsic (safeguards).

The effectiveness of each barrier, which is described either using qualitative description (“insignificant” to “very high”) or using numerical values (1 to 5), is assessed for different diversion scenarios. Increasing the strength of the barriers will increase the PR as more effort and cost would be needed for diversion. The PR is determined for the NES as a whole.

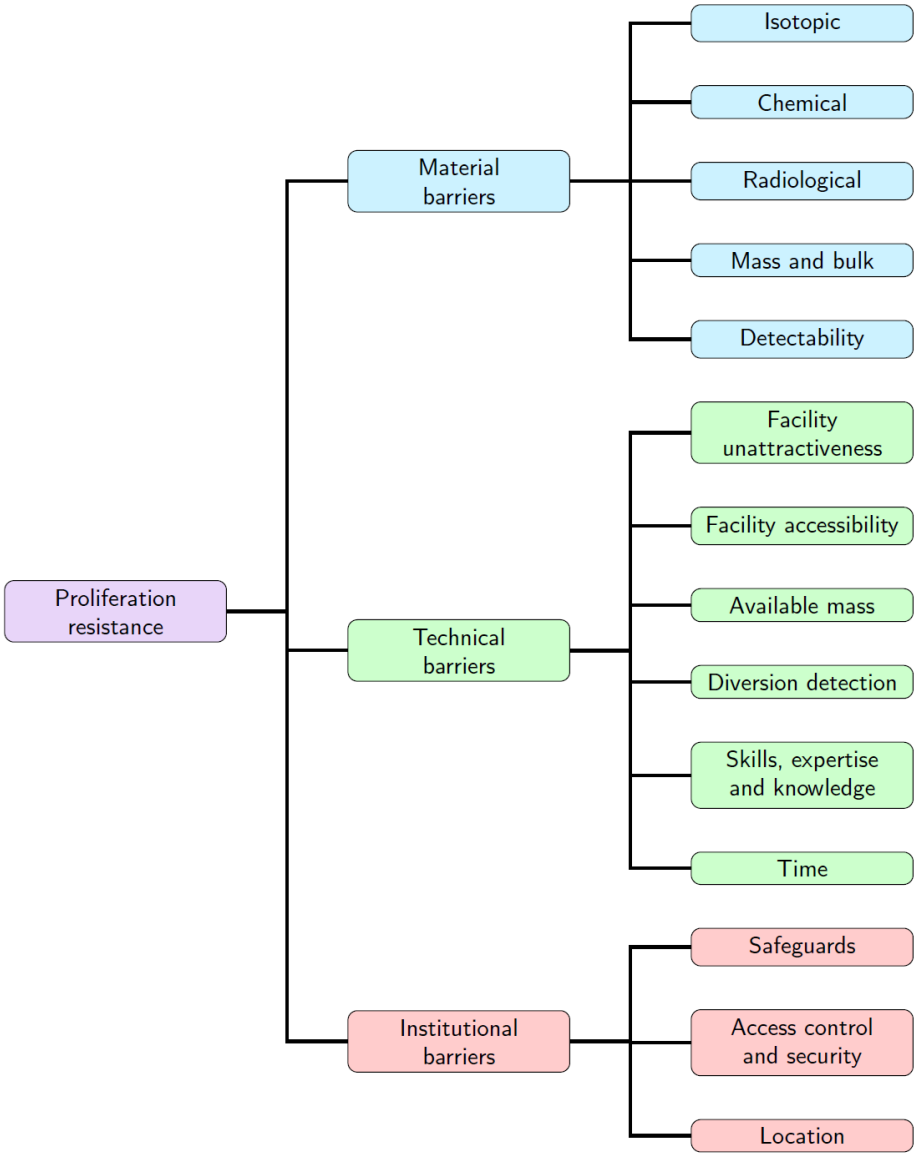

Figure 3.7: Overview of TOPS methodology [64]

3.2.1.2 PR&PP

As increasing the PR is one of the stated GEN-IV goals, a specific methodology for assessing the PR of GEN-IV systems was proposed, which is PR&PP. Figure 3.8 shows the basic framework of the PR&PP evaluation methodology [62].

A set of threats to NES (i.e. diversion, undeclared activities, etc.) are identified. The response of the NES against these threats is evaluated by identifying prospective targets, such as materials that can be diverted, as well as all conceivable diversion channels, i.e. steps that can be used to produce nuclear weapons. Following a methodical definition of targets and diversion paths, six measures are assessed for each of the distinct pathways using the qualitative adjectives 'Very low', 'Low', 'Medium', 'High', and 'Very high' resistance.

Four measures are concerning PR, while the other two are related to physical protection. One of the PR measures is the "Fissile Material Type" which is a classification of materials based on how their suitability for use in nuclear weapons. An assessment of this measure shows how the material, in the proposed fuel cycle, is resistant to proliferation.

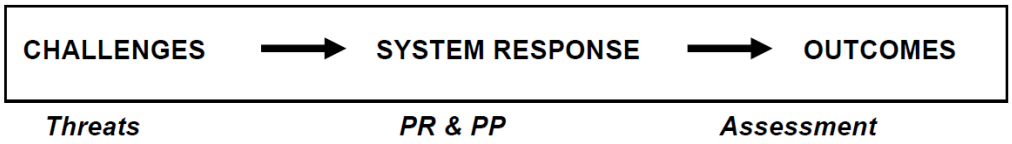

Figure 3.8: Basic framework of PR&PP [62]

3.2.1.3 Proliferation resistance methodology of the INPRO project

INPRO is a project established in 2000 by the IAEA to ensure the sustainability of the Innovative Nuclear energy Systems (INS). Sustainable nuclear energy production has many requirements, one of them being its proliferation resistance. Part of the INPRO project is to develop a methodology for proliferation resistance. In the proposed methodology, a basic principle is defined: "*PR intrinsic features and extrinsic measures shall be implemented throughout the full life cycle for INSs to help ensure that INSs will continue to be an unattractive means to acquire fissile material for a nuclear weapons program. Both intrinsic features and extrinsic measures are essential, and neither shall be considered sufficient by itself"*. [65]

To fulfill this principle, five User Requirements (UR) are determined:

1. State commitments (legal framework).
2. Low attractiveness of nuclear materials and technology.
3. High difficulty and detectability of diversion.
4. Multiple barriers.
5. Optimization of design (costs).

Seventeen Criteria are defined to assess the URs and to check if the INS fulfills the basic principles.

3.2.2 The attractiveness of nuclear materials

As can be seen from all the PR methodologies, the attractiveness of nuclear material which is based on its potential use in a weapons program is an essential part of the barriers against proliferation. Lowering the attractiveness will increase the PR and hence helps in fulfilling the GEN-IV goals.

Attractiveness can be assessed using different methods [66-67]. In this thesis, the "Figure-of-Merit" (FOM) method proposed by Bathke et al. [12] was used to compare different fuel cycles for PT-SCWR. In this methodology, a parameter called FOM is calculated, whose values are related to the attractiveness of the materials, as given in Table 3-1. Any material with FOM > 1 can be used to construct an effective nuclear device, while material with FOM <1 is impractical for weapons but still possible theoretically. Lower FOM is better for proliferation resistance, and each process which can result in a material with a lower FOM should be encouraged. This method is explained more in Chapter 6.

Table 3.1: Meaning of FOM and the attractiveness associated with it

FOM	Weapons utility	Attractiveness
> 2	Preferred	High
1-2	Attractive	Medium
0-1	Unattractive (Theoretically possible)	Low
< 0	Unattractive	Very low

3.2.2.1 Classification of materials

The IAEA classifies nuclear materials into two categories, namely, Direct Use and Indirect Use. Direct Use nuclear materials are those that can be used to construct nuclear weapons without transmutation or further enrichments. Examples are Pu with less than 80% ^{240}Pu, highly enriched uranium, and ^{233}U. While Indirect Use materials are those materials that must be further processed to be suitable for weapons. Examples are low-enriched uranium, depleted and natural uranium, and thorium.

Significant Quantity (SQ) is defined as: "*the approximate amount of nuclear material for which the possibility of manufacturing a nuclear explosive device cannot be excluded*" [68]. The SQ differs between the Direct and Indirect Use materials as shown in Table 3.2. The relationship between the classification of materials according to IAEA and FOM is given in Table 3.3 [62].

Table 3.2: The significant quantities of different nuclear materials

Material	SQ
Direct Use	
Pu (less than 80% ^{238}Pu)	8 kg
HEU (^{235}U ≥ 20%)	25 kg
^{233}U	8 kg
Indirect Use	
LEU (^{235}U < 20%)	75 kg
Natural Uranium	10 tons
Depleted uranium / Th	20 tons

Table 3.3: Relationship between IAEA classification and FOM values

IAEA Material Category	Materials	FOM Value Range	Significant Quantity
Direct use nuclear material	Optimal weapons materials (WG-Pu, HEU w/ ^{235}U > 90 %, ^{233}U w/ ^{232}U < 25 ppm)	2 < FOM	8 kg Pu 25 kg HEU 8 kg ^{233}U
	Pu, Np, HEU w/ ^{235}U > 70%, ^{233}U w/ ^{232}U > 25 ppm	2 < FOM	
	HEU w/ ^{235}U > 20 %, Fresh TRU, Pu w/ ^{238}Pu > 5%	1 < FOM < 2	
Indirect use nuclear material	Am + Cm, LEU w/ ^{235}U < 20%, Pu w/ ^{238}Pu > 80%	0 < FOM < 1	75 kg ^{235}U (10 t natural U or 20 t depleted U)
	Cm, LEU w/ ^{235}U < 10%, HLW solution	FOM < 0	
	LEU w/ ^{235}U < 5%, Natural Uranium, Depleted Uranium, Th	FOM << 0	

Chapter 4 Evaluation of the Canister Spacing and Criticality Safety of Spent Plutonium-Thorium Nuclear Fuel

Citation:

Remon Ibrahim, Adriaan Buijs, John Luxat, July 2022, “Evaluation of the canister spacing and criticality safety of spent plutonium-thorium nuclear fuel”, Ann. Nucl. Energy 172, 109056.

https://doi.org/https://doi.org/10.1016/j.anucene.2022.109056

Reduction of the burden of the long-term management of nuclear waste is one of GEN-IV goals. This requires minimizing the mass, volume, decay heat and the radiotoxicity of the spent fuel. In the article reproduced in this chapter, the decay heat of spent Pu/Th and LEU fuels, which were burned in PT-SCWR till 60 GWd/MTHM, was estimated. The decay heat of Pu/Th is one order of magnitude higher than that of uranium fuel.

The PT-SCWR is a once-through reactor, and its spent fuel is supposed to go to DGR according to the Canadian plan for long-term waste management. As the decay heat of Pu/Th spent fuel is higher than that of LEU, the DGR needed to store Pu/Th fuel is expected to be larger. A quantitative estimation and optimization of a DGR storing Pu/Th was a novel aspect of this work.

The layout of the DGR storing Pu/Th was estimated for many scenarios, including different cooling times of the spent fuel and different numbers of spent fuel channels per canister, to find the optimal size of DGR without violating the thermal safety limit.

Comparison between the space needed to store Pu/Th and LEU was performed as well. It was found that the DGR needed for Pu/Th would be between three to four times larger than that for uranium.

Finally, the criticality safety analysis was performed for canisters holding Pu/Th and LEU fuels in the most reactive situations. The effective multiplication factor was found to be less than the criticality limit of 0.95, without taking any burnup credit, for both fuels. This is mainly due to the special design of the PT-SCWR which uses the heavy water as a moderator and light water as coolant.

In this article the comparison was between Pu/Th and LEU fuels. During the progress of the research, other fuel cycles were proposed, namely LEU/Th (with 48% and 38.4% of UO_2/ThO_2 in the inner and outer rings, respectively), and reprocessed uranium (RepU). This was not included in this publication. Comparison between the decay heats of Pu/Th, LEU, LEU/Th, and RepU was estimated using the same method used in this article and shown in Figure 4.1.

As can be seen, there is no significant difference between the decay heat of all uranium-based fuels; namely LEU, LEU/Th and RepU. Therefore, the results mentioned in the publication concerning LEU are applicable to both LEU/Th and RepU. Hence Pu/Th will need a DGR between three to four times larger than that needed for LEU, LEU/Th, or RepU.

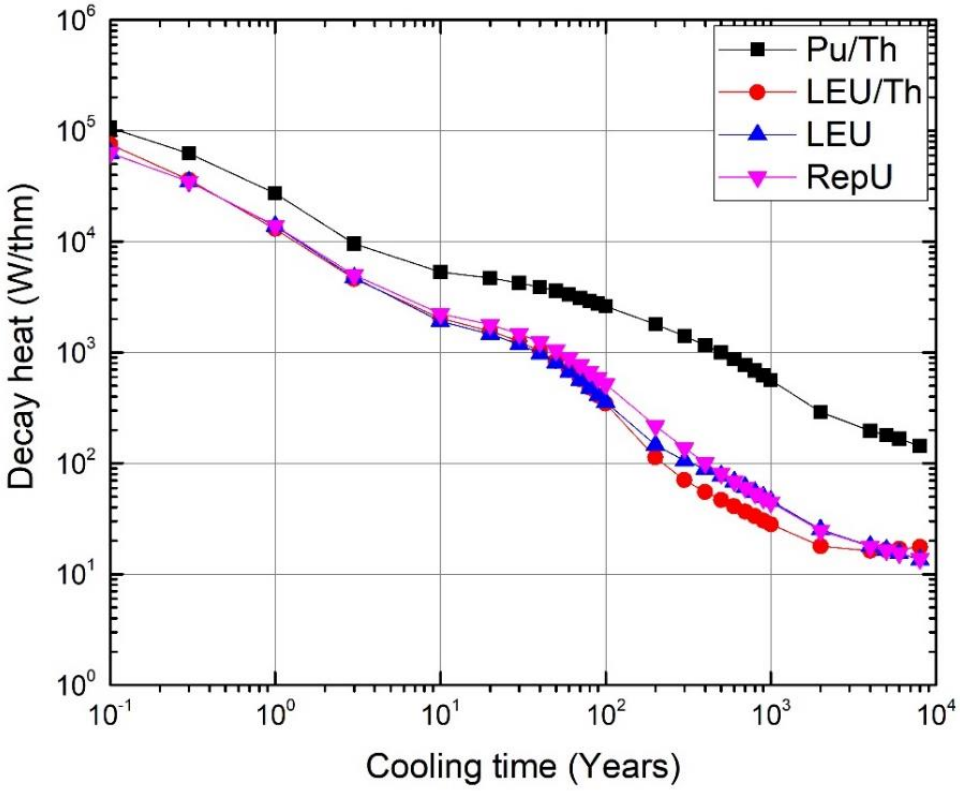

Figure 4.1: Decay heat as function of cooling time for different fuels

Evaluation of the canister spacing and criticality safety of spent plutonium-thorium nuclear fuel

Remon Ibrahim [a,b], Adriaan Buijs [a] , John Luxat [a]

[a] McMaster University, 1280 Main Street West, Hamilton, ON, L8S 4L7, Canada

[b] Nuclear and Radiological Regulatory Authority, N. City, Cairo, Egypt

Abstract

The Canadian conceptual design of the Super-Critical-Water Reactor (SCWR), known as Pressure-Tube –SCWR (PT-SCWR) is a GEN-IV design that employs the Pu/Th direct fuel cycle. The spent Pu/Th fuel is expected to be stored into Deep Geological Repository (DGR). In this study, a thermal analysis for a repository with Pu/Th spent fuel was performed using the computer code CODE_BRIGHT. The maximum temperature of the bentonite was obtained, and the minimum canister spacing was calculated for different cooling times and different numbers of channels per canister.

The size of the repository needed for Pu/Th fuel was found to be three to four times larger than that for uranium for the same electrical energy output. This increases the cost of the long-term management of the spent fuel.

The nuclear criticality safety aspect of storing Pu/Th spent fuel in the DGR was evaluated as well using MCNP. The effective multiplication factor, for the most reactive situations was 0.858, which is less than the acceptance criterion of 0.95.

Keywords:

Deep geological repository; Plutonium/Thorium fuel cycle; Thermal analysis, Canister spacing; Nuclear criticality safety; PT-SCWR

1. Introduction

Management of the spent nuclear fuel (SNF) is one of the major challenges in the nuclear industry. One of the proposed ways to deal with the SNF is to store it in a Deep Geological Repository (DGR), excavated in suitable rock formations like crystalline or sedimentary rock. Different conceptual designs for DGRs were proposed in the past (Lee et al., 2007; SKB, 2006a; SNC-Lavalin, 2011).

Generally, the DGR consists of horizontal placement rooms (tunnels) separated from each other by a certain distance. The canisters holding the SNF are placed inside boreholes, drilled into the tunnels, and surrounded by a blocks of buffer material (bentonite). The layout of the DGR is determined by the tunnel spacing (TS) and canister spacing (CS), which are chosen in a way to fulfill the thermal criterion of the DGR.

The maximum temperature of the bentonite, in contact with the canister's surface, must be below 100 °C to maintain the integrity of the bentonite (SKB, 2006b). Due to the uncertainties in thermal analysis, the calculated maximum temperature is set to 90 °C in this study, giving a safety margin of 10 °C. The temperature at the canister/bentonite interface depends on the distance between the different canisters, the distance between tunnels, the power of the canister at time of deposition, the rate of the power decay, and on the thermal properties of the bentonite and rock.

Different methods, either analytical or numerical, have been used before for the thermal analysis of DGRs (Guo, 2017; Hökmark and Claesson, 2005; Ikonen et al., 2018; Li et al., 2011; Sizgek, 2005; Zhou et al., 2020; Zhou et al., 2022). The previously performed thermal analyses assumed that all spent fuels are uranium oxide fuels (UOX). On the other hand, there is an increasing interest to use other fuels, either in the existing reactors or in the next-generation reactors (Insulander Björk, 2013; Trellue et al., 2011).

One of these fuel cycles is plutonium-thorium, which is the proposed fuel for the Canadian design of the Super-Critical-Water Reactor (SCWR), one of the Generation-IV (GEN-IV) concepts (GIF, 2002).

The Canadian design, known as Pressure-Tube SCWR (PT-SCWR), is a heavy-water moderated, light-water cooled reactor. It consists of 336 pressure tubes which hold the 64-element, five-meter-long fuel assemblies. The fuel assembly consists of two concentric fuel rings with 32 fuel pins each. The fuel is a mix of reactor-grade plutonium and thorium. The plutonium is assumed to originate from recycling of used fuel of LWRs. The weight percentages of PuO_2 in the inner and outer rings are 15% and 12% respectively (Pencer and Colton, 2013). The isotopic composition of Pu was taken as that of sample SF97-4 mentioned in (Nakahara et al, 2002). The expected exit burnup is 60 Giga-Watt-day per ton of heavy metals (60 GWd/thm) (Hummel, 2015)

The PT-SCWR uses a once-through fuel cycle; Its spent fuel is planned to be stored in the DGR. After 50 years of decay, which is a typical decay time for final disposal, the decay heat of the spent fuel of Pu/Th is about two orders of magnitudes higher than that of uranium (Ade et al., 2014; Ibrahim et al., 2019), thus a larger separation between the canisters is required. Also, the decay heat of Pu/Th decreases slower than that of UOX, making the previously preformed thermal analysis for UOX not valid for the Pu/Th case.

The objective of this study was to estimate the minimum canister spacing required to store the Pu/Th spent fuel from the operation of PT-SCWR. This was done for different numbers of channels per canister and for different cooling times. The size of the DGR was estimated for each case, and hence the conditions which give the minimal size of the DGR can be identified. Reduction of the DGR's size has an economical advantage, which is one of GEN-IV goals. For comparison purposes the area of DGR when UOX from PT-SCWR is stored instead of Pu/Th was evaluated as well.

In addition to the thermal criterion, there is a limit on the quantities of the fissile materials which can be stored together to prevent criticality accidents. This is a regulatory requirement; nuclear criticality safety is part of the safety analysis report of the DGR. The regulatory limit is that the effective multiplication factor, k_{eff}, for any collection of fissile materials must be less than 0.95 for the most reactive situations (CNSC, 2020). The

criticality safety of disposal canisters holding Pu/Th fuels was addressed in this work as well.

The outcome of this study may help in choosing a fuel cycle for PT-SCWR that fulfills the GEN-IV goals, which include reducing the costs of the fuel cycle as well as reducing the burden of the long-term management of the SNF.

2. Methods and materials

2.1. The Canadian conceptual DGR

The Canadian conceptual design of the in-floor deep geological repository (referred to here as CANDU DGR), consists of eight panels excavated in the gneiss rock at a depth of 500 meters. Each panel consists of several placement rooms (tunnels) where the boreholes are drilled vertically. There are 124 tunnels in the conceptual design, with 89 holes each. The tunnel spacing is 40 meter while canister spacing is 4.2 meter; hence the length of each tunnel (only the boreholes section) is 369.6 meter. There are segments of eight meter at the end of each tunnel and 16 meters at the entrance (Figure 1). Therefore, the overall length of each tunnel is 395.6 meter. The entrance to the tunnel is an elliptical arch which has a base and height of 5.5 meter. The overall dimension of the DGR is thus 1565 m × 2001 m (SNC-Lavalin, 2011).

The canisters containing the SNF are surrounded by high–compact bentonite (HCB). There are two gaps of 50 mm (filled with bentonite pellets) between the canister and bentonite and between the bentonite and the rock.

The depth of the borehole in the conceptual design is set to 6.918 meter. This is based on the assumption that the height of the canisters, which store CANDU bundles, is 3.909 meter. In this study, canisters are assumed to store channels from PT-SCWR which are five meter long. Accordingly, the height of the canisters in this study is set to 5.323 meter making the depth of the borehole equal to 8.323 meter (a description of the canister is given in section 2.3). The diameter of the borehole is 1.771 meter (which is less than that of the conceptual design which has a diameter of 1.968 meter).

After placement of the canisters, the floors of the tunnels are leveled by 25 cm of light backfill; blocks of dense backfill will be used to close the tunnel. The space between the blocks of the dense backfill will be filled with light backfill. Figure 2 shows a cross-sectional view of a tunnel with a borehole.

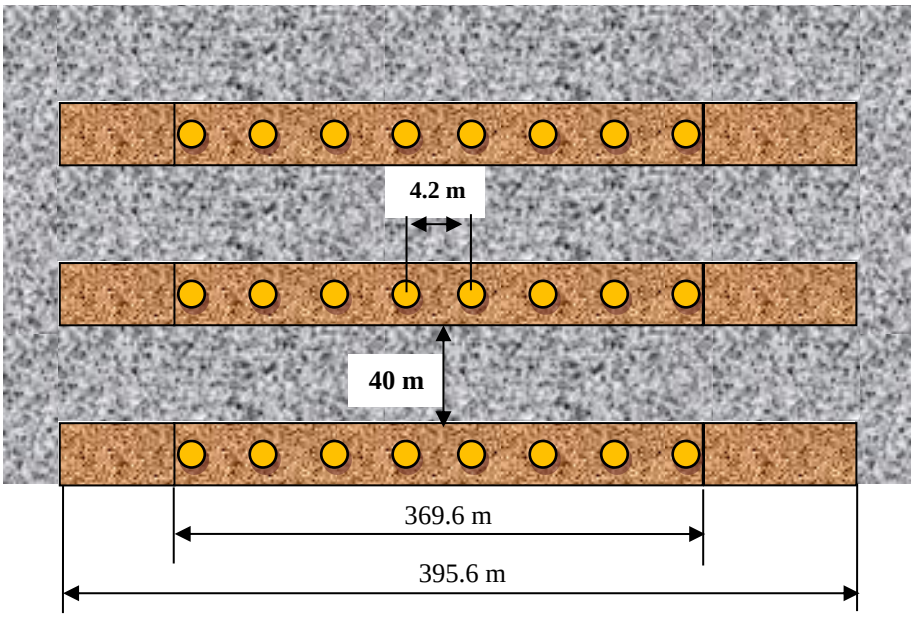

Figure 1. A schematic view of the tunnels in the CANDU DGR.

2.2 Thermal model

The evolution of the temperature of the bentonite in contact with a canister is determined not only by the heat load of the canister, but also by the heat load of all other canisters, either in the same tunnel or in the adjacent tunnels. To estimate the maximum temperature of the bentonite, the effect of adjacent canisters must be taken into account.

Modeling the whole DGR is impractical due to its size. Instead, the whole DGR is represented by a unit cell with adiabatic boundary conditions (near-field model). The DGR would have infinite dimensions in this case; as this is not realistic, the results of the near-field model should be corrected using a far-field model. In the far-field model, the whole

DGR is modeled as a homogenous 3D parallelepiped. Previous work found that there is no significant difference between the results of near- and far-field models for the first 1000 years after deposition (Guo, 2007).

The thermal analysis was performed using the verified and validated code CODE_BRIGHT (version: Code_bright_2021_06) which is a finite-element method program, developed at the Department of Civil and Environmental Engineering of the Polytechnic University of Catalonia (UPC). CODE_BRIGHT is used for the modeling of the coupled thermo-hydro-mechanical (THM) processes in geological media (Olivia et al., 2021).

The pre/post-processor GID, developed by the International Center for Numerical Methods in Engineering (CIMNE), was used with CODE_BRIGHT for the definition of the geometry, materials, boundary conditions, and for the generation of the meshing. CODE_BRIGHT/GID was used previously in the thermal analysis of the CANDU DGR (Guo, 2007; Guo, 2008).

2.2.1 Near-field model

In the near-field model, a unit cell, which is considered as representative of the whole DGR, is modeled in detail with adiabatic boundary conditions. The unit cell used in this study is shown in Figure 3.

It consists of one quarter of the canister, half of canister spacing, and half of the tunnel spacing. The depth of the tunnel is 500 meter below ground. The model extends to 2500 meter below the ground. The boundary conditions are:

- Isothermal boundary conditions at the surface. The temperature was set to 5 °C (Baumgartner et al., 1994). A vertical temperature gradient of 0.012°C/m is used (Baumgartner et al., 1994). Therefore, the lower surface of the model is kept at a temperature of 35 °C.
- Adiabatic boundary conditions (no heat flow at the boundaries) are applied for the outer vertical sides.

The initial temperature of the canister is not an important parameter for the calculation of the peak buffer temperature. This is because the heat transport inside the deposition hole is quasi stationary after a few days (Hökmark et al., 2009)

The materials used in the thermal analysis, as well as their thermal properties are given in Table 1. These are the properties used for the conceptual design of CANDU DGR (SNC-Lavalin, 2011). Fine meshing was used close to the canister's region. The number of eight-noded elements, used for meshing, depends on the CS; For example, for a CS of eight meter and 40-meter tunnel spacing, the number of elements was 353,000.

Table 1. Thermal properties of the materials used in the thermal analysis

Material	Thermal conductivity W/(m.K)	Specific heat J/(kg.K)
Gneiss rock	3.00	845
High-compact bentonite	1.00	1440
Bentonite pellets	0.40	910
Dense backfill	2.00	1110
Light backfill	0.70	1280

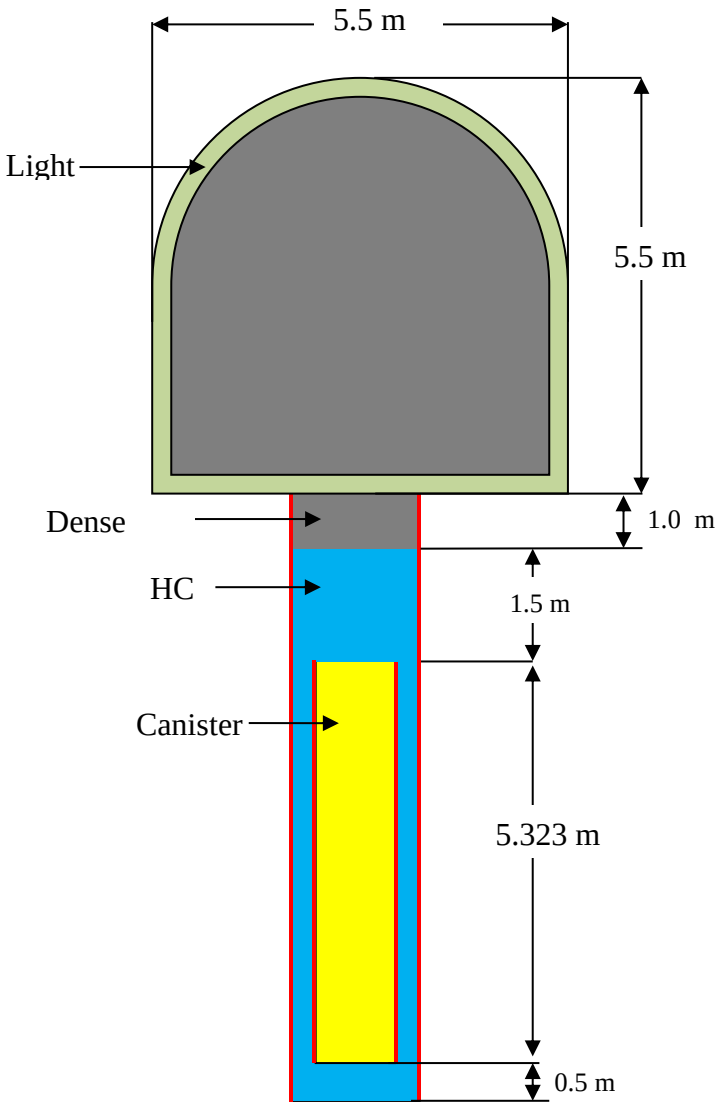

Figure 2. Cross-sectional view of one borehole. The dimensions are the dimensions used in this study.

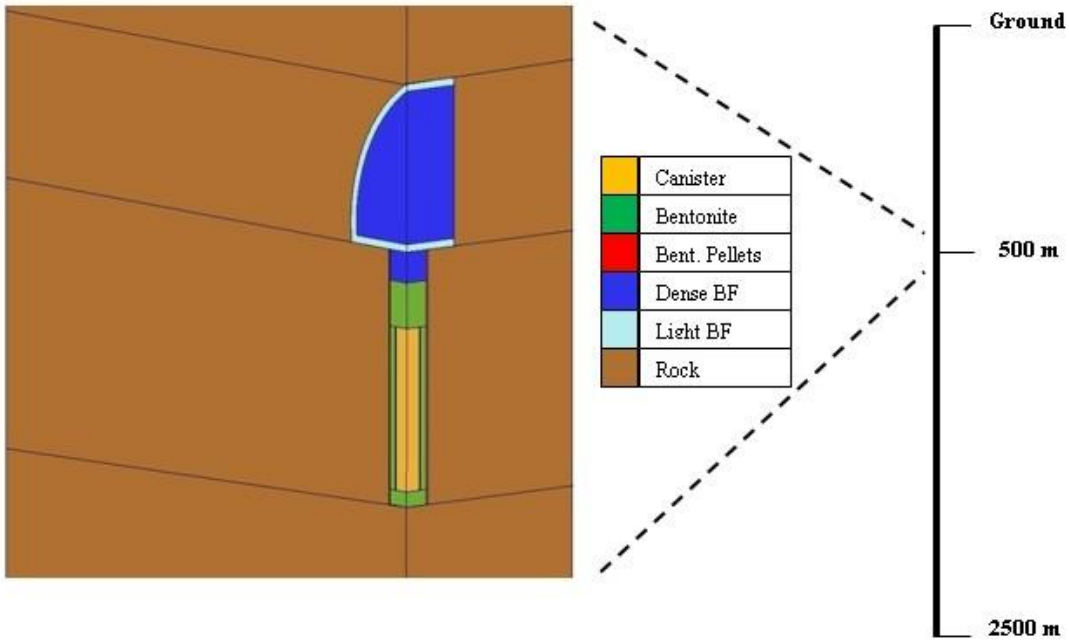

Figure 3. 3D view of the near-field model.

2.2.2 Heat load

The spent Pu/Th fuel is that from the PT-SCWR. A 2D cross-sectional view of the fuel cell of PT-SCWR is shown in Fig 4. This unit cell has been modeled using TRITON, which is part of the SCALE package used in previous work (Ibrahim et al., 2019). The fuel was burnt to an exit burnup of 60 GWd/thm, using a constant specific thermal power of 47.27 MW/thm. The average power per fuel assembly is 7.56 MW_{th}. The decay heat was obtained from TRITON as a function of decay time after discharging from the core. Table 2 gives the power of one channel as function of decay time.

While Pu/Th is the proposed fuel for PT-SCWR, other fuels can be used as well. Uranium oxide fuel, enriched to 9.1% in the inner ring and 7.28% in outer rings, was found to give the same burnup as Pu/Th (Ibrahim et al., 2021). UOX fuel was modeled in TRITON as well; Its decay heat was calculated as a function of the decay time (Table 2). As only one quarter of the canister is modeled, the heat load per channel of the spent fuel will be a quarter of that in Table 2.

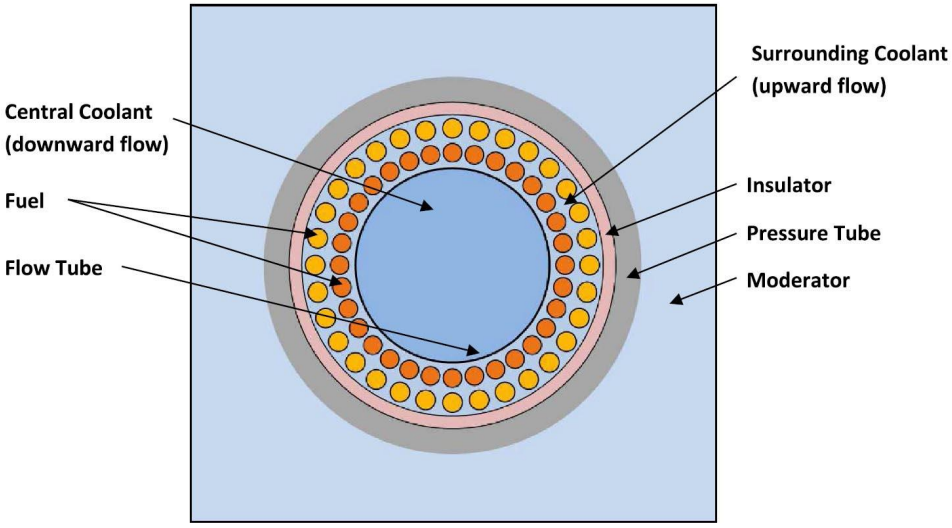

Figure 4. Cross-sectional view of the fuel channel of PT-SCWR.

Table 2. The power of one spent fuel channel in watt as function of time after discharge from the core.

Time after discharge (Years)	Heat load for one fuel channel (W)	
	Pu/Th	UOX
50	573.7	128.7
54	556.5	119.5
60	532.6	107.2
70	497.6	90.1
90	441.6	65.4
120	381.3	43.9
160	332.2	31.1
190	296.1	24.5
240	257.8	19.9
350	203.1	15.4
470	166.2	12.8
620	135.5	10.7
820	107.7	8.6
1000	88.3	7.2
1300	70.7	5.9

2.3 Canister specifications

The canister originally proposed to store the CANDU bundles will not be suitable for storing SNF from PT-SCWR. Instead, a modified version of the canister designed for the SNF of the light water reactors was used in this study (Raiko, 2012). It is a cylinder of nodular graphite cast iron coated with a layer of copper for corrosion resistance. The height of the canister used in this study is 5.323 meter and the radius is 0.525 meter. The channels are stored inside circular compartments in the cast iron with diameter of 17.4 cm. Figure 5 shows a cross-sectional and a top view of the canister holding twelve fuel channels. The materials and dimensions of the cast iron, steel lid, and copper are the same as that given in (Raiko, 2012).

As the outer layer of the canister is covered with copper, which has a high thermal conductivity, a nearly uniform temperature distribution exists on the canister's exterior surface. Accordingly, the canister was considered to be homogenous for thermal analysis.

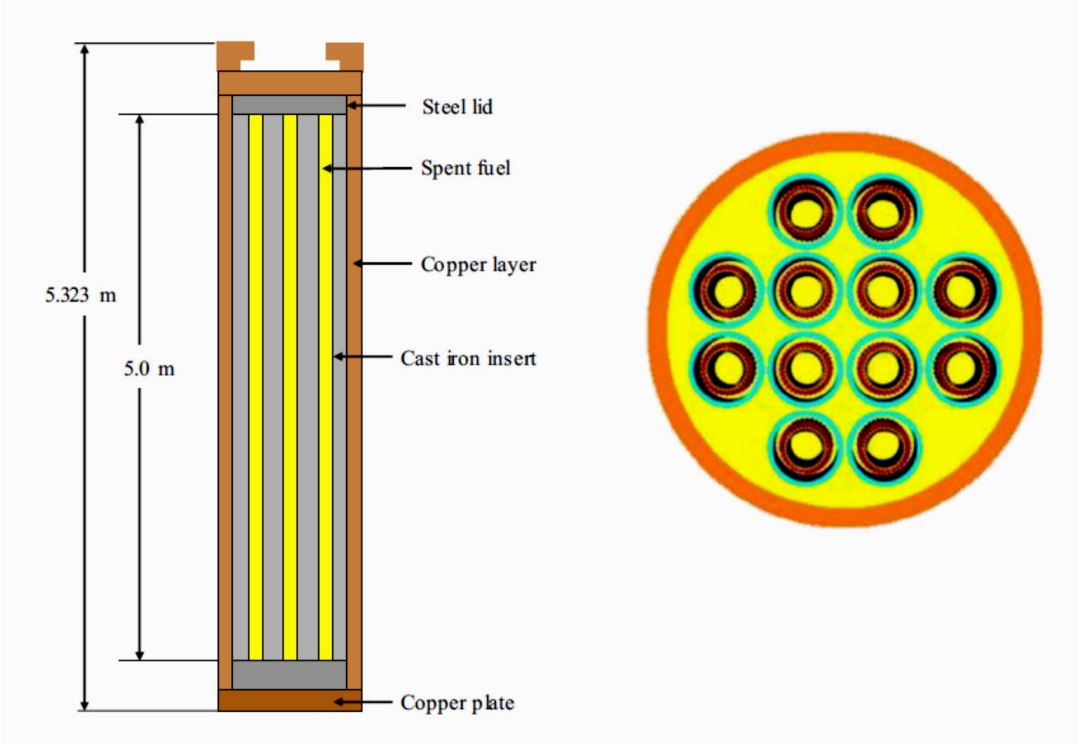

Figure 5. Cross-sectional view (left) and top view (right) of the canister.

2.4 Criticality safety

The criticality safety was studied using the computer code MCNP 6.1. MCNP is a general-purpose, continuous energy Monte-Carlo transport code developed by Los Alamos National Laboratory (Goorley et al., 2013). MCNP can be used for very complex geometries and gives accurate results with few approximations.

The canister was modeled in detail using the data given in (Raiko, 2012) for the structural materials. Fresh fuel was modeled instead of burnt fuel as it is more reactive. Light water is assumed to fill the holes where the channels are placed inside the canister. The canister is surrounded with the bentonite, then rock. The canister spacing was assumed to be six meter in this model. Figure 6 depicts the geometry of the model in MCNP. By running several cases with different canister spacing, no significant effect on the k_{eff} was found for different canister spacings.

The criticality calculation was done using 3,000 cycles with 10,000 histories per cycle. The first 30 cycles were omitted. The cross-section library was based on the ENDF/B-VII.0 evaluated data library. Thermal neutron scattering was considered using the ENDF/B-VII.0-based thermal *S(alpha, beta)* cross section library.

3. Results and discussion

The decay heat per ton of heavy metals for Pu/Th and UOX spent fuels (burnt to 60 GWd/thm in PT-SCWR) was calculated using ORIGEN/SCALE as a function of the cooling time. The results are shown in Figure 7. The decay heat of Pu/Th was always higher than that of UOX. This is due to the higher concentrations of heat-generating nuclei; namely Pu-239, Pu-240, Am-241 and Am-243 in the Pu/Th fuel compared with that in the UOX fuel. Figure 7 also illustrates that the decay heat of Pu/Th decreases slower rate than that of UOX spent fuel.

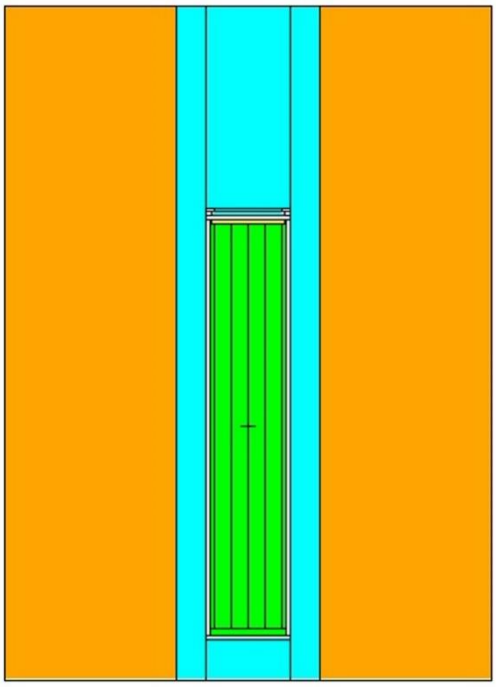

Figure 6. Cross-sectional view of the MCNP model. The canister is surrounded with bentonite and then rock.

To estimate the effect of the different decay rates on the thermal response of the DGR, two CODE_BRIGHT near-field models were constructed. The first one was for a canister having Pu/Th spent fuel, while the other was for a canister having UOX spent fuel. Both canisters had the same initial power of 1545 W. This power corresponds to three and twelve fuel channels of Pu/Th and UOX, respectively. Both fuels were discharged from the PT-SCWR and decayed for 50 years before placement inside the corresponding canister.

Figure 8 illustrates the evolution of the temperature at the canister/bentonite interface with time after deposition. Although both canisters had the same initial power the temperature increased to a higher value for Pu/Th compared to UOX. For UOX fuel, the maximum temperature achieved was 66.5 °C, while for Pu/Th, it was 77.7 °C.

These results show that using the initial power of a canister as a sole parameter to estimate the CS is not a valid procedure. Accordingly, the previously performed thermal analyses for UOX fuel, either for the Finnish repository (Ikonen et al., 2018) or for the CANDU DGR with high-burnup fuel (Freire-Canosa, 2012), cannot be used for the case of Pu/Th.

Therefore, an alternate thermal analysis for Pu/Th fuel was performed in this study. The minimum canister spacing (CS), required for maximum allowable temperature of 90 °C, was estimated, using near-field models.

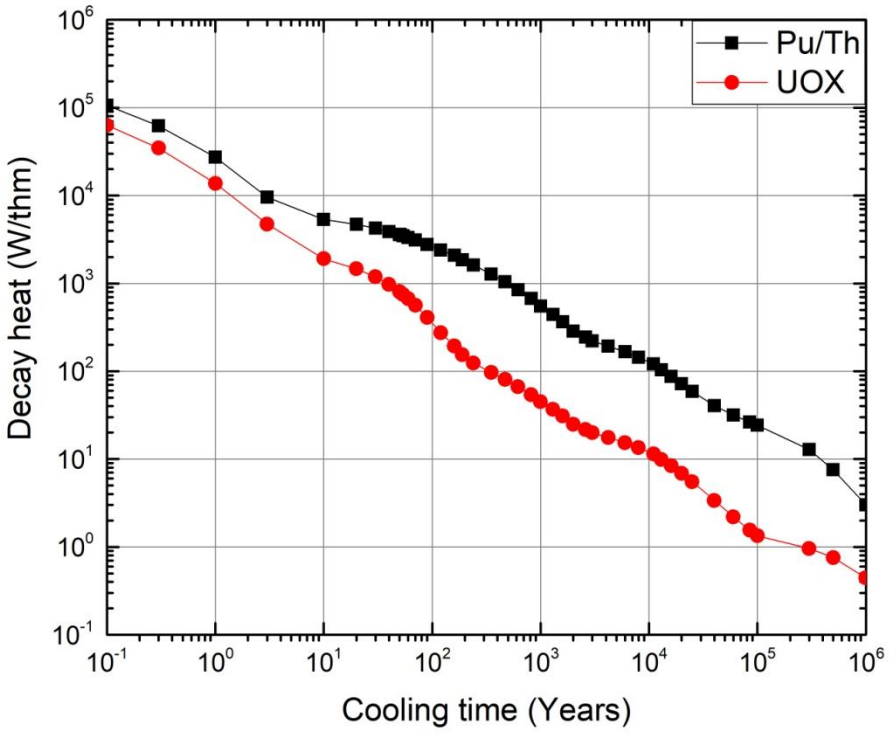

Figure 7. Decay heat per ton of heavy metals, as function of cooling time for Pu/Th and UOX fuel.

3.1 Thermal analysis

The previously proposed designs of the canisters for LWR were used in this study. One of the canister's designs has four channels per canister, while another has twelve. The design with four channels was used for Pu/Th spent fuel, while the one with twelve channels was used for UOX fuel, due to the higher decay heat of Pu/Th spent fuels.

3.1.1. Pu/Th spent fuel

A canister with four channels of Pu/Th spent fuel was modeled as a homogenous heat source in CODE_BRIGHT. The temperature increase of the bentonite pellets, which are in contact with the canister's surface, was calculated for the first 1000 years after deposition. The maximum temperature of the bentonite pellets is given in Table 3 as a function of different CS ranging from eight to 14 meter, for various decay times (initial powers). The tunnel spacing was 40 meter.

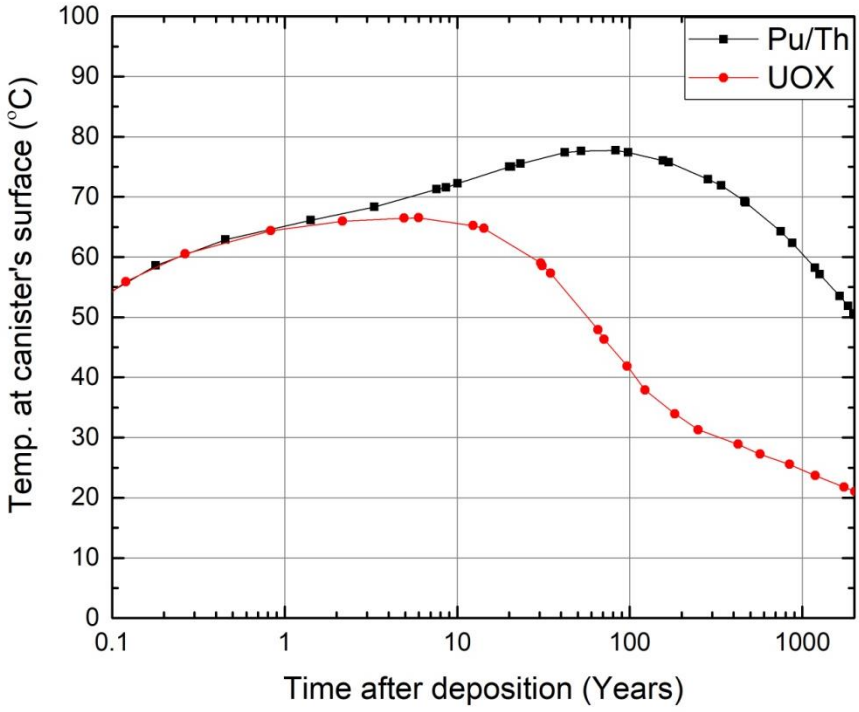

Figure 8. Evolution of the temperature at the canister/bentonite interface for two canisters having the same initial power, one canister with Pu/Th and the other with UOX spent fuel.

Figure 9 shows the variation of the maximum temperature with the canister spacing for some selected initial powers. The curves in Figure 8 can be fitted using a two-term exponential relationship (in the form given by equation (1)).

$$T(x) = a\exp(bx) + c\exp(dx) \quad (1)$$

where x and T are the canister spacing and maximum temperature of the bentonite pellets, respectively, while a, b, c & d are parameters which can be found by fitting the data in Table 3.

Using this relationship, the minimum canister spacing, required to get maximum temperature of 90 °C, was estimated and given in the last column of Table 3 and Figure 10.

A correlation between the initial power of a canister, having four channels, and the minimum canister spacing can be suggested by fitting the data in Figure 10. This correlation is given in equation (2).

The suggested correlation can be used for an initial power less than 2000 W. Using this equation, the minimum canister spacing for a given initial power can be estimated.

$$x_{min} = 3.897 \times \exp(4.77 \times 10^{-4}P) + 7.45 \times 10^{-5}\exp(4.79 \times 10^{-3}P) \quad (2)$$

where x_{min} is the minimum canister spacing in meter, while P is the initial power of the canister in watt.

3.1.2 Size of repository for Pu/Th

The size of the Pu/Th repository was estimated based on the results of section 3.1.1. The CANDU DGR is assumed to store fuel bundles corresponding to an output electricity of 4,930 TWhe (Terawatt-hour). This is the reference value used to estimate the size of the repository for Pu/Th fuel.

Table 3. The maximum temperature of the bentonite pellets as function of CS, and the minimum CS to satisfy the thermal criterion of the repository for different initial powers.

Cooling Time (Years)	Initial Power (W)	Canister spacing (m)							Min. CS (m)
		8	9	10	11	12	13	14	
70	1990	105.9	99.3	94.3	90.4	87.4	84.7	83.0	11.1
80	1870	102.5	95.8	90.6	86.4	83.6	81.1	79.2	10.1
90	1767	99.0	92.4	87.3	83.4	80.1	77.4	75.8	9.4
100	1676	96.4	89.6	84.4	80.3	77.2	74.6	72.7	8.9
110	1596	93.6	87.0	82.0	77.8	74.8	72.1	70.3	8.5
120	1525	91.5	84.8	79.6	75.6	72.6	69.8	68.0	8.2
130	1462	89.5	82.8	77.6	73.6	70.4	68.0	65.8	7.9

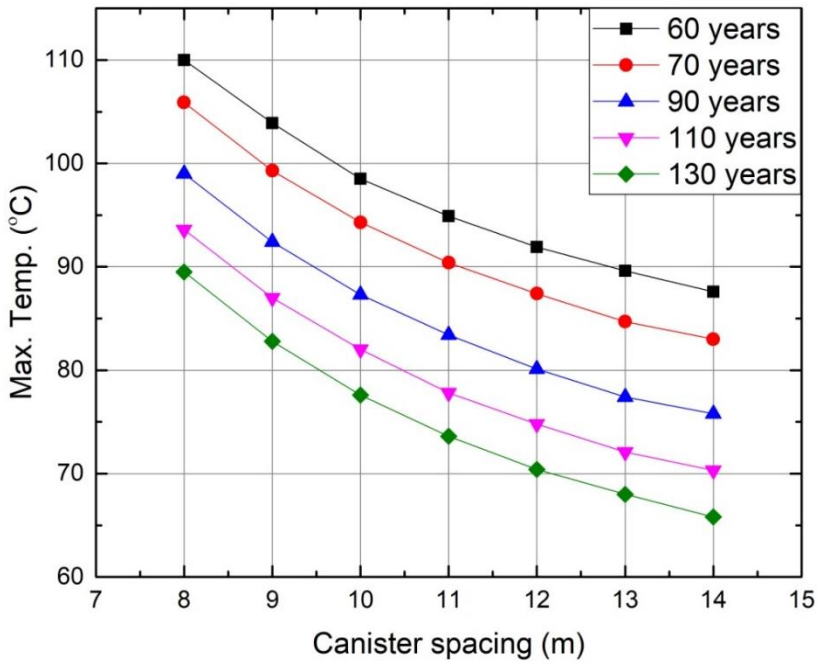

Figure 9. Change of the maximum temperature at the canister/bentonite with CS.

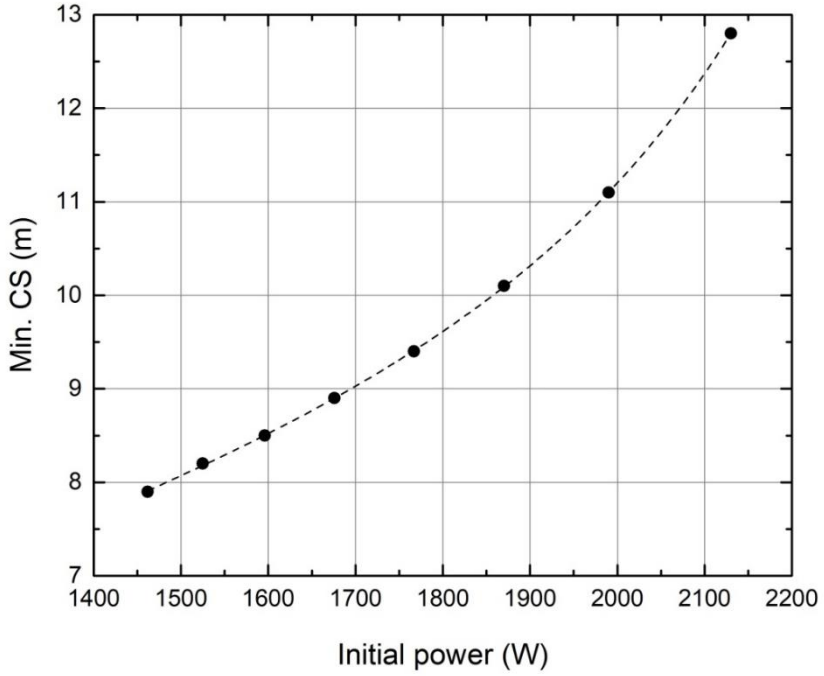

Figure 10. Variation of minimum CS with initial power of a canister having four Pu/Th spent fuel channels. The dotted line is the fitted function given by equation (2).

The burnt fuel was assumed to be 60 GWd/thm, and the PT-SCWR has an efficiency of about 47%. Each channel has a mass of 160 kg of heavy metals. Therefore, 45,327 channels are needed to get the same electric output as the reference CANDU DGR. For a canister with four channels, 11,332 canisters (boreholes) would be needed. Given that 10% of extra boreholes are needed for emergency situations and the number of tunnels is 124, the number of boreholes per tunnel is 101.

Referring to Figure 1, the estimated size of the Pu/Th repository with four channels per canister was calculated and given in Table 4 for the different initial powers.

To give a fair comparison between the effect of the two fuels Pu/Th and UOX, on the size of the repository, a UOX fuel was assumed to be used in PT-SCWR instead of Pu/Th.

To get the same exit burnup, the enrichment of the uranium was 9.1% for the inner ring and 7.28% for the outer ring. The canister used in this case was the one with twelve channels. The cooling time was 40 years (to give a canister's power compared with that of Pu/Th and of that of previously reported results). The canister's power was 1870 W. The minimum canister spacing required to fulfill the maximum allowable temperature of 90 °C was found to be 6.1 meter (last row in Table 4).

As can be seen in Table 4, the size of the repository with Pu/Th would have to be at least three times larger than that with UOX, with longer cooling time. This will certainly increase the cost of the fuel cycle for PT-SCWR.

3.1.3 Different number of channels per canister for Pu/Th

The size of repository for Pu/Th spent fuel was calculated based on four channels per canister. As mentioned in section 3.1.2, the size of the Pu/Th repository would have to be between three to four times larger than UOX repository. To check if using a different number of channels per canister would reduce the repository's required size, two more cases were investigated: three and five channels per canister. The results are presented in this section.

The same methodology used for the four-channels case was followed here as well. The results of the minimum CS and the size of the repository are given in Tables 5 & 6, for three and five channels per canister respectively.

Equations 3 and 4 give the correlations for the minimum CS required as a function of initial power of canister having three and five channels per canister respectively.

$$x_{min} = 3.782 \exp(3.76 \times 10^{-4} P) + 3.1 \times 10^{-4} \exp(4.12 \times 10^{-3} P) \qquad (3)$$

$$x_{min} = 4.209 \exp(5.25 \times 10^{-4} P) + 2.2 \times 10^{-5} \exp(5.34 x 10^{-3} P) \qquad (4)$$

Table 4. Size of the repository needed to store number of channels of Pu/Th equivalent to 4,930 TWhe.

Cooling Time (Years)	Initial Power (W)	Min. CS (m)	DGR size		m^2/TWhe	Ratio of Pu/Th repository's size to that of UOX
			Dim. (m × m)	Area (10^6 m^2)		
70	1990	11.1	1564 × 4924	7.70	1562.1	3.8
80	1870	10.1	1564 × 4533	7.09	1438.1	3.5
90	1767	9.4	1564 × 4261	6.66	1351.8	3.3
100	1676	8.9	1564 × 4064	6.36	1289.2	3.1
110	1596	8.5	1564 × 3894	6.09	1235.4	3.0
120	1525	8.2	1564 × 3770	5.90	1196.1	2.9
130	1462	7.9	1564 × 3659	5.72	1160.7	2.8
UOX 40 years	1870	6.1	1564 × 1295	2.03	410.8	1.0

The effect of using different number of channels per canister can be seen by comparing the area per TWhe for all cases at the same initial power. The results are given in Table 7. Data in Table 7 were calculated using the correlations given by equations (2 – 4).

Table 7 shows that, for the same initial power, a larger CS would be needed if the number of channels per canister is increased. This can be explained by Figure 11, which shows the decay of the canister's power as a function of time after deposition. Even if the initial power was the same, increasing the number of channels will increase the canister's power at the same time after deposition. This shows that a larger CS would be needed, for the same initial power, when the number of channels per canister is increased.

Table 5. Minimum CS required for maximum allowable temperature of 90 °C, size of the repository for the case of *three channels* of Pu/Th per canister.

Decay Time	Initial Power (W)	Min. CS (meter)	DGR size		m^2/TWhe	Ratio of Pu/Th repository's size to that of UOX
			Dims. (m × m)	Area (10^6 m^2)		
40	1867	8.3	1564 × 4920	7.7	1560.7	3.8
50	1721	7.6	1564 × 4531	7.09	1437.5	3.5
60	1598	7.1	1564 × 4283	6.70	1358.8	3.3
70	1493	6.8	1564 × 4117	6.44	1306.0	3.2
80	1403	6.5	1564 × 3958	6.19	1255.7	3.1
90	1325	6.3	1564 × 3833	6.00	1216.0	3.0

Although a larger CS would be needed for the same initial power, the overall size of the repository would be reduced by increasing the number of channels. A smaller number of boreholes per tunnel would be needed, and thus shorter tunnels and a smaller area would be required for the repository. However, increasing the number of channels will require a longer cooling time. For example, a canister with 2000 W will need to be cooled for 32, 69 or 110 years if three, four or five channels are to be used respectively.

In conclusion, even with five channels per canister and a cooling time of 110 years, the size of the repository will be 3.6 times larger than that for UOX. Decreasing the number of channels will decrease the cooling time but increase the size of the repository

Table 6. Minimum CS required for maximum allowable temperature of 90 °C, size of the repository for the case of *five channels* of Pu/Th per canister

Decay Time	Initial Power (W)	Min. CS (m)	DGR size		m^2/TWhe	Ratio of Pu/Th repository's size to that of UOX
			Dims. (m × m)	Area (10^6 m^2)		
110	1995	12.9	1564 × 4611	7.21	1462.7	3.6
120	1907	12.0	1564 × 4322	6.76	1371.0	3.3
130	1828	11.4	1564 × 4118	6.44	1306.5	3.2
140	1756	10.9	1564 × 3950	6.18	1253.1	3.1
150	1691	10.4	1564 × 3810	5.96	1208.7	2.9

Table 7. Comparison of the minimum CS and repository area for different numbers of Pu/Th channels per canister as a function of the initial power.

Initial power (w)	Cooling time (years)			Min. CS (m)			m^2/TWhe (ratio to size of UOX repository)		
	3	4	5	3	4	5	3	4	5
2000	32	69	110	10.2	11.2	12.9	1876.4 (4.6)	1573.4 (3.8)	1463.0 (3.6)
1900	38	77	121	8.6	10.3	12.0	1611.4 (3.9)	1462.5 (3.6)	1367.3 (3.3)
1800	44	87	134	7.9	9.6	11.2	1496.6 (3.6)	1373.8 (3.3)	1285.3 (3.1)
1700	52	97	149	7.5	9.0	10.5	1422.3 (3.5)	1299.8 (3.2)	1214.5 (3.0)
1600	60	110	166	7.1	8.5	9.9	1363.2 (3.3)	1235.8 (3.0)	1152.6 (2.8)
1500	69	124	186	6.8	8.1	9.3	1307.5 (3.2)	1178.9 (2.9)	1098.0 (2.7)

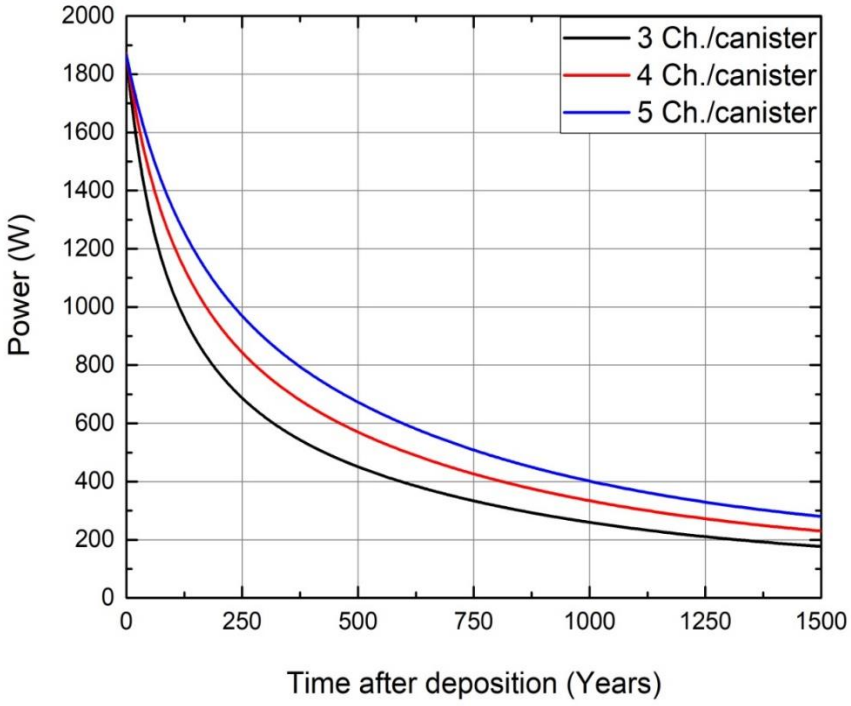

Figure 11. Decay of the power of three canisters that have the same initial power with time after deposition.

3.2 Criticality safety

In normal situations the spent fuel channels will be stored inside the disposal canister under dry conditions. Argon should fill the compartments where the channels are located. The canister is surrounded with bentonite and rock as explained before. For criticality calculations, the most reactive situations are used.

In this work, to represent an accident situation, it was assumed that water leaked inside the canister. The k_{eff} was calculated using MCNP 6.1 for Pu/Th and for UOX fuels. Both fuels were modeled as fresh fuel. Also, both fuels were assumed to be disposed into twelve-channel canister. It is not foreseen that twelve channels of Pu/Th will be stored together, as indicated before, but this will give a conservative result. Reflective boundary conditions were applied at the outer edge of the rock to take the effect of all other canisters into account.

Under these conditions, k_{eff} was found to be 0.84327 ± $1.3\times10^{-4}$and 0.85811 ± 1.3×10^{-4} for Pu/Th and UOX fuel, respectively.

The case where reflective boundary conditions were applied at the outer surface of the canister was studied as well. This is not realistic but can represent a highly reactive situation. in this case k_{eff} was 0.87477 ± 1.3×10^{-4}, and 0.88987 ± 1.3×10^{-4} for Pu/Th and UOX respectively.

These effective multiplication factors are less than the limit of 0.95 for all cases, even without crediting burnup. It was found before that the burnup credit must be applied for UOX fuel in BWR and PWR/EPR in order to fulfill the criteria of criticality safety (Anttila, 2005; SKB, 2010). For PT-SCWR, this is not the case, mainly because it uses heavy water as a moderator. In conclusion, neither Pu/Th nor UOX spent fuel from PT-SCWR would pose any hazard concerning criticality accidents.

4. Conclusion

The objective of this work is to give a quantitative estimate of the size of Canadian conceptual design of Deep Geological Repository when Pu/Th spent fuel is stored.

The maximum temperature of the bentonite in contact with the canister surface was estimated using the computer code CODE_BRIGHT. The minimum canister spacing required to fulfill the thermal criterion for the design of DGR (maximum temperature of the bentonite should be less than 90 °C with 10 °C as safety margin), was calculated. The size of the whole repository was estimated based on the minimum canister spacing. For comparison, the size of the repository if uranium-oxide fuel were used in PT-SCWR instead of Pu/Th was calculated as well. The investigated cases involved different cooling times, between 60 – 150 years after discharge from the reactor, and different numbers of channels per canister, three, four and five channels per canister.

It was found that switching to Pu/Th fuel will increase the size of the repository between three to four times compared with uranium oxide fuel. For the same initial power of the canister but using more channels per canister a larger canister spacing will be

required, but the overall size of the repository will be reduced. Using four or five channels per canister would reduce the size of the repository by 9 % or 16 % compared with using three channels per canister. This will, however, require longer cooling times. For five channels per canister and a cooling time of 110 years, the size of the repository will be 3.6 times larger than that for uranium fuel.

For the same cooling time, using fewer channels per canister would decrease the size of the repository (due to the reduced initial power of the canister), but the reduction in size of the repository will require increased cost for the extra canisters needed and extra excavation costs (134 and 101 boreholes are needed for three and four channels per canister respectively).

The criticality safety for the storage of Pu/Th in the repository was evaluated using MCNP, assuming fresh fuel and water-filled canisters. The effective neutron multiplication factor was found to be $0.84327 \pm 1.3\times10^{-4}$ and $0.85811 \pm 1.3\times10^{-4}$ for Pu/Th and UOX fuel respectively, which are both less than the criticality safety limit of 0.95, without taking any fuel burnup credit.

5. Acknowledgments

The authors would like to thank Dr. Shinya Nagasaki, for his valuable comments and suggestions. This work was partly funded by the University Network of Excellence in Nuclear Engineering (UNENE), Canada, and by the Natural Sciences and Engineering Research Council of Canada (NSERC), under grant no. RGPIN-2020-06897.

6. References

Ade, B., Worrall, A., Powers, J., Bowman, S., Flanagan, G., Gehin, J., 2014. Safety and regulatory issues of the thorium fuel cycle. (No. ORNL/TM-2013/543; NUREG/CR-7176). Oak Ridge National Lab.(ORNL), Oak Ridge, TN (United States).

Anttila, M., 2005. Criticality Safety Calculations for Three Types of Final Disposal Canisters. POSIVA working report 2005-13.

Baumgartner, P., Tran, T. V, Burgher, R., 1994. Sensitivity analyses for the thermal response of a nuclear fuel waste disposal vault. Atomic Energy of Canada Limited. Technical Report, TR-621, COG-94-258.

CNSC, 2020. Nuclear Criticality Safety. Canadian Nuclear Safety Commission. Regulatory document REGDOC-2.4.3, Version 1.1.

Freire-Canosa, J., 2012. Implications of Placing High Burnup Used Fuel in a Deep Geological Repository. Nuclear Waste Management Organization, NWMO TR-2012-15.

GIF, 2002. A Technology Roadmap for Generation IV Nuclear Energy Systems. Generation IV International Forum. GIF-002-00. Available at: https://www.gen-4.org/gif/jcms/c_9352/technologyroadmap

Goorley, J.T., James, M.R., Booth, T.E., Brown, F.B., Bull, J.S., Cox, L.J., Durkee Jr, J.W., Elson, J.S., Fensin, M.L., Forster III, R.A. and Hendricks, J.S., 2013. Initial MCNP6 release overview-MCNP6 version 1.0 (No. LA-UR-13-22934). Los Alamos National Lab. (LANL), Los Alamos, NM (United States). https://doi.org/10.2172/1086758.

Guo, R., 2007. Numerical Modeling of a Deep Geological Repository Using the In-Floor Borehole Placement Method. Nuclear Waste Management Organization, NWMO TR-2007-14.

Guo, R., 2008. Sensitivity Analyses to Investigate the Influence of the Container Spacing and Tunnel Spacing on the Thermal Response in a Deep Geological Repository. Nuclear Waste Management Organization, NWMO TR-2008-24.

Guo, R., 2017. Thermal response of a Canadian conceptual deep geological repository in crystalline rock and a method to correct the influence of the near-field adiabatic boundary condition. Eng. Geol. 218, 50–62. https://doi.org/10.1016/j.enggeo.2016.12.014

Hökmark, H., Claesson, J., 2005. Use of an analytical solution for calculating temperatures in repository host rock. Eng. Geol. 81, 353–364. https://doi.org/10.1016/j.enggeo.2005.06.016

Hökmark H., Lönnqvist M., Kristensson O., 2009. Strategy for thermal dimensioning of the final repository for spent nuclear fuel. SKB Report R-09-04, Svensk Kärnbränslehantering AB

Hummel, D.W., 2015. Transient neutronic-thermalhydraulic coupling in a PT-SCWR, PhD Thesis, 295.

Ibrahim R., Buijs, A., Luxat, J. 2019. Assessment of the Long-Term Storage of PT-SCWR Fuel Bundles in CANDU Deep Geological Repository. 39th Annual Conference of the Canadian Nuclear Society and 43rd Annual CNS/CNA Student Conference.

Ibrahim R., Buijs, A., Luxat, J. 2021. Assessment of the occupational dose rate and radiotoxicity of various fuel cycles used in the super-critical water reactors and the impact on deep geological repository performance. Submitted to Progress in Nuclear Energy

Ikonen, K., Kuutti, J., Raiko, H., 2018. Thermal Dimensioning for the Olkiluoto Repository 2018 update. POSIVA working report 2018-26.

Insulander Björk, K., 2013. A BWR fuel assembly design for efficient use of plutonium in thorium-plutonium fuel. Prog. Nucl. Energy 65, 56–63. https://doi.org/10.1016/j.pnucene.2013.01.010.

Lee, J., Cho, D., Choi, H., Choi, J., 2007. Concept of a Korean reference disposal system for spent fuels. J. Nucl. Sci. Technol. 44, 1565–1573. https://doi.org/10.1080/18811248.2007.9711407

Li, J., Yim, M.S., McNelis, D., 2011. A simplified methodology for nuclear waste repository thermal analysis. Ann. Nucl. Energy 38, 243–253. https://doi.org/10.1016/j.anucene.2010.11.002

Nakahara, Y., Suyama, K., Inagawa, J., Nagaishi, R., Kurosawa, S., Kohno, N., Onuki, M., Mochizuki, H., 2002. Nuclide Composition Benchmark Data Set for Verifying Burnup Codes on Spent Light Water Reactor Fuels. Nucl. Technol. 137, 111–126. https://doi.org/10.13182/NT02-2

Olivia, S., Vaunat, J., Rodriguez-Dono, A., 2021. Code_Bright 2021 User's Guide. Available to download at https://deca.upc.edu/en/projects/code_bright.

Pencer, J., Colton, A., 2013. Progression of the lattice physics concept for the Canadian supercritical water reactor. Proceedings of the 34th Annual Conference of the Canadian Nuclear Society. Toronto, Ontario (Canada).

Sizgek, G.D., 2005. Three-dimensional thermal analysis of in-floor type nuclear waste repository for a ceramic waste form. Nucl. Eng. Des. 235, 101–109. https://doi.org/10.1016/j.nucengdes.2004.09.010

SKB, 2006a. Long-term safety for KBS-3 repositories at Forsmark and Laxemar – a first evaluation: Main Report of the SR-Can project. Tech. Rep. TR-06-09.

SKB, 2006b. Buffer and backfill process report for the safety assessment SR-Can. Tech. Rep. TR-06-18.

SKB, 2012. Criticality safety calculations of disposal canisters. Document ID 1193244.

SNC-Lavalin, 2011. APM Conceptual Design and Cost Estimate Update Deep Geological Repository Design Report Crystalline Rock Environment Copper Used Fuel Container. SLN report No. 020606-6100-REPT-0001.

Trellue, H.R., Bathke, C.G., Sadasivan, P., 2011. Neutronics and material attractiveness for PWR thorium systems using monte carlo techniques. Prog. Nucl. Energy 53, 698–707. https://doi.org/10.1016/j.pnucene.2011.04.007.

Zhou, X. Yun, Sun, D., Tan, Y., Zhou, A., 2020. Canister spacing in high-level radioactive nuclear waste repository. Ann. Nucl. Energy 141. https://doi.org/10.1016/j.anucene.2020.107335

Zhou, X., Sun, D., Tan, Y., Zhou, A., 2020. Canister spacing in high-level radioactive nuclear waste repository. Ann. Nucl. Energy 141, 107335. https://doi.org/10.1016/j.anucene.2020.107335.

Chapter 5 Assessment of the Occupational Dose Rate During Fuel Handling and Storage of Various Fuel Cycles Used in the Super-Critical Water Reactor and the Impact on Deep Geological Repository Performance

Citation:

Remon Ibrahim, A. Buijs, J. Luxat, 2022. “Assessment of the occupational dose rate during fuel handling and storage of various fuel cycles used in the super-critical water reactor and the impact on deep geological repository performance”, Prog. Nucl. Energy 147, 104178.

https://doi.org/https://doi.org/10.1016/j.pnucene.2022.104178

In addition to the decay heat described in the previous chapter, the total occupational doses associated with the whole life cycle was proposed before as a comparative metric between different fuels.

Ault et al. [69] reported the collective doses for the whole life cycle of each fuel cycle. But they did not report the occupational doses resulting from the fuel handling and storage into DGR.

The key feature of this study was to estimate the occupational dose rate to the workers in the surface facility of the Canadian DGR, for different types of fuel proposed for PT-SCWR.

The results of this article can be used to estimate the total occupational doses associated with the management of spent fuel, which is part of the total occupational doses received during the life cycle of the nuclear fuel. In addition to that, the dose rate to the public was estimated after-closure of the DGR.

It was found that using Pu/Th and U/Th would increase the occupational doses to the workers by 8% and 5% comparing with uranium oxide fuel respectively. To get the same dose rate as LEU, about 13% and 10% thicker shielding would be needed for Pu/Th and U/Th respectively.

The peak dose rate to the public, in case of a failure of canisters, was found to be 75% higher in the Pu/Th case than in UOX. Using Pu/Th will not cause the public's peak dose rate to exceed the recommended limit of 0.3mSv/a, but it must be justified according to the ALARA principle.

Assessment of the occupational dose rate during fuel handling and storage of various fuel cycles used in the super-critical water reactor and the impact on deep geological repository performance

Remon Ibrahim [a,b], A. Buijs [a] , J. Luxat [a]

[a] McMaster University, 1280 Main Street West, Hamilton, ON, L8S 4L7, Canada

[b] Nuclear and Radiological Regulatory Authority, N. City, Cairo, Egypt

Abstract

The Canadian concept of the Pressure-Tube Super-Critical Water-Reactor (PT-SCWR) uses Pu/Th in a once-through fuel cycle. The implication of using Pu/Th in a PT-SCWR on the safety of the workers in the Deep Geological Repository (DGR) facilities as well as on the public after the closure of the DGR was investigated.

A comparison between the Pu/Th and other fuel cycles, namely, U/Th (two U/Th fuels with different enrichments and different UO_2/ThO_2 ratios), and the regular UO_2 was also made. The enrichment of U-235 in U/Th and UO_2 was adjusted to give the same exit burnup of the proposed Pu/Th fuel, namely 60 GWd per ton of heavy metals (THM).

The dose rate as a function of distance from the surface of a canister holding different types of spent fuel, and the thickness of the shielding required to reduce this dose rate to 10 μSv/h were estimated.

The dose rate after 50 years of decay for Pu/Th fuel channel is higher than that of uranium by about 8%. This will increase the dose to the workers in DGR facilities unless more shielding is used. Pu/Th will need 13% more thickness of concrete compared to UO_2. Using U/Th fuel will also increase the dose received by workers, compared with uranium-only fuel, but less than using Pu/Th. The neutron dose rate of the Pu/Th fuel is the highest dose rate from all fuels studied.

Pu/Th spent fuel will cause the highest dose to the public in case of an accident of the DGR after closure as it will produce the largest amount of I-129 per THM. Although the exact dose received by the critical group is not expected to exceed the dose limit for DGR, it is higher than alternative fuels.

Keywords: PT-SCWR, fuel cycle, uranium, plutonium, thorium, dose rate, radiotoxicity, post-closure safety

1. Introduction

The long-term management of nuclear spent fuel is a major challenge in the nuclear industry. The current approach is to store the spent nuclear fuels (SNF) in an on-site interim storage facility till the final disposal. Canadian's plan for the long-term management of SNF is known as Adaptive Phased Management (APM). According to this plan, the SNF, after being packaged into a suitable canister, will be placed into a deep geological repository (DGR) hosted in a suitable rock formation for final disposal, with the ability to retrieve the spent nuclear fuel, if needed (NWMO, 2005).

The conceptual design of the Canadian DGR consists of two main facilities. The first is the underground repository which is excavated at a depth of about 500 meter in certain rock formations like crystalline or sedimentary rocks. The underground repository consists of a network of tunnels where the containers holding the SNF will be placed either vertically, in holes drilled vertically, or horizontally. The second is the surface facility where the SNF is packaged into the canisters and stored for the final underground disposal (Noronha, 2016).

The dose received by the workers in the surface facility was estimated for the Canadian DGR (NWMO, 2014). It was found that the highest doses will be received by the workers who are involved with reception of the SNF.

On the other hand, the main safety indicator for the DGR is the effective dose rate to a group of humans (know as critical group) who are assumed to receive the highest dose from the repository (ICRP, 2013). The dose rates to the critical group were studied for the Canadian DGR; The doses are not expected to exceed the dose constraint of 0.3 mSv/a (NWMO 2017, 2018).

All the dose estimations were based on the assumption that all the disposed spent fuels are fuel bundles from CANDU reactors, which consist of natural uranium dioxide.

Canada is developing the Super-Critical-Water-Reactor (SCWR), one of the Generation-IV (GEN-IV) concepts (GIF, 2002). The Canadian design, known as Pressure Tube SCWR (PT-SCWR), is a heavy-water moderated, light-water cooled reactor. It consists of 336 pressure tubes which hold the 64-element, five-meter-long fuel bundle. The fuel is a mix of reactor-grade plutonium and thorium (Pencer and Colton, 2013).

The PT-SCWR is a once-though concept, so the spent fuel will be eventually disposed in the DGR. The impact of disposing the high-burnup Pu/Th fuel from PT-SCWR on the operational safety and public safety was assessed in this study.

The occupational hazards to the workers are assessed by modelling the gamma and neutrons dose rates around spent fuel channels and around canisters which are loaded with the SNF. The shielding thickness required to reduce the radiation doses to acceptable levels were calculated as well.

A preliminary post-closure safety assessment was done by estimating the dose rate received by the critical group in case the engineered-safety barriers are breached, and contaminated water reaches the biosphere.

In addition to Pu/Th, other fuel types can be used in PT-SCWR; thorium mixed with low enriched uranium (LEU/Th) and low enriched uranium-oxide (UOX). The occupational and public hazards associated with handling and storing of these fuels were assessed in this study as well, and a comparative assessment with Pu/Th was presented.

Occupational dose is one of the metrics used for comparing the performance of different fuel cycles as suggested by (Ault et al., 2017). As the occupational doses associated with the back end of the spent fuel are part of the total occupational doses for the fuel's life cycle, the results of this study can help to estimate the total collective occupational doses associated with different fuel cycles, and therefore, can help the decision makers in choosing the optimal fuel cycle for the Gen-IV PT-SCWR.

The occupational dose is not the only metric for comparison between different fuels; other metrics, like volume of low-level waste, decay heat, radiotoxicity, fuel cost and resource stewardship can also be used for comparison (Ashley et al., 2014; Croff and Krahn, 2016). Only the occupational doses were considered here; comparison based on other metrics would be part of a future study.

2. Material and Methods

2.1 Fuel channel design of the PT-SCWR

The core of the PT-SCWR consists of 336 pressure tubes surrounded by low-pressure, heavy water moderator (Leung et al., 2011). Fig. 1 shows a 2-D representation of the lattice cell of the PT-SCWR concept. The coolant is a high-pressure light water that operates above the thermodynamic critical point of water (374°C, 22.1 MPa). It enters the fuel channel from the top through the central flow tube, then goes downwards till the bottom of the channel, where its direction is reversed and it flows upwards through the fuel elements (Yetisir et al., 2013). The active length of the fuel channel is five meters while the lattice pitch is 25 cm.

The fuel elements are arranged into two concentric rings with 32 fuel elements each. The fuel is a mixture of PuO_2 and ThO_2. The ratio of PuO_2 to ThO_2 is 15% in the inner ring and 12% in the outer ring. This difference in ratios will help to flatten the radial power distribution across the fuel element. The plutonium is assumed to be produced by recycling of LWR's spent fuel. The isotopic vector of Pu is Pu-238: 2.75%; Pu-239: 51.96%; Pu-240: 22.96%; Pu-241: 15.23%; Pu-242: 7.1%.

As the coolant is in the supercritical conditions, the density of the outer coolant varies drastically between the bottom and top of the channel. This axial variation is not considered in this study. Instead, the thermal conditions at the middle of the channel were used to represent the whole channel. This will give conservative results as the neutron flux and burnup are the highest at the mid-height of the channel.

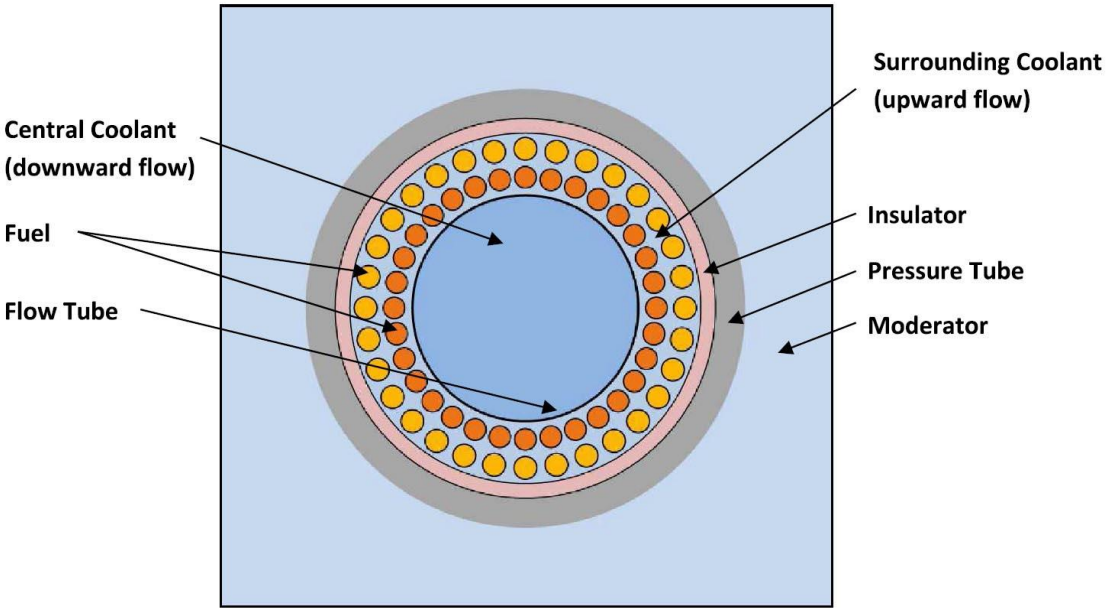

Fig 1. Cross-sectional view of the fuel channel of PT-SCWR

The PT-SCWR is assumed to be a three-batch-fueled reactor, so one-third of the core will be disposed as high-level waste at each refueling. In this study the disposed spent fuel consists of the burnt fuel elements, the activated cladding and the central flow tube.

Table 1. The weight percentages and enrichments of the investigated fuel cycles.

Fuel Cycle	UO_2/ThO_2		U-235 enrichment	
	Inner rings	Outer rings	Inner rings	Outer rings
U/Th-48%	48%	38.4%	19.75%	19.75%
U/Th-75%	75%	60%	12.4%	12.4%
UOX	100%	100%	9.1%	7.28%

The dimensions and material compositions of the lattice cell, shown in Fig. 1, are given in (Pencer and Colton, 2013). In addition to the nominal fuel of Pu/Th, three other fuel types were investigated. The exit burnup and radial power distributions of the investigated fuels were made the same as those of the nominal Pu/Th fuel. The target exit burnup of LEU/Th fuel can be achieved using different combinations of thorium mass and uranium enrichment. To investigate the effect of increasing the mass of thorium (which must be accompanied with increasing the enrichment of uranium to achieve the target exit burnup) on the occupational dose, two different LEU/Th fuels were investigated as shown in Table 1. Also, increasing the amount of thorium can be desirable in case that recycling of the spent fuel, to extract U-233, is needed. Uranium-oxide fuel (UOX) was also investigated as a reference for comparison between different fuels.

2.2 Source-Term Calculations

To estimate the dose rates, the gamma and neutron source terms of the spent fuel have to be calculated first. These source terms were obtained using the SCALE 6.2.3 package (Rearden and Jessee, 2018).

The SCALE code, which is developed by Oak Ridge National Laboratory (ORNL), is a verified and validated code which has been used extensively for criticality safety, lattice physics and source-term calculations. It consists of several modules. Each module performs a certain function like cross-section processing, transport calculations, depletion decay and sensitivity/uncertainty calculation. In this study, two modules were used: TRITON and ORIGEN.

The geometry of the PT-SCWR unit cell was modeled in TRITON which depleted the fuel elements using a constant power of 47.27 MW. The discharge burnup is assumed to be 60 Giga-watt-day per ton of heavy metals (GWd/THM) as obtained from full-core modeling of PT-SCWR (Hummel, 2015).

The first step in the depletion calculations is the preparation of a multi-group, problem-dependent, cross-section library which accounts for the self-shielding effects. TRITON has some reference unit-cell types which are used to account for the self-shielding effects. As the geometry of PT-SCWR fuel cell is not one of these default unit cells, a Dancoff Factor (DF) must be calculated first to be used in the preparation of the self-shielded library (Jessee and DeHart, 2018).

This was done using the MCDANCOFF module within SCALE 6.2.3. The DF associated with each pin was calculated. For the fuel pins inside the same ring, the DFs were found to be quite comparable, therefore, the average DFs for the inner and outer rings were used: They were 0.4395 and 0.3854 respectively, with standard division of 1.88×10^{-3} and 2.06×10^{-3} respectively.

As the fuel lattice of PT-SCWR, as shown in Fig. 1, has one-eighth symmetry, only one-eighth of the lattice was modeled in TRITON. A 238 energy-group library based on ENDF/B-VII was used in this study. Reflective boundary conditions were used for all boundaries. Fig. 2 shows the simulated fuel cell with the applied meshing.

At the end of the depletion calculation, the composition of the burnt fuels, and the gamma and neutron data were stored in a binary file which was used as an input to the ORIGEN module.

ORIGEN was used to follow the change in the isotopic compositions and the source terms with time after the discharge from the reactor. The decay period was taken to be two million years.

The gamma and neutron spectra were obtained using 21 and 47 energy groups, which have the BUGLE (White et al., 1996) structure for energy groups, respectively. The neutron source, as obtained from TRITON/ORIGEN, includes the neutrons resulted from spontaneous fission and from the interaction of alpha particles with light nuclei. The time of disposal to the DGR was assumed to be 50 years after reactor discharge.

2.3 Canisters

Before the underground disposal, the spent fuel is stored in cylindrical containers (canisters) which act as a barrier against the transport of the radionuclides to the biosphere.

Several disposal canisters have been proposed before (Noronha, 2016; Raiko, 2005) depending on the geometry of the fuel assemblies. The canisters proposed for the disposal of Finnish spent LWR fuels were used in this study. The Finnish design of the canisters has three versions. Two versions can hold 12 assemblies of BWR and VVER 440 fuel while the third one holds four assemblies of EPR fuel. (Raiko, 2005). All versions consist of a nodular graphite cast iron insert, where the fuel assemblies are stored in holes. The surface of the cast iron is covered by a five cm layer of copper for corrosion resistance.

Regarding the PT-SCWR fuel assembly, it was found that four assemblies can be disposed in the same canister for Pu/Th fuel, while 12 assemblies can be disposed together for uranium-based fuel (Ibrahim et al., 2019). This is due to the higher decay heat of Pu/Th compared with that of uranium-based fuels and the thermal constraint for the maximum temperature at the surface of the canister which should not exceed 100 °C.

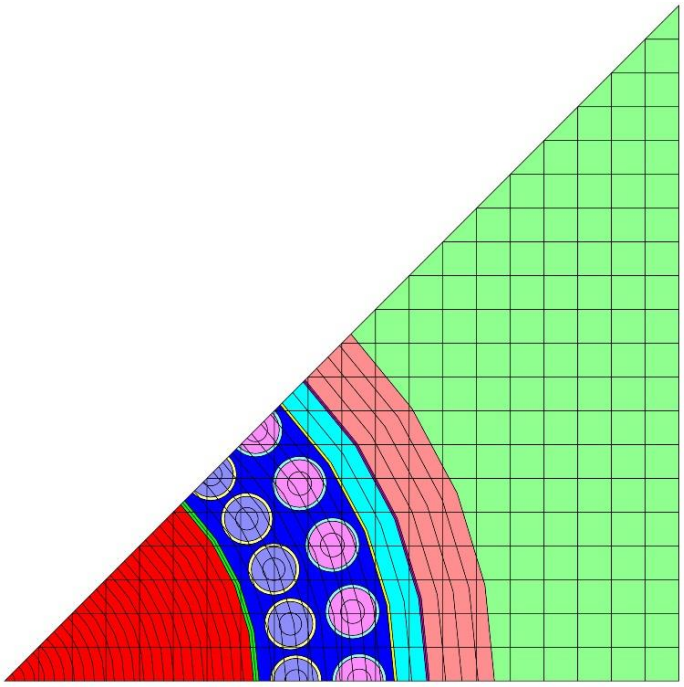

Fig 2. One-eighth of a PT-SCWR unit cell with meshing.

The Finnish canisters, which were designed for VVER 440 fuel assemblies, were modified to store the uranium-based fuels in this study. The modification is only in the height of the canister which was extended to be able to hold the five-meter-long fuel assembly of PT-SCWR (compared with 3.127 meter of VVER 440).

The Finnish EPR canisters were modified to store the Pu/Th fuels for this study. In the original design, the holes, inside which the fuel assemblies are stored, are rectangular with side length equal to 23.5 cm. In the modified version, the holes are circles with a diameter of 17.4 cm. All other design features and the compositions of the used materials are the same as mentioned in (Raiko, 2005). Fig. 3 depicts cross-sectional views of the disposed fuel channel, the Pu/Th canister (four assemblies per canister) and the uranium-based canister (12 assemblies per canister).

2.4 Dose rate calculations

The radiation dose rate and the thickness of shielding required to reduce the dose rate to acceptable levels were estimated using MCNP6.1 (Goorley et al., 2013).

MCNP is a continuous-energy Monte-Carlo radiation transport code developed by Los Alamos National Laboratory. It is a very flexible computational tool as it can transport different types of particles through any complex geometry. Also, MCNP has various types of tallies and various variance reduction techniques.

In this study, 3-D models of an individual spent fuel channel and of a canister holding different numbers of spent fuel channels were constructed in MCNP. The continuous-energy, ENDF/B-VII.0 cross-section library was used for neutron transport, while the continuous-energy, photoatomic library based on ENDF/B-VI.8 was used for photon transport.

The exact compositions of burnt fuel and the gamma and neutron energy spectra, as obtained from ORIGEN/SCALE, were used in the MCNP input file. The axial power distribution at End-of-Cycle (EOC) is nearly flat along the fuel channel but not around the top and bottom of the channel (Hummel, 2015).

The axial distributions of the gamma and neutron sources were modeled in MCNP in a way which represents the power axial distribution at EOC.

The gamma and neutron fluxes at the mid-height of the channel/canister were tallied using the F2 surface flux tally. These fluxes were converted to effective dose rates using the flux-to-dose conversion factors as given by ICRP 74 (ICRP, 1996). The number of particles used in the simulation was 10^9 particles in order to get an error less than 0.1% in the tallies.

Various reduction techniques were used in the calculation of the dose rates around canisters and behind the shielding to reduce the relative error and accelerate the convergence process. The ADVANTG-3.2 code (Mosher et al., 2015), developed at Oak Ridge National Laboratory, was used to automate the generation of variance reduction parameters.

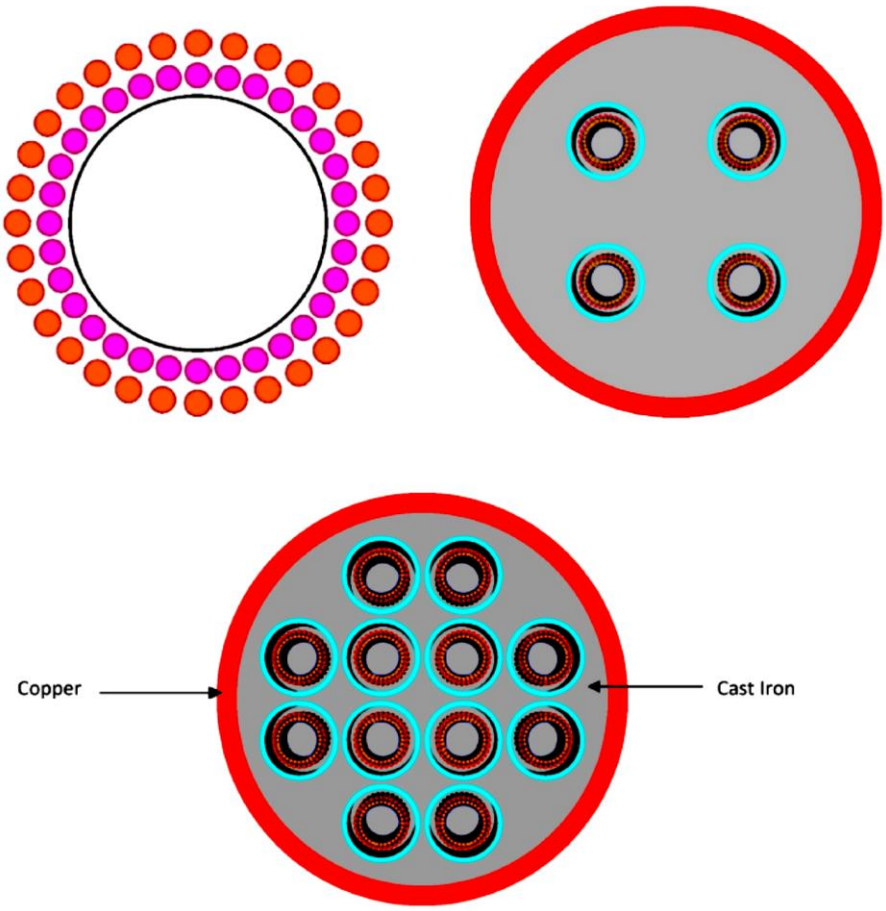

Fig 3. Cross-section view of the disposed fuel channel, and of canisters holding Pu/Th and U-based spent fuels.

ADVANTG implements two methods for automatic generation of variance reduction parameters, the Consistent Adjoint Driven Importance Sampling (CADIS) method and the Forward-Weighted CADIS (FW-CADIS) method. The CADIS, which was developed for accelerating individual tallies, was used in this study along the 27-neutron/19-gamma (27n19g) ENDF/B-VII.0 cross section libraries. The input file of MCNP was modified by adding the generated weight windows and source biasing generated by ADVANTG.

3. Results and discussion

The Deep Geological Repository (DGR) consists of the underground repository, where the canisters containing the spent fuel are stored, and the surface facility, known as Used Fuel Packaging Plant (UFPP) in the Canadian-DGR concept, where the used fuel assemblies are received, loaded into canisters, and stored till the underground final storage.

The workers within the DGR are exposed to various configurations of the radiation sources. It can be bare (not inside the canister) fuel channels, or canisters loaded with many spent fuel channels, depending on the location and the specific role of the worker (NWMO, 2014; Ranta-aho, 2008).

To assess the implication of using different fuel cycles in PT-SCWR on the radiological hazards to the workers in the DGR, the gamma and neutron dose rates at different distance from a bare fuel channel as well as from a filled canister were calculated using MCNP 6.1 and the ICRP74 flux-to-dose conversion factors. The fuel channels were assumed to decay for 50 years after discharge with an exit burnup of 60 GWd/THM.

In the next sections, the gamma and neutron emission rates as function of decay time are discussed for the various fuel cycles studied. Then, the gamma and neutron dose rates around a fuel channel and around a loaded canister were presented alongside with the dose rate as a function of the shielding thickness. In the last section, the hazards to the public from using various fuel cycles in PT-SCWR were assessed by comparing the dose rates after the closure of the repository.

3.1 Source terms

3.1.1 Gamma source term

Fig. 4 shows the gamma emission rate per THM, resulting from different spent fuel cycles, as a function of the decay time. There is no significant difference in the emission rate till around 100 years of decay. Between 100 years and 40,000 years of decay, the gamma emissions from Pu/Th fuel are higher than those of uranium-based fuel by around one order of magnitude. After 40,000 years of decay, Fig. 4 shows that the gamma

emissions of thorium-based fuel, either mixed with plutonium or uranium, were very close and higher than that of uranium-only fuel. After about one million years of decay, the gamma emissions of uranium-based fuel are the same and always lower than those of plutonium-based fuel.

To explain the above-mentioned behaviour of gamma emissions, the principal gamma emitters after different decay times (representing the different eras mentioned before), namely 50, 300, 10^5 and 10^6 years, were identified using ORIGEN/SCALE and are shown in Fig. 5 (a-c).

Fig. 5 (a) shows the main contributors to the gamma emissions after 50 years of decay. The total gamma source is almost the same for all the studied fuel types (as can be seen in Fig. 4), but the principal emitters are different, which results in different gamma spectra. The main gamma emitters, as shown in this figure, are Cs-137/Ba-137m, Sr-90/Y-90, Pu-238 and Am-241.

The contributions of Cs-137/Ba-137m to the different fuel cycles are almost the same. The contributions of Am-241 and Pu-238 to the gamma emissions of Pu/Th fuel are much higher than those of uranium-based fuel. Fig. 6 shows the mass of selected actinides (per THM) as a function of the cooling time. The higher concentration of americium and plutonium isotopes in the spent fuel of Pu/Th, as shown in Fig. 6, is due to the existence of plutonium in the fresh fuel.

On the other hand, the contribution of Sr-90/Y-90 is higher in uranium-based fuel compared with the plutonium fuel. This is due to the higher fission yield of Sr-90 from U-235 (5.73 ± 0.13 %) compared with the fission yield from Pu-239 (2.013 ± 0.054 %) (Nichols et al., 2008).

Although Sr-90/Y-90 is a pure beta emitter, it was given by ORIGEN as a gamma emitter. This is due to the fact that the gamma emissions calculated by ORIGEN include the Bremsstrahlung radiation, which is emitted when electrons from the beta emitters, like Sr-90/Y-90, de-accelerate in the medium (Rearden and Jessee, 2018). Therefore Sr-90/Y-90 is found to be a principal gamma emitter, as shown in Fig. 5(a).

Ignoring the Bremsstrahlung radiation reduces the gamma emissions, after 50 years of decay, by about 60% for uranium-based fuel and by only 30% for plutonium-based fuel. This confirms that the fission products, which are mainly beta emitters, are the main contributors to the gamma emissions for uranium fuel. After 300 years of decay, when most of the fission products are decayed away, the Bremsstrahlung radiation contributes by only 1% for Pu/Th and 10% for uranium-based fuel.

After 300 years of decay, the gamma source for Pu/Th fuel is about one order of magnitude higher than that of uranium-based fuel, as shown in Fig. 4. The main contributors to the gamma source at this decay time is Am-241 with smaller contributions from Pu-238, Pu-240 and Am-234 (Fig. 5 (b)). All these isotopes exist in much higher concentration in the spent fuel of Pu/Th than in uranium-based fuel as shown in Fig. 6.

Starting from around 40,000 years of decay to one million years, the gamma sources for thorium-based fuels are comparable and higher than uranium alone. At this time span, the SNF are assumed to be inside the DGR; however, as mentioned before, the spent fuel may be retrieved from DGR if needed, and hence the radiation fields (gamma and neutron) could be important to estimate at this time span.

By investigating the principal gamma emitters at this period, it was found that the main contributors for gammas are Th-229 and its decay products (Ra-225, Ac-225, Fr-221, etc). Th-229, with its half life of 7,340 years, is a decay product of U-233 which is produced in the thorium fuel cycle (by neutron capture of Th-232 to produce Th-233 which decays by beta to Pa-233 which in turn decays to U-233). Therefore, fuels containing thorium will have higher gamma emissions due to Th-229 than fuel without thorium within this decay period.

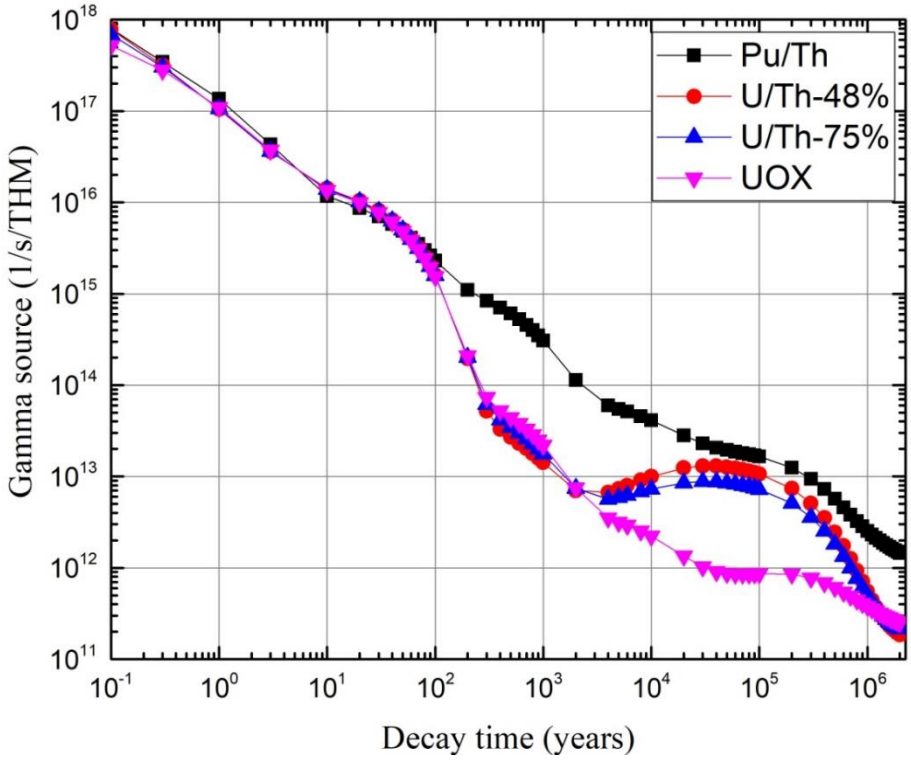

Fig. 4. Variation of the gamma emission rate per THM with the cooling time for different fuel cycles.

Between one-million and two million years of decay, where the emission rate of Pu/Th is higher than all other fuels, The principal gamma emitters are still Th-229 and its decay products (plus Bi-214 from the uranium decay series). In Fig. 5(c), the ratio of gamma emission rate at different decay times to the emission rate at 100,000 years is plotted, against the decay period of 100,000 years to two million years, for Pu/Th fuel and U/Th-48% as a representative for uranium-based fuels.

Fig. 5(c) shows that Th-229 decays at a higher rate in case of U/Th than in Pu/Th fuel. This may be attributed to a higher production of U-233 and Th-229 in Pu/Th fuel compared with U/Th due to the decay of Np-237. Np-237 is a decay product of Am-241 which exists in higher quantity per THM for Pu/Th as mentioned above (Fig. 6).

This higher production of U-233 (and hence Th-229) explains the higher emission rate of Pu/Th after one million years of decay compared with uranium-based fuels.

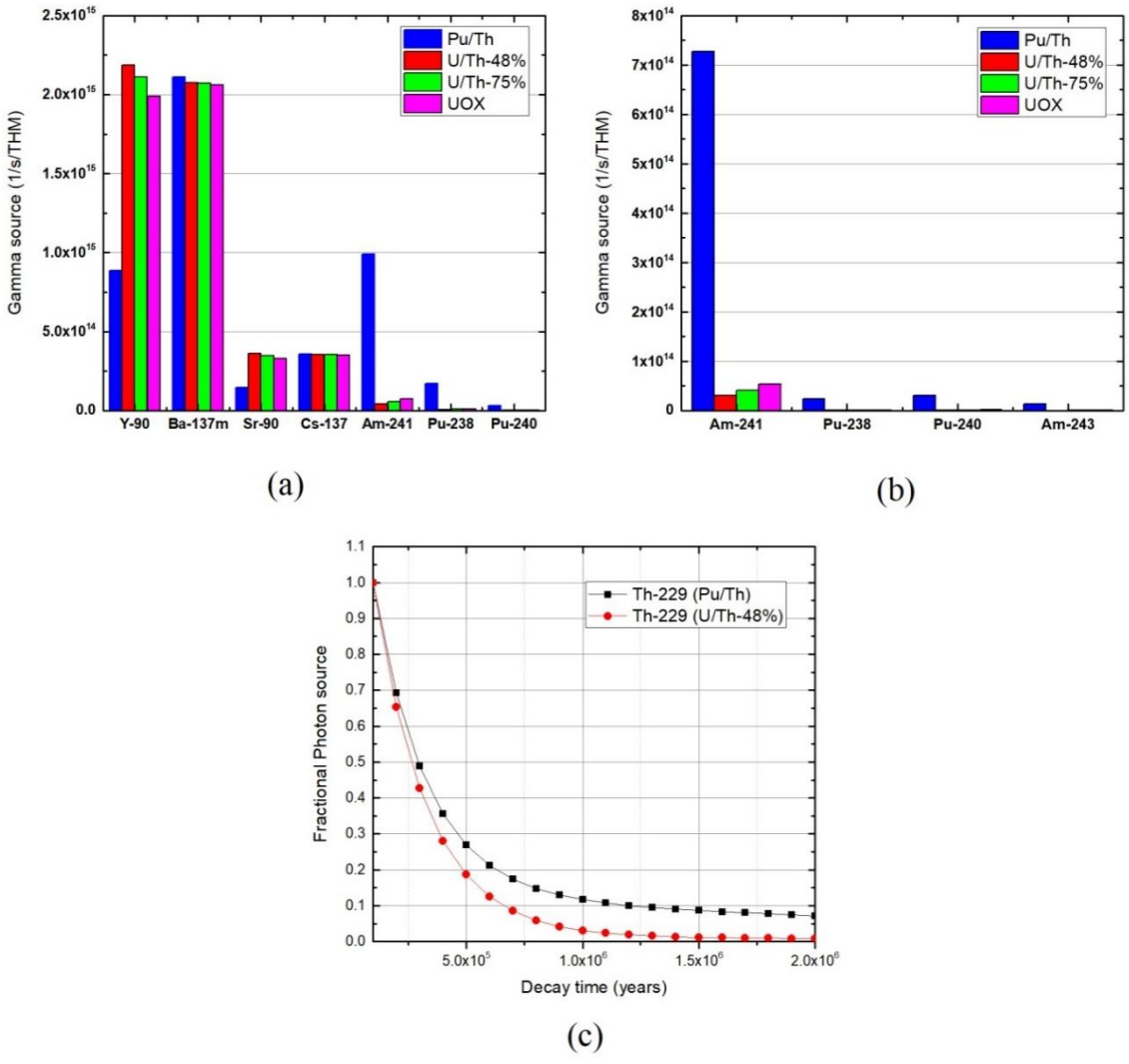

Fig. 5. Principal gamma emitters for different fuel cycles.

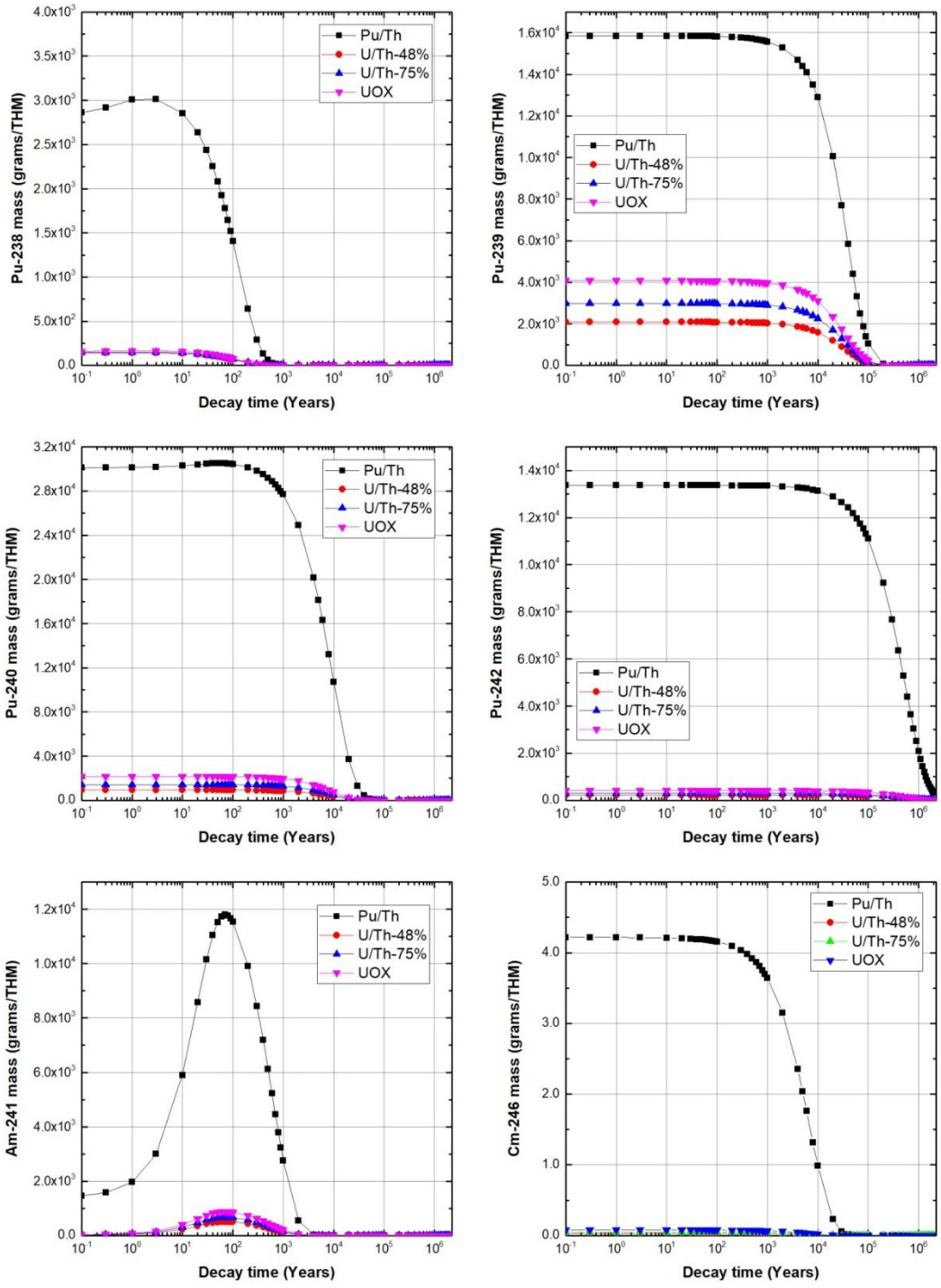

Fig. 6. Change of the mass of selected actinides with decay time for different fuel cycles.

3.1.2 Neutron source term

Fig. 7 shows the neutron emission rate per THM. It shows that the neutron emissions for Pu/Th spent fuel are always higher than those of uranium-based fuel. The main part of the neutron emission is the spontaneous fission of the actinides, especially Cm-244, Cm-246, Cm-242, Pu-240 and Pu-242 as given by ORIGEN and shown in Fig. 8 for Pu/Th fuel.

Till about 100 years, the main contributors are Cm-244 which has a half life of 18.1 years. After 100 years, the neutrons are mainly due to Pu-240, Pu-242 and Cm-246. Starting from around 40,000 years, Pu-242 is the sole contributor to the neutron source. All of these elements exist in higher concentrations in the spent Pu/Th fuel.

The neutron source of uranium-based fuels is higher for UOX than that of uranium mixed with thorium. This is because of the higher enrichment of U/Th fuel compared with that of UOX. Higher enrichments imply a lower mass of U-238 which is the main nuclide generating actinides by neutron absorptions.

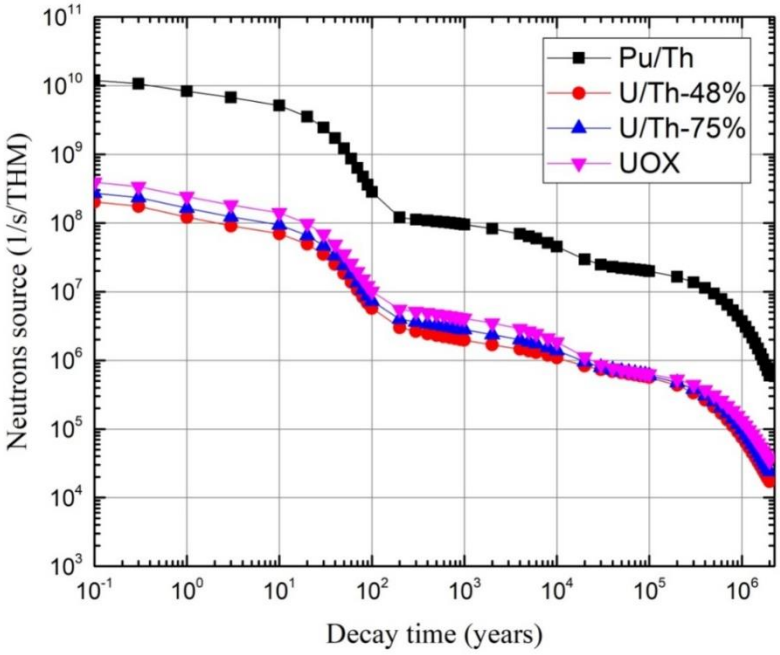

Fig. 7. Neutron emission rate per THM for different fuel cycles.

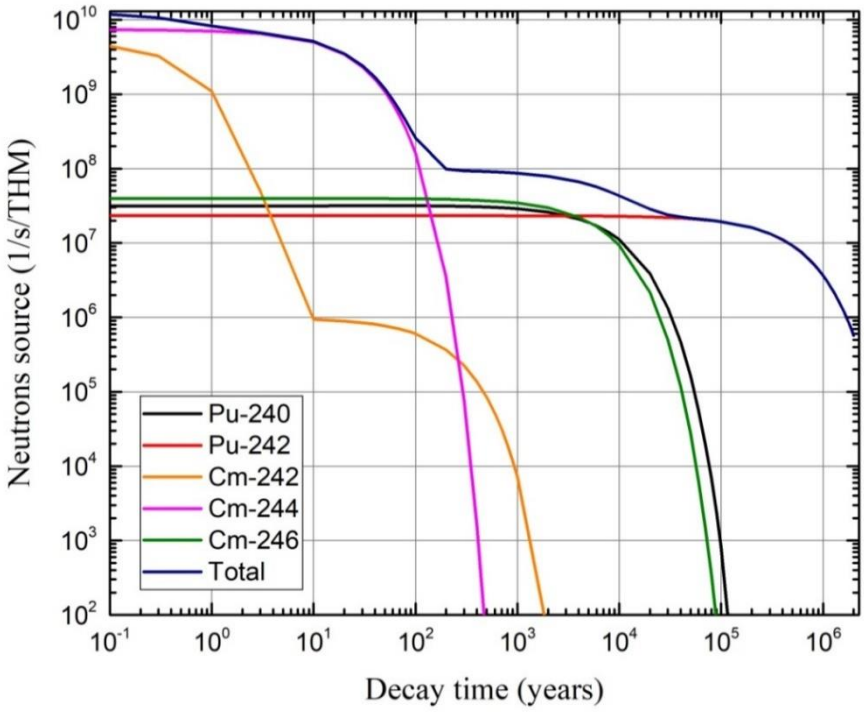

Fig. 8. Neutron emissions rate from spontaneous fission of some isotopes from Pu/Th fuel.

3.2 Dose rate and shielding thickness for an individual spent fuel channel.

3.2.1 Gamma and neutron dose rate

Some tasks in the surface facility of DGR involve dealing with individual spent fuel channels. For example, the crane operator who moves the spent channel from transport cask to the fuel handling cell is exposed to the bare spent fuel channel. The gamma and neutron dose rates at different distances from the surface of the spent fuel channel, after 50 years of decay (this is assumed cooling period before disposal) were calculated using MCNP 6.1.

As mentioned in section 3.1.1, the Bremsstrahlung radiation is given by ORIGEN as gamma source. In this study, only the gamma source, including the Bremsstrahlung, was used in the MCNP coupled photon and electron transport, to calculate the dose rate. To validate this approach, another case was investigated. In this case, two MCNP coupled photon and electron transports were performed. The first one used gamma, without the

Bremsstrahlung part, as a source and the second one used betas (electrons). The dose rates from both files were added and compared with the dose rates resulting from gammas with Bremsstrahlung radiation. The difference between the two approaches was less than the statistical error. This validated the approach of using the gamma source with Bremsstrahlung radiation.

The gamma and neutron source terms obtained from ORIGEN are shown in Table 2, while Table 3, shows the gamma and neutron dose rates in mSv/h at the mid-height of the spent fuel channel as a function of the distance from the surface. The uncertainties in the results were less than 0.1%.

Fig. 9 illustrates the relative dose rates of Pu/Th and LEU/Th to that of UOX. Table 3 , and Fig. 9, show that Pu/Th, the suggested fuel for PT-SCWR, will have an 8% higher gamma dose rate than the most commonly used fuel, uranium oxide fuel (UOX), despite the fact that the total gamma emission rates for both fuels are almost the same (Table 1). This is due to the harder gamma spectrum of Pu/Th as will be explained later.

Pu/Th fuel will always have a higher gamma dose rate than U/Th fuel even if the total gamma emissions rate is higher in the U/Th fuel. This is also due to the harder gamma spectrum of Pu/Th fuel. Accordingly, more shielding would be needed for handling the spent Pu/Th.

Finally, Table 3 shows that increasing the uranium enrichment will increase the gamma emission rates and the dose rate. This is mainly due to higher production of Sr-90/Y-90 with increasing the uranium enrichment (Fig. 5.a).

The neutron dose rate is less than 1% of the gamma dose rate for all fuel cycles (Table 3). Pu/Th fuel has the highest neutron dose rates because the main neutron source, after 50 years of decay, is Cm-244 which has the highest concentration in Pu/Th spent fuel (section 3.1.2).

Table 2. The gamma and neutron source terms after 50 years of decay.

	Gamma emission rate (Bq/THM)	**Neutron emission rate (Bq/THM)**
Pu/Th	7.77E+14	1.95E+08
U/Th-48%	8.13E+14	3.06E+06
U/Th-75%	7.98E+14	3.99E+06
UO_2	7.73E+14	5.71E+06

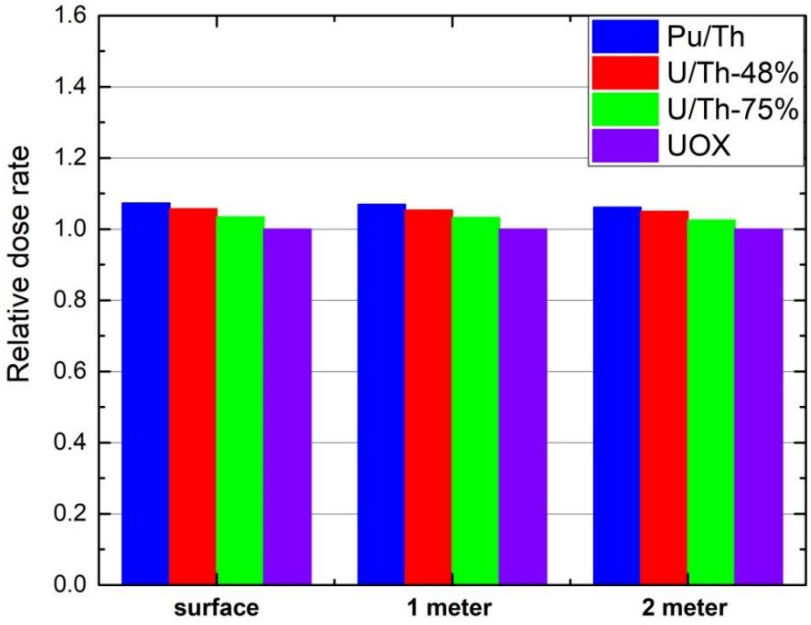

Fig. 9. Relative dose rate, with respect to UOX of various fuels at different distances from the surface of fuel channel.

Table 3. Gamma and neutron dose rate in mSv/h for different fuel channels as function of distance.

Dist.	Pu/Th		U/Th-48%		U/Th-75%		UOX	
	Gamma	Neutron	Gamma	Neutron	Gamma	Neutron	Gamma	Neutron
Surf.	44,091.02	17.607	43,423	0.2821	42,493.99	0.3662	41,086.25	0.5267
1m	2,009.62	0.768	1,979	0.0122	1,937.34	0.0159	1,877.51	0.0227
2m	861.9	0.314	849.2	0.0050	831.3	0.0065	806.5	0.0093
3m	471.1	0.168	464.5	0.0027	454.5	0.0035	440.9	0.0050
4m	291.6	0.103	287.6	0.0016	281.4	0.0021	273.2	0.0030
5m	197.0	0.069	194.1	0.0011	190.1	0.0014	184.3	0.0020
6m	140.9	0.049	138.7	0.0008	135.8	0.0010	131.8	0.0014
7m	104.9	0.037	103.5	0.0006	101.4	0.0008	98.3	0.0011
8m	81.2	0.028	80.0	0.0004	78.3	0.0006	75.9	0.0008
9m	64.2	0.022	63.3	0.0004	62.0	0.0005	60.1	0.0007
10m	52.2	0.018	51.4	0.0003	50.3	0.0004	48.8	0.0005

3.2.2 Gamma energy spectrum at 50 years of decay

As mentioned in the previous section, the Pu/Th fuel showed the highest gamma dose rate compared with all other fuels although the emission rates were almost the same or even lower. This can be explained by the difference in gamma spectra between the different fuels.

Fig. 10 shows the multi-group gamma emission rate as a function of the mid-energy of each energy group. The thorium-based fuels have a higher gamma emission at energy groups with mid-energy 2.5 and 3.5 MeV compared to fuel without thorium. This is mainly due to Tl-208 which emits “hard” gamma rays with energy 2.6 MeV.

For the energy range between 4.0 MeV and 14 MeV, the principal gamma source is Cm-244, which, as was mentioned in section 3.1.1, exists in higher quantities in Pu/Th fuel than in all other fuels studied.

The above observations explain why the Pu/Th fuels have the highest dose rate compared with uranium, either mixed with thorium or not. The high-energy gammas between 4.0 and 14.0 MeV are responsible for the higher gamma dose rate of Pu/Th compared with U/Th. The gamma from Tl-208 was the main cause of the higher dose rate of U/Th compared with UOX.

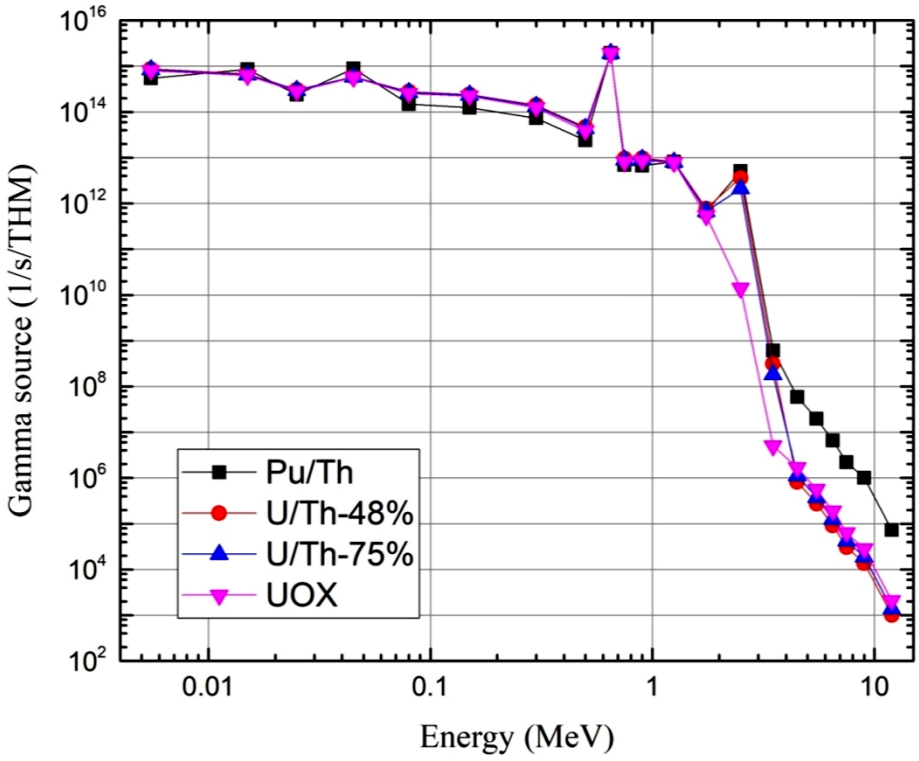

Fig. 10. Gamma spectrum after 50 years of decay.

3.2.3 Shielding thickness

The bare spent fuel channels are transported to the disposal facility using special transport cask. Upon arrival to the disposal facility, they are transferred, using a crane, to the fuel handling cell. Inside the fuel handling cell, which is a shielded chamber, the bare fuel channels are stored before insertion into the final disposal canister.

To study the effect of using different fuel cycles on the shielding requirements, the gamma dose rate of a fuel channel is calculated using MCNP as a function of the thickness of regular concrete which is used as a shielding material (McConn et al., 2011). The dose rate is given in μSv/h at the contact of the concrete. There is 60 cm distance between the fuel channel and the concrete (Ranta-aho, 2008).

Fig. 11 shows the dose rate as function of the thickness of concrete on a logarithmic scale. The same thickness of shielding reduced the dose for UOX fuel much more effectively than for thorium-containing fuels, either Pu or U. This is mainly due to the hard gamma emitter Tl-208 that exists in thorium fuel. Therefore, more shielding will be needed for thorium-containing fuel than for UOX with the Pu/Th fuel needing the thickest shielding.

Table 4 gives the dose rate, with an uncertainty less than 0.1%, as function of the thickness of shielding and the thickness of concrete which is needed to get a dose rate less than 10 μSv/h. Pu/Th will need to be around 13% and 7% thicker than UOX and uranium mixed with thorium, respectively.

3.3 Dose rate and shielding thickness for disposal canister

3.3.1 Gamma and neutron dose rate

The disposal canisters, after being filled with spent fuels, are moved into the storage area before their final underground disposal. During moving and storage of the canisters, they represent a radiological hazard, and an adequate shielding must be used to protect the personnel around the storage area and transfer corridor.

As mentioned in section 2, due to the thermal limitation, only four Pu/Th channels can be disposed into a single canister, while twelve uranium channels can be disposed into a single canister.

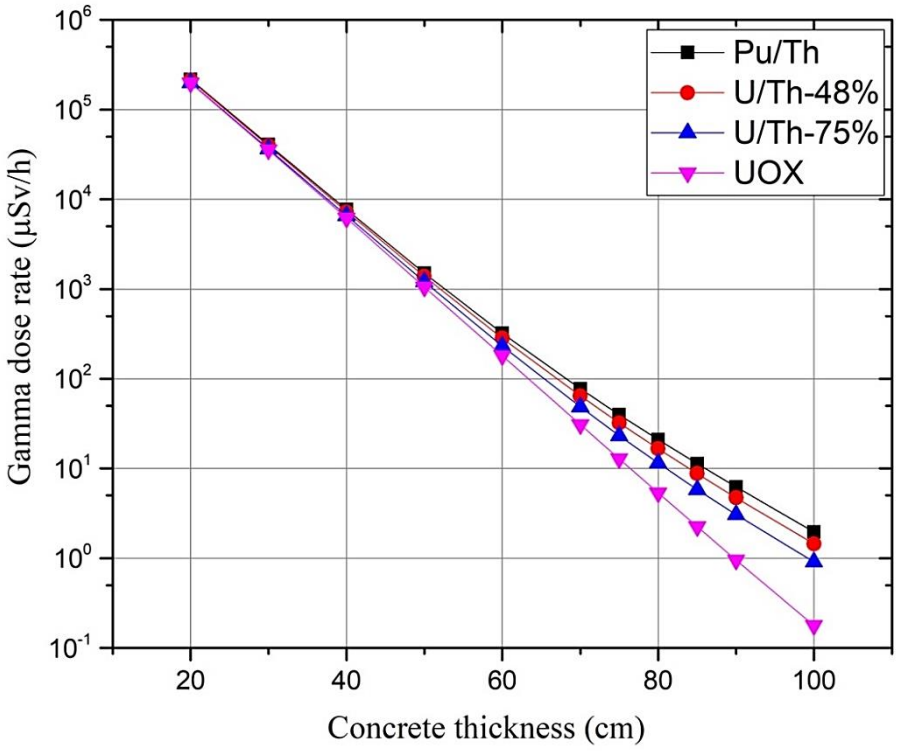

Fig. 11. Gamma dose rate as a function of thickness of concrete after 50 years of decay.

Table 4 Gamma dose rate at different thickness of concrete and the thickness of concrete needed to reduce the total dose rate to below 10 µSv/h.

Fuel	Dose rate (µSv/h)					Minimum Thickness (cm)
	60 cm	70 cm	80 cm	90 cm	100 cm	
Pu/Th	321.71	77.41	20.93	6.22	1.96	87.0
U/Th-48%	283.56	64.43	16.60	4.73	1.45	84.7
U/Th-75%	232.14	48.74	11.48	3.05	0.91	81.5
UOX	180.35	30.74	5.32	0.96	0.18	76.8

The gamma and neutron dose rates around a loaded canister were assessed for different fuel cycles and the results are given in Table 5. The following observations about the gamma dose rates can be made.

First, while the dose rate of a single fuel channel is the highest for Pu/Th fuel, the dose rate of canister containing Pu/Th is the lowest. This is mainly because the canister loaded with Pu/Th contains only four channels, compared with twelve channels for uranium-based fuel.

Secondly, Table 5 shows that the dose rate for U/Th fuel was 27% higher compared with UOX. This is due to the hard gamma emitter, Tl-208. Accordingly, a thicker shielding will be needed for U/Th fuel.

The neutron dose rate was found to be negligible for canisters containing uranium-based fuel, less than 0.5% of the total dose rate, while it was about 60% of the total dose rate for Pu/Th canisters. The neutron dose rate for Pu/Th was the highest one among all studied fuels. Hence, a neutron shielding may be needed when moving/storing canister containing Pu/Th.

3.3.2 Shielding thickness for disposal canisters

The gamma and neutron dose rates for different canisters are given in Table 6 as a function of the shielding thickness. The last row of the table gives an estimation of the thickness needed to reduce the total dose rate below 10 µSv/h, assuming that only one canister is behind the shielding.

In reality, many canisters would be together (around 12 canisters in the Finnish concept of DGR (Ranta-aho, 2008). Therefore, the objective of this table is to illustrate the effect of different fuel cycles on the shielding requirements.

Table 6 shows that around 27% thicker shielding would be needed for U/Th fuel compared with UOX.

The neutron dose rate plays an important role in determining the shielding thickness for the Pu/Th canister. Without it the thickness needed to achieve the limit of 10 µSv/h would be much smaller.

This estimation of shielding is based on the assumption of only one canister behind the shielding. Therefore, three canisters for Pu/Th will be needed to store the same amount of fuel channels as canister containing uranium. This will further increase the required shielding. Using a specific material for neutron shielding should be considered in this case. In conclusion, using U/Th or Pu/Th will increase the shielding needed compared with UOX.

3.3.3 Directional Dose Rate

Due to the design of the disposal canister, the dose rate will depend on the azimuthal angle. Fig. 12shows the contour of gamma and neutron dose rates for the two different types of canisters studied here. One that holds the Pu/Th fuel channels (four fuel channels per canister) and one that holds uranium-based fuel (12 fuel channels per canister).

Table 5. Gamma and neutron dose rates in mSv/h for disposal canisters after 50 years of cooling

Dist.	Pu/Th		U/Th-48%		U/Th-75%		UOX	
	Gamma	Neutron	Gamma	Neutron	Gamma	Neutron	Gamma	Neutron
Surf.	1.045	1.49	18.87	0.111	17.15	0.143	14.70	0.202
1m	0.156	0.36	5.40	0.027	4.90	0.035	4.21	0.049
2m	0.080	0.18	3.01	0.014	2.75	0.018	2.36	0.025
3m	0.050	0.11	1.93	0.008	1.75	0.011	1.51	0.015
4m	0.034	0.07	1.32	0.005	1.20	0.007	1.04	0.010
5m	0.024	0.05	0.95	0.004	0.86	0.005	0.75	0.007

Table 6. The gamma and neutron dose rate as function of shielding thickness and the thickness of concrete needed to reduce the total dose rate below 10 µSv/h (uncertainty is less than 0.1%).

Thickness (cm)	Pu/Th		U/Th-48%		U/Th-75%		UOX	
	G	N	G	N	G	N	G	N
20	18.9	86.6	626.0	6.50	528.1	8.40	387.9	11.90
40	1.8	8.7	37.9	2.04	27.1	2.64	12.3	3.73
60	0.20	0.9	3.23	0.67	2.04	0.86	0.41	1.22
80	0.02	0.1	0.33	0.22	0.20	0.28	0.02	0.40
Thickness to 10 µSv/h	40.3		49.0		46.3		42.0	

There is a strong angular dependence of the gamma dose rate especially for the Pu/Th canister. No significant dependence is observed for the other canister or for neutron dose rates of both canisters. The gamma dose rate mentioned in Table 5 is the maximum dose rate for Pu/Th canisters and the average one for other canisters and for the neutron dose rate.

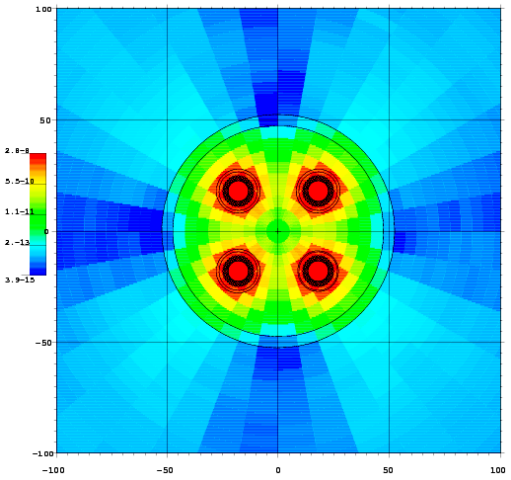

Gamma dose Pu/Th fuel

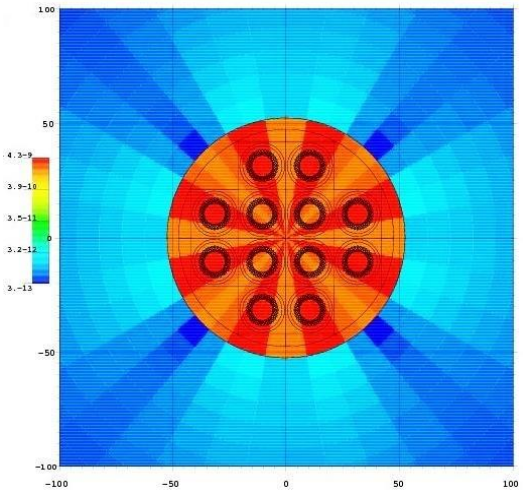

Gamma dose uranium fuel

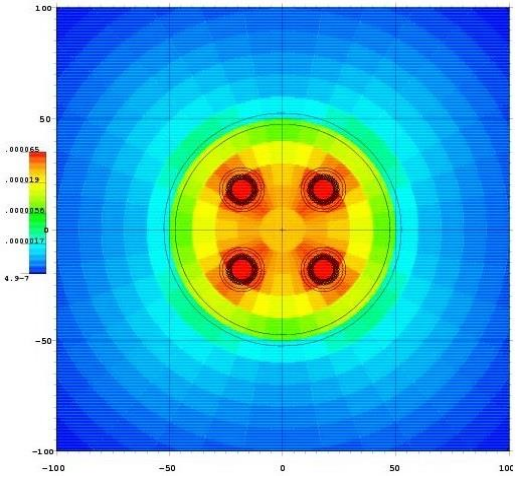

Neutron dose Pu/Th fuel

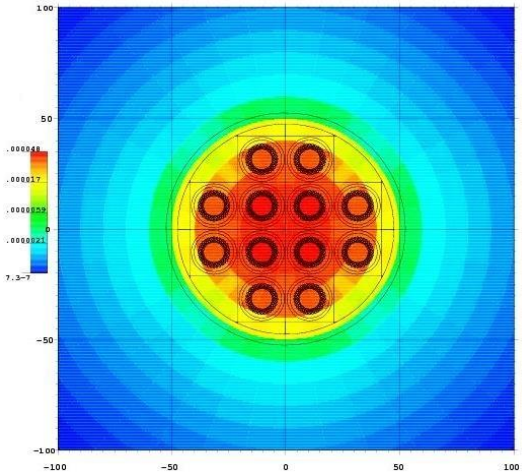

Neutron dose uranium fuel

Fig. 12. Dependence of the gamma and neutron dose rate on the azimuthal angle.

3.4 Post-closure performance

The implications of using various fuel cycles in PT-SCWR on the occupational hazard were assessed in the previous sections; It was concluded that the Pu/Th fuel cycle caused the highest dose rate to the workers. In this section, the hazards to the public are assessed using the dose rate to a critical group of the public after the closure of the repository.

As a regulatory requirement, the dose received by public due to any planned or potential exposure from the DGR must not exceed the 1.0 mSv/a limit, and this exposure should be kept as low as reasonably achievable (ALARA) (IAEA, 2011). A dose constraint below the regulatory limit is used to account for the possibility of future exposure to various sources. The adopted dose constraint in Canada is 0.3mSv/a, which is also recommended by ICRP (CNSC, 2006; ICRP, 2007). The dose rate to the public caused by the DGR must be below this dose constraint.

The lifetime of the disposal facility has two main phases: the operational phase and the post operational phase when the repository is fully sealed and closed. After the closure of the repository, no active controls exist and the protection of the public from any radiological hazards from the repository depends only on the passive safety integrated into the design of the repository (which, in normal situations, prevent the radioisotopes from reaching to the biosphere), (ICRP, 2013).

The post-closure safety assessments of different concepts of DGR were studied before (Chornoboy et al., 2018; NWMO, 2017; NWMO, 2018; Prítrský and Nečas, 2012). It was found there that the main contributors to the dose rate to the public is I-129 which contributes around 99.0% of the total dose rate. This result was used in this study to investigate the post-closure performance of the Canadian DGR containing different types of fuel.

Fig. 13 illustrates the change of the mass of I-129, per THM, in the spent fuel of the different fuel cycles as a function of the decay time. Pu/Th contains the most I-129. This is attributed to the higher yields of I-129 from the fission of Pu-239, Pu-241 and U-233, which are 1.407±0.027 %, 1.28±0.36 % and 1.63±0.26 % respectively, compared with that of U-235, which is 0.706±0.032 %. (Nichols et al., 2008). Comparing UOX with U/Th fuel shows that U/Th will have more I-129 inventory than UOX. This can be attributed to the different fissile elements of these two fuels.

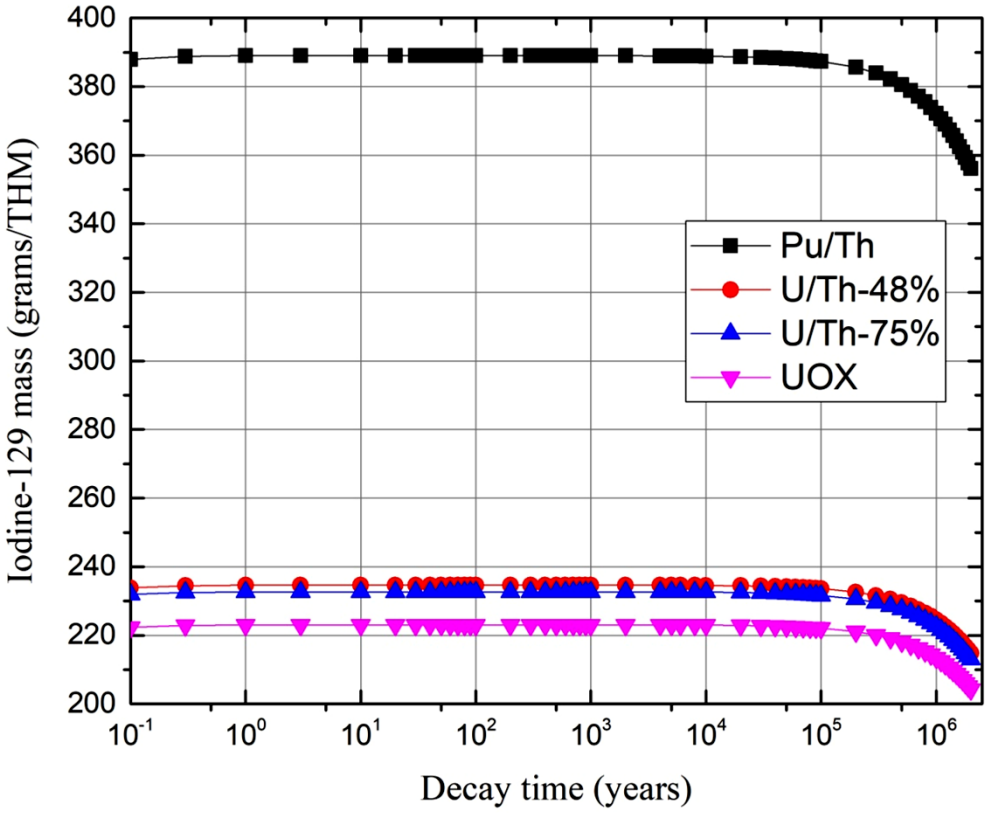

Fig. 13. The mass of I-129 as function of decay time for different fuel cycles.

The cumulative contributions of different fissile nuclides to the total energy produced by each fuel were estimated using TRITON (Jessee et al., 2018). The results are given in Table 7. About 7.45% and 10.75% of fissions are caused by Pu-239 and U-233 respectively for U/Th-48% while for UOX about 15.66% of the fissions are caused by Pu-239 and none by U-233. As the yield of I-129 from U-233 fission is slightly higher than that of Pu-239, this explains why U/Th fuel will have more I-129 compared with UOX.

The dose rate to the public was estimated here by scaling the previously reported doses. Only a comparative study was done here, where the dose rate to the critical group is estimated by scaling the previously reported results comparing the amount of I-129 in each investigated fuel cycle to that of CANDU.

The Canadian DGR post-closure performance was studied previously, assuming different accident scenarios (NWMO, 2017). It was found that simultaneous failures of 10 canisters after 1000 years resulted in a peak dose rate equal to 2.6×10^{-3} mSv/a. This is the scenario used in this study, as it gave the highest dose rate among all studied scenarios, to estimate the peak dose rate when different types of fuel cycles are used.

A detailed modeling has to be done to predict the exact dose rate to the public, taking into consideration the specific layout, the number and distributions of canisters, the underground pathway, etc. (NDA, 2010); This is out of scope of the present study.

The dose rates reported here were estimated by comparing the I-129 inventories of each fuel cycle to that of CANDU canisters used to estimate the peak dose rate of 2.6×10^{-3} mSv/a.

Table 8 shows, after 1000 years of decay, the mass of I-129 per ton of initial heavy materials as well as the peak dose rate for different fuel cycles assuming 10 canisters failed simultaneously. Since the Pu/Th canisters have only four fuel channels compared with 12 fuel channels in uranium-based fuel, the peak dose rate per unit of electric output, in TWde, is given as well (assuming the efficiency is 47% for SCWR and 33% for CANDU).

Table 7. The cumulative contribution of each isotope to total energy produced for different fuel cycles.

Fuel Cycle	Fission percentage (%)			
	Pu-239	**Pu-241**	**U-233**	**U-235**
Pu/Th	58.03	31.25	8.51	0.04
U/Th-48%	7.45	1.28	10.75	78.88
U/Th-75%	10.61	1.73	7.22	78.20
UOX	15.66	2.53	0.0	78.78

Table 8. Mass of I-129, peak dose rate and normalized peak dose rate per terawatt day electric (TWde).

	I-129 inventory (g/THM)	**Peak Dose rate (mSv/a)**	**Normalized Peak dose rate (mSv/a/TWde)**
Pu/Th	3.89E+02	9.9E-03	5.49E-02
U/Th-48%	2.35E+02	1.8E-02	3.31E-02
U/Th-75%	2.33E+02	1.8E-02	3.28E-02
UOX	2.23E+02	1.7E-02	3.15E-02
CANDU	7.04E+01	2.6E-03	3.14E-03

Table 8 shows that the Pu/Th will have the highest dose rate to the public per unit of electricity produced. This means that using Pu/Th will increase the dose to public in case of failure of canisters by 75% compared to that of uranium.

The dose rate for Pu/Th given in the second column of Table 8 is the lowest because of the assumption that the Pu/Th spent fuel will be stored in the canisters which contain only four channels. In case of using Pu/Th in canisters with 12 fuel channels, the peak dose rate will be 3.0×10^{-2} mSv/a, which would be the highest dose rate. On the other hand, using

thorium with uranium will not significantly affect the dose rate, as shown in Table 8, and hence, the dose limit will not be exceeded.

Using Pu/Th will not cause the peak dose rate to exceed the recommended dose constraint of 0.3mSv/a, but the storage of Pu/Th spent fuel in deep geological repository will increase the risk to the public, and this increased risk must be justified against the ALARA principle. Also, the margin to the constraint was reduced in the case of Pu/Th fuel, given the large uncertainties involved with the dose assessment from DGR.

3.4.1 Effect of origin of Pu on the dose rate

As Pu will come from reprocessing the exiting spent fuels from an LWR, during reprocessing the I-129, as a gas, will escape. It is trapped in the reprocessing facility using silver (Ag) to form AgI. The management of this radioactive AgI depends on each country's policy; For example, in Japan, it is planned to be stored in the DGR (Nagasaki)

This means that the reprocessing of the original fuel will not help in the reduction of the amount of I-129 to be stored and hence, to the public dose rate in case of an accident to the DGR containing AgI.

If the original fuel has to be taken into consideration, the public dose rate from a DGR containing AgI has to be calculated. This requires the specific design of such a DGR, such as the layout, the amount of AgI stored into each borehole, etc. All of this data is not available and such study is outside the scope of this work.

But, hypothetically, if AgI would be stored in the same DGR as the spent fuel, according to data presented in (Ault et al., 2017), 21.09 MT of uranium will produce 0.874 GWe-year in PWR with exit burnup of 50 GWd/THM and efficiency of 33.33%. The amount of I-129 per 1 MTU is 223.6 grams, therefore, for 21.09 MT of UOX, there will be 4.72 kg of I-129 in the spent fuel.

During reprocessing, this amount of I-129 would be released; Assuming that 99% of it would be trapped, 4.67 kg of I-129 would go to the DGR. The peak dose rate to public from this amount is 1.87×10^{-2} mSv/a, using the same methodology used before to estimate the peak dose rate).

Reprocessing of 21.09 MT would produce Pu. Ten channels of Pu/Th would be needed to give 0.126 GWe-year in a PT-SCWR with efficiency of 47.24% (so the combined energy production of both reactor systems is 1 GWe-year). The mass of I-129, in case of Pu/Th, is 389 gram per ton of heavy metals. This amount of I-129, would give a peak dose rate of 3.73×10^{-3} mSv/a. Hence, the combined dose rate per 1 GWe-year of both reactor systems is 2.12×10^{-2} mSv/a.

For UOX in a PT-SCWR, 80 channels are needed for 1 GWe-year; The amount of I-129 in case of UOX in PT-SCWT is 223.1 gram/MTU (lower than that in PWR, due to the higher enrichment needed in PT-SCWR). This amount would give a dose rate of 1.15×10^{-2} mSv/a.

Therefore, when the origin of the Pu is taken into consideration, the peak dose rate caused by Pu/Th fuel was 84% higher than that of UOX. This confirms that considering the spent fuel of Pu/Th without the origin is justified for post-closure safety assessment.

3.5 Mass of Uranium Ore

The mass of natural uranium ore needed for a full core of PT-SCWR was estimated in this section using equation (1) (Lamarsh and Baratta, 2001)

$$M_F = \left(\frac{X_p - X_T}{X_F - X_T}\right) M_p \qquad (1)$$

Where M_F is the mass of the feed (natural uranium) and M_p is the mass of the product (enriched uranium), X_p , X_F and X_T are the enrichments of the product, feed and tail respectively.

Assuming the feed and tail's enrichments are 0.711% and 0.2% respectively, the mass of natural uranium required for the full core of PT-SCWR were found to be 884.6, 862.5, and 836.7 tons for U/Th-48%, U/Th-75% and UOX fuels respectively.

This indicates that using U/Th will require more uranium ore than UOX and, hence, no better resource utilization is expected when using U/Th over UOX. This is due to the higher enrichment needed for U/Th fuel.

4. Conclusion

The dose rate for occupational workers in the DGR as well as the peak dose rate received by the public after the closure of the DGR were investigated for different fuel cycles assumed to be used in the PT-SCWR.,. The investigated fuel cycles were Pu/Th, LEU/Th and UOX.

As the occupational doses is one of the metrics which can be used to compare between different fuel cycles, the results of this study can help the decision makers in choosing the optimal fuel cycle for the Gen-IV PT-SCWR. The following conclusions were made:

1. The gamma source term is almost the same for all fuel cycles till 100 years of decay. The main gamma emitters here were the fission products (Cs-137/Ba-137m).
2. Between 100 and 40,000 years of decay, the gamma emissions from Pu/Th fuel are higher than those of uranium-based fuel by around one order of magnitude as the main gamma emitters here are the actinides which exist in higher mass in spent fuel of Pu/Th than in uranium-based fuel. Between 40,000 and one million years of decay, the thorium-based fuels, Pu/Th and U/Th , have higher gamma emissions than UOX due to the decay products of U-233. After one million years of decay, the gamma emissions of Pu/Th are the highest. This is attributed to the decay of Np-237.

3. Although the gamma emissions were almost the same for all fuels after 50 years of decay, the gamma dose rate to the workers from exposure to Pu/Th fuel was 8% higher than that of UOX, and hence 13% thicker shielding was found to be needed. This is due to the hard gammas emitted from Tl-208 and from Cm-244.
4. Comparing U/Th with UOX, it was found that a 5% higher gamma dose resulted from U/Th due to high-energy gammas from Tl-208. Around 10% thicker shielding will be needed.
5. Using LEU/Th instead of UOX does not show any better utilization of the uranium ore as more uranium will be needed given the higher enrichment needed for LEU/Th fuel cycle.
6. The peak dose rate to the public in case of a failure of canisters was found to be 75% higher in the Pu/Th case than in UOX. Using Pu/Th will not cause the public's peak dose rate to exceed the recommended limit of 0.3mSv/a, but the storage of Pu/Th spent fuel in deep geological repository will increase the dose to the public, and this increased dose has to be justified against the ALARA principle.

5. Acknowledgments

The authors would like to thank Dr. Jeremy Pencer and Dr. Shinya Nagasaki for their valuable comments and suggestions. This work was partly funded by the University Network of Excellence in Nuclear Engineering (UNENE), Canada, and by the Natural Sciences and Engineering Research Council of Canada (NSERC), under grant no. RGPIN-2020-06897.

6. References

Ashley, S.F., Lindley, B.A., Parks, G.T., Nuttall, W.J., Gregg, R., Hesketh, K.W., Kannan, U., Krishnani, P.D., Singh, B., Thakur, A., Cowper, M., Talamo, A., 2014. Fuel cycle modelling of open cycle thorium-fuelled nuclear energy systems. Ann. Nucl. Energy 69, 314–330. https://doi.org/10.1016/j.anucene.2014.01.042 .

Ault, T., Krahn, S., Croff, A., 2017. Comparing the environmental impacts of uranium- and thorium-based fuel cycles with different recycle options. Prog. Nucl. Energy 100, 114–134. https://doi.org/10.1016/j.pnucene.2017.05.010

Chornoboy, N., Levinsky, A., Kitson, C., Bromley, B.P., 2018. Postclosure Performance Assessment of a Hypothetical Canadian Deep Geological Repository for Thorium-Containing Advanced Heavy Water Reactor Fuels. Nucl. Technol. 204, 110–118. https://doi.org/10.1080/00295450.2018.1454229 .

CNSC, 2006. Assessing the Long Term Safety of Radioactive Waste Management. Canadian Nuclear Safety Commission, Regulatory Guide G-320 .

Croff, A.G., Krahn, S.L., 2016. Comparative assessment of thorium fuel cycle radiotoxicity. Nucl. Technol. 194, 271–280. https://doi.org/10.13182/NT15-46 .

GIF, 2002. A Technology Roadmap for Generation IV Nuclear Energy Systems. Generation IV International Forum. GIF-002-00. Available at: https://www.gen-4.org/gif/jcms/c_9352/technologyroadmap .

Goorley, J.T., James, M.R., Booth, T.E., Brown, F.B., Bull, J.S., Cox, L.J., Durkee Jr, J.W., Elson, J.S., Fensin, M.L., Forster III, R.A. and Hendricks, J.S., 2013. Initial MCNP6 release overview-MCNP6 version 1.0 (No. LA-UR-13-22934). Los Alamos National Lab.(LANL), Los Alamos, NM (United States). https://doi.org/10.2172/1086758.

Hummel, D.W., 2015. Transient neutronic-thermalhydraulic coupling in a PT-SCWR, PhD Thesis, 295.

IAEA, 2011. Disposal of Radioactive Waste, INTERNATIONAL ATOMIC ENERGY AGENCY Safety Standards Series No. SSR-5.

Ibrahim R. , Buijs, A., Luxat, J. , 2019. Assessment of the Long-Term Storage of PT-SCWR Fuel Bundles in CANDU Deep Geological Repository. 39th Annual Conference of the Canadian Nuclear Society and 43rd Annual CNS/CNA Student Conference.

ICRP , 1996. Conversion coefficients for use in radiological protection against external radiation, International Commission on Radiological Protection Publication 74. Ann. ICRP 26, 3-4 https://doi.org/10.1016/j.icrp.2013.01.001.

ICRP, 2007. The 2007 Recommendations of the International Commission on Radiological Protection. ICRP Publication 103. Ann. ICRP 37, 2-4.

ICRP , 2013. Radiological Protection in geological disposal of long-lived solid radioactive waste, International Commission on Radiological Protection Publication 122. Ann. ICRP 42, 1–57. https://doi.org/10.1016/j.icrp.2013.01.001 .

Jessee, M.A. and DeHart, M.D., 2018. Triton: a multipurpose transport, depletion, and sensitivity and uncertainty analysis module. ORNL/TM-2005/39, Version 6.2.3, Section 3.

Lamarsh, J.R. and Baratta, A.J., 2001. Introduction to nuclear engineering, third ed. Upper Saddle River, NJ: Prentice hall, pp 202.

Leung, L.K.H., Yetisir, M., Diamond, W., Martin, D., Pencer, J., Hyland, B., Hamilton, H., Guzonas, D., Duffey, R., 2011. A next generation heavy water nuclear reactor with supercritical water as coolant. International conference on Future of Heavy Water Reactors, Ottawa, Ontario (Canada).

Mosher, S.W., Johnson, S.R., Bevill, A.M., Ibrahim, A.M., Daily, C.R., Evans, T.M., Wagner, J.C., Johnson, J.O., Grove, R.E., 2015. ADVANTG: An Automated Variance Reduction Parameter Generator, ORNL/TM-2013/416 Rev 1. https://doi.org/10.2172/1210162 .

Nagasaki, S., personal communication.

NDA, 2010. Geological Disposal: Generic Operational Environmental Safety Assessment. Nuclear Decommissioning Authority. Report no. NDA/RWMD/030.

Nichols, A.L., Aldama, D.L., Verpelli, M., 2008. Handbook of Nuclear data for safeguards: database extensions. IAEA. https://www-nds.iaea.org/sgnucdat/ .

Noronha, J., 2016. Deep Geological Repository Conceptual Design Report Crystalline / Sedimentary Rock Environment. Nuclear Waste Management Organization, APM-REP-00440-0015 R001.

NWMO, 2005. Choosing a way forward: the future management of Canada's Used Nuclear Fuel. Nuclear Waste Management Organization. report submitted to the Minister, Natural Resource Canada.

NWMO, 2014. Preliminary ALARA Dose Assessment for Three APM DGR Concepts. Nuclear Waste Management Organization, TR-2014-18.

NWMO, 2017. Postclosure Safety Assessment of a Used Fuel Repository in Crystalline Rock. Nuclear Waste Management Organization. TR-2017-02.

NWMO, 2018. Postclosure Safety Assessment of a Used Fuel Repository in Sedimentary Crystalline Rock. Nuclear Waste Management Organization. TR-2018-08.

Pencer, J., Colton, A., 2013. Progression of the lattice physics concept for the Canadian supercritical water reactor. Proceedings of the 34th Annual Conference of the Canadian Nuclear Society. Toronto, Ontario (Canada).

Prítrský, J., Nečas, V., 2012. Impact of advanced nuclear fuel cycle IMF on geological repository performance. Prog. Nucl. Energy 54, 36–40. https://doi.org/10.1016/j.pnucene.2011.09.005

Raiko, H., 2005. Disposal Canister for Spent Nuclear Fuel – Design Report Disposal Canister for Spent Nuclear Fuel. Design Report, Posiva Report 2005-02 .

Ranta-aho, A., 2008. Review of the Radiation Protection Calculations for the Encapsulation Plant Review of the Radiation Protection Calculations for the Encapsulation Plant. Posiva Report 2008-63 .

Rearden, B.T., Jessee, M.A., 2018. SCALE Code System, Oak Ridge National Laboratory. ORNL/TM-2005/39, Version 6.2.3.

White, J.E., Ingersoll, D.T., Slater, C.O., Roussin, R.W., 1996. BUGLE-96: A revised multigroup cross section library for LWR applications based on ENDF/B-VI Release 3. American Nuclear Society (ANS) Radiation Protection and Shielding Division topical meeting on advancements and applications in radiation protection and shielding, Falmouth, MA (United States).

Yetisir, M., Gaudet, M., Rhodes, D., Fuel, C., 2013. Development and integration of Canadian SCWR concept with counter-flow fuel assembly. The 6th International Symposium on Supercritical Water-Cooled Reactors (ISSCWR-6); Shenzhen, Guangdong (China).

Chapter 6 Assessment of the Material Attractiveness and Reactivity Feedback Coefficients of Various Fuel Cycles for the Canadian Concept of Super-Critical Water Reactors

Citation:

Remon Ibrahim, Adriaan Buijs, John Luxat, 2022, "Assessment of the material attractiveness and reactivity feedback coefficients of various fuel cycles for the Canadian concept of Super-Critical Water Reactors", Nuclear Engineering and Technology 54 (2022) 2660 – 2669. https://doi.org/10.1016/j.net.2022.01.036

Increasing the proliferation resistance is another goal of GEN-IV systems. As mentioned in Chapter 3, reduction of the attractiveness of nuclear materials enhances the overall proliferation resistance.

In this publication, the attractiveness of different types of nuclear fuel, proposed for the PT-SCWR, was estimated using the Figure-of-Merit (FOM) method. A novel contribution in this article was proposing a numerical assessment system, based on the attractiveness of fresh and spent fuel, to compare between different fuel cycles.

The investigated fuels were, Pu/Th, LEU, LEU/Th, RepU, Pu/Th/U. It was found that, according to the proposed numerical system, Pu/Th is the least proliferation resistant fuel, while RepU is the most proliferating resistant fuel for PT-SCWR.

The optimal amount of natural uranium, which can be added to Pu/Th to “denature” the U-233, was determined as well in this study.

Finally, the reactivity coefficients of the studied fuels were investigated. It was found that all fuels have the same sign of reactivity feedback as the originally proposed fuel, which is Pu/Th.

Assessment of the material attractiveness and reactivity feedback coefficients of various fuel cycles for the Canadian concept of Super-Critical Water Reactors

Remon Ibrahim [a,b], Adriaan Buijs [a] , John Luxat [a]

[a] McMaster University, 1280 Main Street West, Hamilton, ON, L8S 4L7, Canada

[b] Nuclear and Radiological Regulatory Authority, N. City, Cairo, Egypt

Abstract

The attractiveness for weapons usage of the proposed fuel cycle for the PT-SCWR was evaluated in this study using the Figure-of-Merit methodology. It was compared to the attractiveness of other fuel cycles namely, Low Enriched Uranium (LEU), U/Th, Re-enriched Reprocessed Uranium (RepU), and Pu/Th/U. The optimal content of natural uranium, which can be added to Pu/Th to render the produced U-233 unattractive, was found to be 9%.

A ranking system to compare the attractiveness of the various fuel cycles is proposed. RepU was found to be the most proliferation resistant fuel cycle for the first 100 years, while the least proliferation resistant fuel cycle was the originally proposed Pu/Th one.

The reactivity feedback coefficients were calculated for all proposed fuel cycles. All studied reactivity coefficients have the same sign implying that all the fuel cycles will behave neutronically in a similar way. The Pu/Th/U fuel was found to have the most negative value of the Coolant Void Reactivity which will help to restore the core to a safe status faster in case of a loss-of-coolant accident. The fuel and moderator temperature coefficients did not show significant differences between the fuels studied.

Keywords: Proliferation resistance; material attractiveness; PT-SCWR; nuclear fuel cycles; reactivity coefficients

1. Introduction

The supercritical water reactor (SCWR) is one of the six concepts of the generation-IV nuclear systems selected by the Generation-IV International Forum (GIF) [1]. Canada, as a member of GIF, is developing the concept of the supercritical water reactor. The Canadian concept of SCWR, known as Pressure Tube SCWR (PT-SCWR), uses a once-through Pu/Th fuel cycle [2].

Increasing the proliferation resistance is one of the goals of GEN-IV nuclear energy systems (NESs). Different methodologies were proposed [3-5] to evaluate the proliferation resistance of any proposed design. One of those methodologies is the Proliferation Resistance and Physical Protection (PR&PP) evaluation methodology developed by GIF [4] which recommends performing an evaluation of the proliferation resistance at the earliest stage of the design. This will help in detecting any vulnerabilities of a proposed design and to change it accordingly. Using a different fuel cycle or changing the layout to more easily implement the safeguards are examples of the possible changes in design to increase its proliferation resistance.

As the PT-SCWR is in the design stage, its proliferation resistance will mainly depend on the attractiveness of the existing fissile materials to be used in nuclear weapons. Different methods were proposed to assess the attractiveness of fissile materials [6-8]. This study uses the "Figure-of-Merit" (FOM) method proposed by Bathke et al. [8]. They defined a parameter, FOM, which can be calculated using equation (1) or equation (2). The difference between FOM_1 and FOM_2 is that FOM_2 accounts for the spontaneous fission neutrons. A high neutron yield from spontaneous fission can result in pre-initiation of the nuclear explosive devices, which reduces the nuclear yield of the nuclear explosive [9].

For a sub-national actor, any nuclear yield would be acceptable, and therefore, FOM_1 represents the worst-case scenario and was used in this study.

$$FOM_1 = 1 - \log_{10}\left[\frac{M}{800} + \frac{Mh}{4500} + \frac{M}{50}\left[\frac{D}{500}\right]^{1/\log_{10} 2}\right] \quad (1)$$

$$FOM_2 = 1 - \log_{10}\left[\frac{M}{800} + \frac{Mh}{4500} + \frac{MS}{6.8(10)^6} + \frac{M}{50}\left[\frac{D}{500}\right]^{1/\log_{10} 2}\right] \quad (2)$$

Where:

M is the bare critical mass of the assessed material (kg);

h is the heat content (W/kg);

S is the intrinsic-fission neutron production rate (n/s.kg^{-1}); and

D is the dose of 20% of the bare critical mass *M* at 1 meter (rad/h).

Table 1 gives the meaning of FOM and its range of values. Any material with FOM > 1 can be used to construct an effective nuclear device, while material with FOM <1 is impractical for weapons but still possible theoretically. The lower the FOM is the better the material is for proliferation resistance, and each process which can result in a material with a lower FOM should be encouraged.

Table 1. Meaning of FOM and the attractiveness associated with it.

FOM	Weapons utility	Attractiveness
> 2	Preferred	High
1-2	Attractive	Medium
0-1	Unattractive (Theoretically possible)	Low
< 0	Unattractive	Very low

In this paper, the attractiveness of the Pu/Th fuel cycle proposed for the PT-SCWR was assessed using the FOM method. The possibility of using different fuel cycles in the PT-SCWR was investigated as well. The attractiveness in terms of FOM, and the neutronic safety coefficients were calculated for each proposed fuel cycle.

The attractiveness was usually evaluated based on the characteristics of the spent fuel as the majority of the current reactors are using either Low Enriched Uranium (LEU) or Natural Uranium (NU), which, as fresh fuel, are unattractive materials for weapons [10]. However, other fuels proposed for the PT-SCWR might contain highly attractive materials when fresh; their attractiveness will be considered in the evaluation of the proliferation resistance as well.

This study proposes a simple numerical ranking system to fairly compare between different proposed fuel cycles. It considers the attractiveness of the materials in both the fresh and spent fuel. The proposed ranking system is explained later.

2. Materials and Methods

2.1. PT-SCWR and the different fuel cycles

The PT-SCWR is a pressure tube reactor cooled with supercritical light water and moderated with heavy water. The reference reactor core concept consists of 336 fuel channels, each housing a 5-m long fuel assembly. The fuel bundle consists of two concentric fuel rings with 32 fuel pins each (Fig. 1). The lattice pitch is 25 cm and the fuel is a mix of reactor-grade plutonium and thorium. The weight percentage of PuO_2 is chosen to be 15% and 12% for the inner and outer rings respectively, to limit the maximum linear element rating (LER) to 40 kW/m [11]. The dimensions and the material compositions are given in [2].

The density of the outer coolant changes dramatically between the bottom and top of the channel because the coolant is under supercritical conditions. This study does not consider axial variance. Instead, the thermal conditions corresponding to those at the center of the channel were used to represent the entire channel.

This is based on an earlier 3D full-core analysis for the PT-SCWR core. It was found that the thermal properties of the middle of the channel may be used for the whole channel. The errors in radial power distribution and exit burnup, resulting from this approximation were not significant [12].

In addition to the nominal Pu/Th fuel, other fuel cycles were investigated in this study from the proliferation resistance's perspective. These fuel cycles are: Low Enriched Uranium (LEU), uranium/thorium (U/Th), plutonium/ uranium /thorium (Pu/U/Th) and Enriched Reprocessed Uranium (RepU). Fig. 2 shows schematic material flow diagrams of the various fuel cycles, while Table 2 shows the wt% and the enrichments for the uranium-based fuels.

The values in Table 2 were estimated using a series of parametric calculations, in such a way to get the exit burnup equal to that of the Pu/Th fuel. For UOX and RepU fuels, the ratios between the enrichments in the inner and outer rings are the same as the ratio of the PuO_2 content between the two rings of Pu/Th fuel (1.25).

The isotopic vectors of the enriched uranium are given in Table 3. The weight percentage of the lighter isotopes will increase in each stage of the enrichment process. Two uranium isotopes that differ by a unit mass number (U-234/U-235), would have a 4:3 enrichment ratio [13].

The enrichment of U-235 needed to achieve the same exit burnup as the nominal Pu/Th fuel was estimated for each fuel cycle. By knowing the final U-235 needed, the weight percentages of U-234 and U-236 were estimated as mentioned above, and the remaining would be U-238.

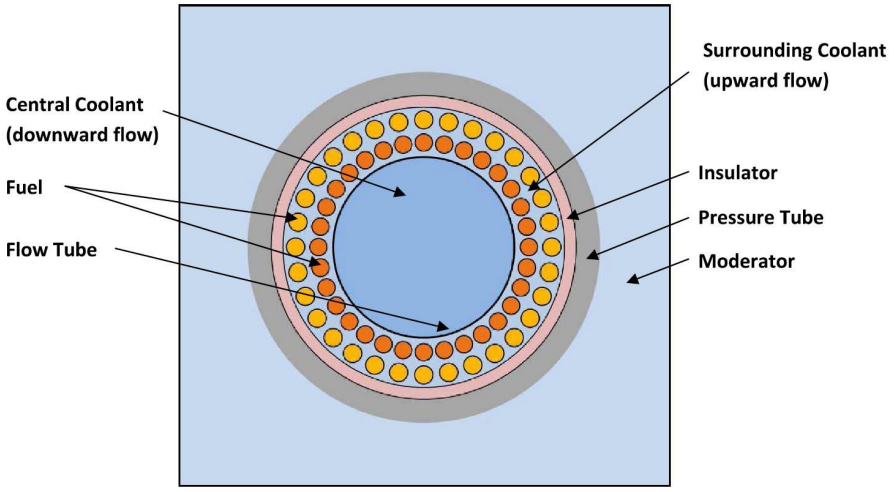

Fig 1. Cross-sectional view of the fuel channel of PT-SCWR.

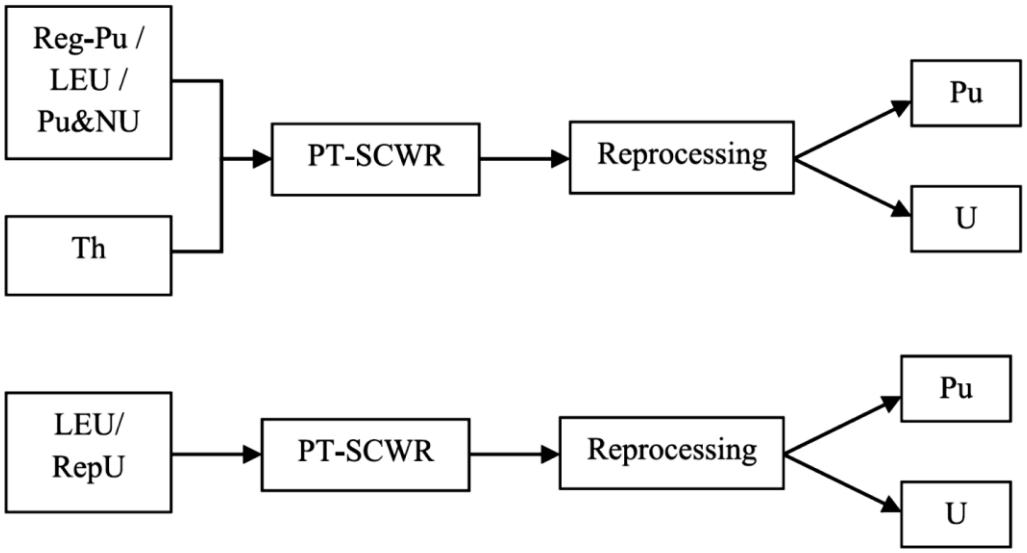

Fig. 2. Schematic material flow diagrams of thorium-based fuel (top) and uranium-based fuels (bottom).

Table 2. Ratio of UO_2/ThO_2 and U-235 enrichment for the investigated fuel cycles

Fuel Cycle	UO_2/ThO_2		U-235 enrichment	
	Inner rings	Outer rings	Inner rings	Outer rings
U/Th-48%	48%	38.4%	19.75%	19.75%
LEU	100%	100%	9.1%	7.28%
RepU	100%	100%	9.55%	7.64%

2.2. Computational methods

The parameters used to calculate the FOM of any material, as defined in Equation (1), depend on the isotopic vector of this material. The computer package SCALE 6.2.3 [14] was employed in this work to calculate the isotopic vector of the reprocessed plutonium and uranium fuels.

SCALE 6.2.3, developed by Oak Ridge National Laboratory (ORNL), is a verified and validated code used extensively for criticality safety, lattice physics and source-term calculations. It consists of different modules for different types of applications.

The irradiation of the different types of fuel used was performed in TRITON, which is a part of the SCALE package. TRITON has the advantage of modeling geometries and fuel compositions which are not provided within SCALE. The fuel has been irradiated to burnup of 60GWd/THM (Giga watt day per ton of heavy metals) using a constant power of 47.27 MW. Due to symmetry, only one-eighth of the lattice cell was modeled.

Due to the irregular configuration of the fuel pins in the PT-SCWR, Dancoff factors have to be calculated for resonance self-shielding. This was done using the MCDANCOFF module within SCALE 6.2.3. The calculated Dancoff factors for the inner and outer rings were 0.4395 and 0.3854, respectively. A 238 energy-group library based on ENDF/B-VII was used. All external boundaries were reflective.

Table 3. The isotopic vectors of the uranium in the different fuel cycles.

Fuel cycles	U-234	U-235	U-236	U-238
Natural uranium	0.006	0.711	0.003	99.279
Enriched uranium (9%)	0.107	9.0	0.031	90.862
Enriched uranium (19.75%) in U/Th	0.234	19.75	0.068	79.948
Reprocessed uranium (Not enriched)	0.015	0.521	0.543	98.920
Reprocessed uranium (Enriched to 9.55%)	0.375	9.550	7.458	82.618

The spent fuel was left to decay at the end of the irradiation period. The isotopic vectors of the Pu and U were calculated at different decay times, starting from the time of discharge from the reactor's core till one million years. The final decay time of one million years was chosen to investigate the attractiveness of the fissile materials after the final disposal of the spent fuel.

2.2.1 Bare Critical Mass

The Bare Critical Mass (BCM), parameter *M* in Equation (1), is the smallest mass of a fissile material required to sustain a nuclear chain reaction without neutron reflectors. As the sphere is the shape of minimum leakage and hence minimum critical mass, the BCM was estimated by finding the radius of a critical sphere. The criticality calculations were performed with the Monte Carlo code MCNP 6.1 [15].

MCNP 6.1, developed by Los Alamos National Laboratory, is a general-purpose code that can be used to transport different types of particles. The continuous-energy ENDF/B-VII.0 cross-section library was used for neutron transport. For criticality calculations 10,000 histories per cycle were used with 3000 active cycles. The critical radius was found by iteration. If it exceeded 20 m, the material was considered non-usable for weapons. The radius of the critical sphere was used to calculate its BCM.

2.2.2 Decay heat and gamma spectrum

The decay heat per kilogram of the fissile material, the parameter *h* in Equation (1), was calculated using the ORIGEN module of the SCALE package. The isotopic compositions of one kilogram of the fissile materials, Pu or U, obtained at different decay times, were used in an ORIGEN run to calculate decay heat, gamma spectrum and gamma strength. The decay heat estimated in this study corresponds to the heating caused by alpha, beta, and gamma radiation. Although the contribution of gamma radiation to the total decay heat is small, it was accounted for in this study [16].

2.2.3 Dose rate

The dose rate was estimated using MCNP 6.1 at one meter from the surface of a sphere with 20% of the BCM. The gamma spectrum and strength, as obtained from ORIGEN, were used in the MCNP file as the source definition. The tally's statistical error was kept below 1% by increasing the importance of the particles leaving the sphere and by transporting a large number of particles (2×10^8). The photoatomic library based on ENDF/B-VI.8 was used for photon transport.

2.2.4 Neutronic feedback coefficients.

The reactivity feedback coefficients for all proposed fuel cycles were calculated using:

$$\Delta\rho = (\rho_o - \rho_{per})/\Delta\alpha, \quad ((3)$$

where ρ_o and ρ_{per} are the unperturbed and perturbed reactivities (in *mk*), respectively, and $\Delta\alpha$ is the perturbed quantity, e.g. the temperature difference (in K) for coefficients involving a change in temperature.

The reactivity coefficients investigated here are the inner coolant void reactivity (ICVR), outer coolant void reactivity (OCVR), total coolant void reactivity (TCVR), fuel temperature coefficient (FTC) and moderator temperature coefficient (MTC). The temperatures of the fuel, inner and/or outer coolant were increased by 100 K, the coolant density in the inner and/or outer was decreased to 0.001 g/cm^3, the temperature of the moderator was increased by 20 K. For each perturbed condition, a new Dancoff factor was calculated.

3. Results and Discussion

3.1 Nominal Pu/Th Fuel Cycle

The FOMs of Pu and U reprocessed from the spent fuel of Pu/Th with discharge burnup of 60 GWd/THM were calculated and plotted in Fig. 3, as a function of the cooling time after the discharge from the core. The isotopic vector of the spent fuel at discharge is given in Table 4.

3.1.1 FOM of Pu

The FOM of reprocessed Pu was found to be dependent on the time of the reprocessing. It was less than 2.0, hence has medium attractiveness, for the first 100 years after discharge. It would be less attractive than Reg-Pu, which has a FOM of 2.13 [8]. After 100 years of decay, the FOM of Pu increases to 2.5 at 30,000 years of decay, then it decreases again to 2.02.

This is due to the variation of BCM and decay heat, which are dependent on the isotopic vector of reprocessed Pu, with the cooling time. Fig. 4 shows the mass of plutonium isotopes in the spent fuel, per THM, and the isotopic vector of the reprocessed Pu, at different cooling times. The absolute mass of each isotope in the spent fuel decreases due to radioactive decay, but due to the different half-lives of the different isotopes, the weight percentage of some isotopes increases. These figures show that after 100 years the main heating isotopes Pu-238 and Pu-240 start to decay, causing the reduction of decay heat and hence an increase of the FOM. However, the decay of Pu-239 caused the increase in BCM after 30,000 years; hence the decrease of the FOM (Fig. 5).

Therefore, the attractiveness level of Pu separated from Pu/Th fuel cycles would be medium only for the first 100 years, afterwards it would be high till at least one-million years.

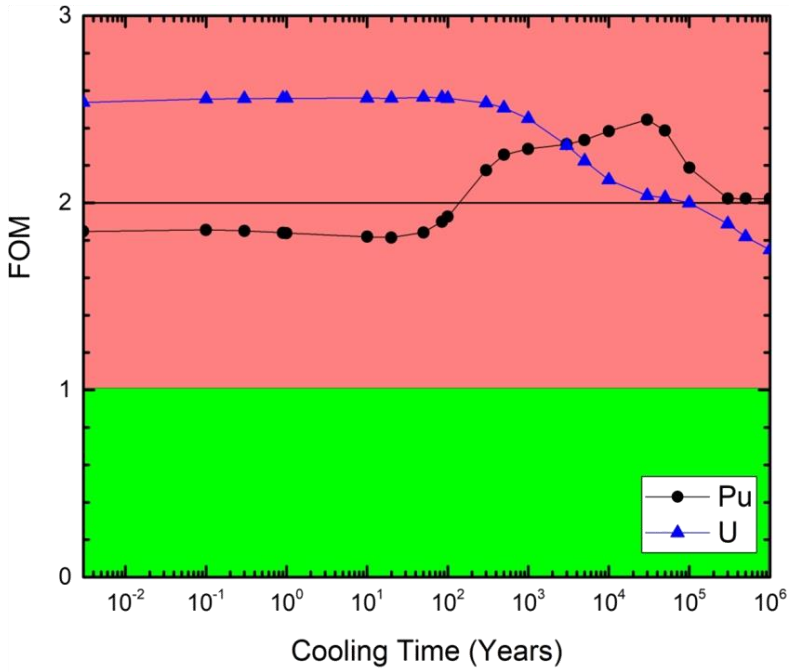

Fig. 3. FOM of Pu and U reprocessed from Pu/Th fuel as function of the cooling time.

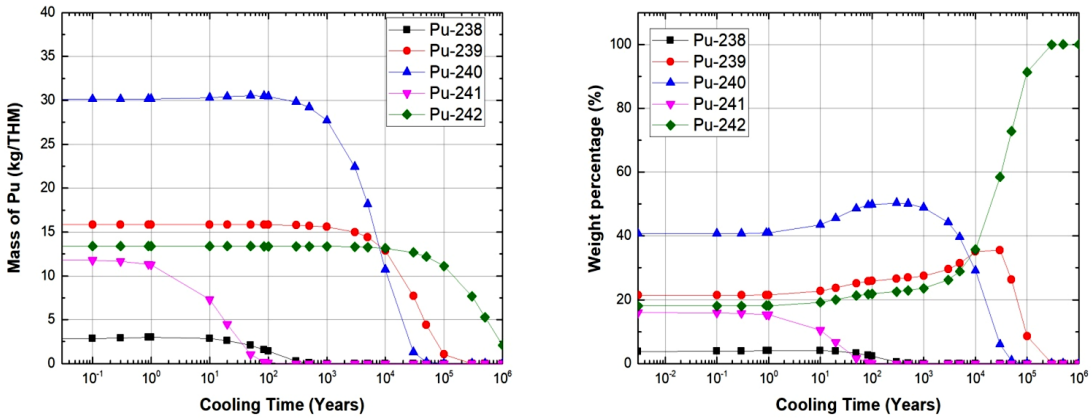

(a) (b)

Fig. 4. (a) Variation of the Mass of Pu isotopes in the spent fuel, (b) the isotopic vector of reprocessed Pu from Pu/Th fuel.

Table 4 The isotopic vector, in wt%, of reprocessed Pu and U from different fuel cycles

Fuel Cycle	Pu					U				
	Pu-242	Pu-241	Pu-240	Pu-239	Pu-238	U-238	U-236	U-235	U-234	U-233
Pu/Th	18.1	16.0	40.7	21.4	3.8	0.0	0.1	0.8	7.2	91.5
LEU (9.0% U-235)	5.5	12.4	28.3	51.7	2.0	96.7	1.1	2.2	0.1	0.0
U/Th (19.75% U-235)	5.7	14.1	23.9	52.7	3.5	88.4	2.8	6.4	0.4	2.0
Pu-Th-U (9% Nat-U)	4.5	11.3	24.7	49.7	9.9	89.2	8.0	2.6	0.3	0.0
Pu-Th-U (20% Nat-U)	17.0	15.6	39.6	24.1	3.7	88.7	0.1	0.4	0.8	10.0
Rep-U (9.55% U-235)	16.5	15.4	39.1	25.5	3.6	95.0	0.1	0.4	0.3	4.2

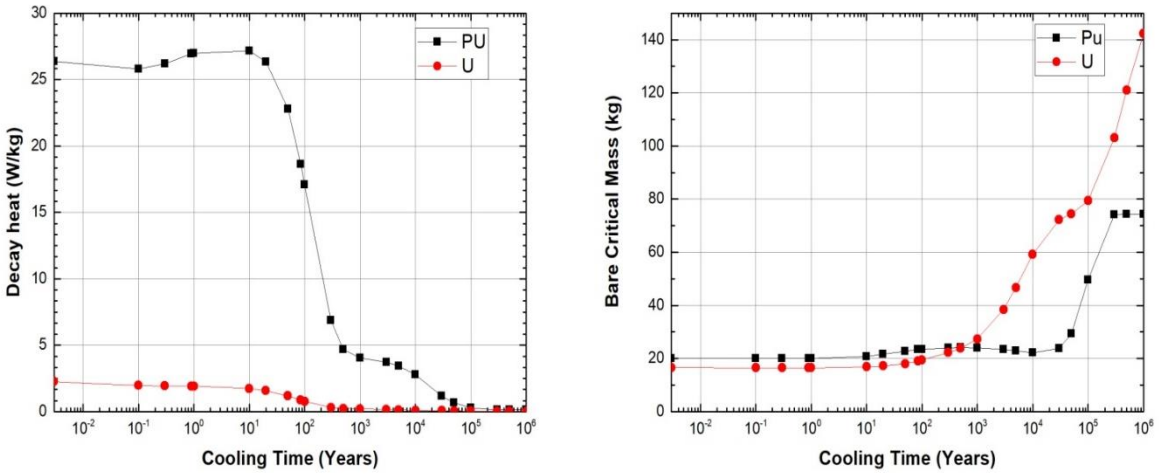

(a) (b)

Fig. 5. (a) Decay heat, (b) Bare critical mass of reprocessed Pu and U from Pu/Th fuel as function of cooling time.

3.1.2 FOM of U

The FOM of uranium reprocessed from the thorium fuel cycle was calculated earlier by Bathke et al. [17], but it was reported that the FOM for U-233 depends on the concentration of U-232 that co-exists with U-233 [18-19]. U-232 reduces the attractiveness of U-233, due to the high-energy gamma rays emitted from the progeny of U-232, mainly Tl-208 [20].

Fig. 6 (a) illustrates the ratio of U-232 (and its precursor Pa-232) to U-233 (and its precursor Pa-233) as a function of burnup. The concentration of U-232 increases with the burnup and reaches around 2500 ppm at the discharge burnup. Comparison with Fig.9 in [21] shows that the U-233 bred in the Pu/Th fuel used in PT-SCWR has less U-232 and is therefore more attractive, than that bred in thorium mixed with enriched uranium used in light water reactor (PWR), at a comparable burnup.

This is explained by the different neutron spectra of the different reactor designs, as the production of U-232 involves the (n,2n) reaction, which has an energy threshold of 6 MeV. The neutron energy spectrum of the PT-SCWR, as obtained from TRITON, is plotted in Fig. 6 (b). The fraction of the neutron spectrum with energy more than 6 MeV, shaded in Fig. 4 (b), is 0.4% while it is typically 0.8% in a PWR [21].

The FOM of uranium reprocessed from Pu/Th fuel used in the PT-SCWR, as shown in Fig 1. was 2.6, implying that it is a highly attractive material for weapons. Variation of the FOM with the cooling time shows no change of the FOM for the first 100 years. After that, the FOM decreases. This can be attributed to the increase of the BCM of the separated uranium due to the decrease of the weight percentage of U-233 (Fig. 7). This decrease was not related to the decrease of the U-233 mass, which was constant for the first 10,000 years (Fig. 7 (a)), but due to the increase of the mass of other uranium isotopes. Mainly of U-234 and U-236 which are the decay products of Pu-238 and Pu-240, respectively. The U-235 mass also shows an increase starting from 1000 years due to the decay of Pu-239. This increase of the fissile isotope U-235 partly offsets the decay of U-233 making it possible to find a BCM, even a large one, after this time of decay.

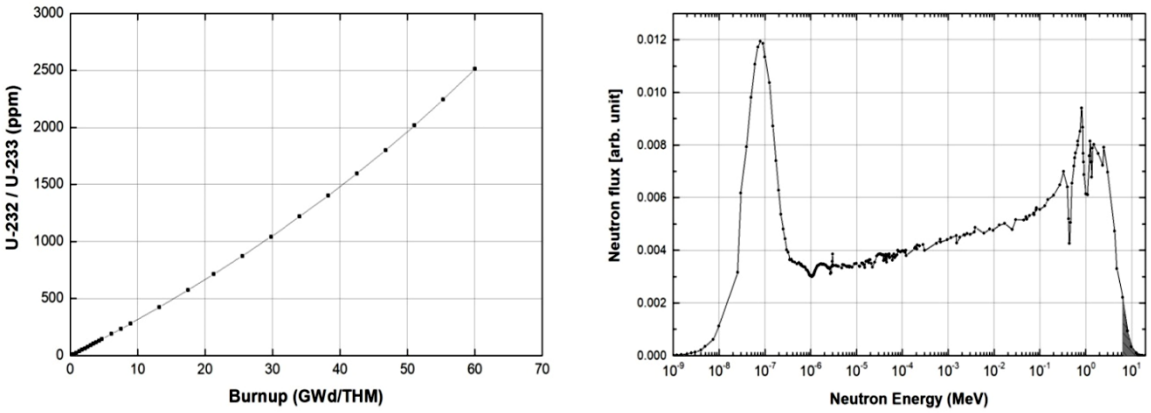

(a) (b)

Fig. 6. (a) The ratio of U-232 to U-233 as function of burnup, (b) the neutron energy spectrum of the PT-SCWR.

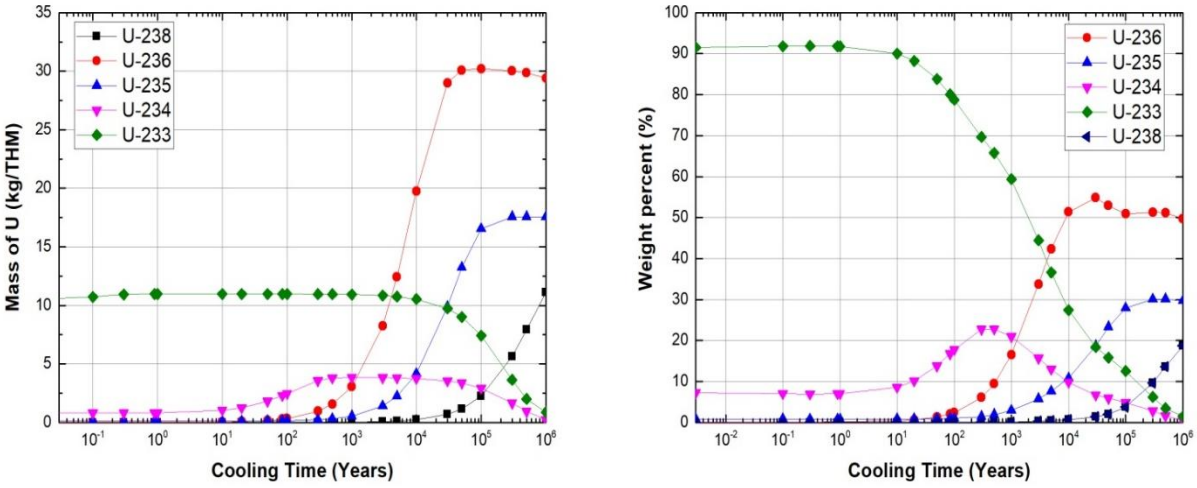

(a) (b)

Fig. 7. (a) Variation of the Mass of U isotopes in the spent fuel, (b) the isotopic vector of reprocessed U from Pu/Th fuel.

3.2 Pu/Th/U Fuel Cycle

The Pu/Th fuel cycle has the advantages of preserving the limited uranium resources and depleting the existing plutonium stockpiles. But, as indicated in the above discussion, it may pose a high proliferation risk. This is caused, partly, by the existence of the Reg-Pu in the fresh fuel, which is not as highly radioactive as the spent fuel would be. One fresh fuel assembly may contain enough plutonium for several nuclear weapons (this was one of the reasons for the worldwide declining interest in MOX [22]). In addition to that, the uranium in the spent fuel is a highly attractive material, with the highest FOM (higher than Reg-Pu and U-233 produced in PWR).

The proliferation risk of Pu/Th can be reduced by mixing the fresh fuel with uranium. This will denature U-233, making it unattractive for weapons, but at the same time more plutonium will be bred in the fuel due to the existence of U-238. In order to find the optimized amount of uranium to be added to Pu/Th, gradually increasing amounts of natural uranium (Nat-U) were added to Pu/Th fresh fuel. The PuO_2 weight percentages were the same as that of nominal Pu/Th, namely 15% and 12% in the inner and outer rings respectively, and the UO_2 was added at the expense of ThO_2. For each amount of the added Nat-U, the FOM of the uranium in the spent fuel was calculated. The minimum Nat-U which reduced FOM below one was considered as the optimal amount.

Fig. 8 illustrates the FOM of uranium and plutonium reprocessed from Pu/Th/U as a function of the cooling time. Adding Nat-U to Pu/Th did not change the attractiveness of the reprocessed plutonium but reduced the attractiveness of the uranium. By adding 9% of Nat-UO_2 to Pu/Th, the FOM of the uranium became less than 1.0; therefore, 9% of Nat-U was considered as the optimal value for Pu/Th/U.

Adding more Nat-U will reduce the FOM more, but more plutonium will be bred which counteracts the main advantages of using Pu/Th, namely to destruct the stockpiles of plutonium.

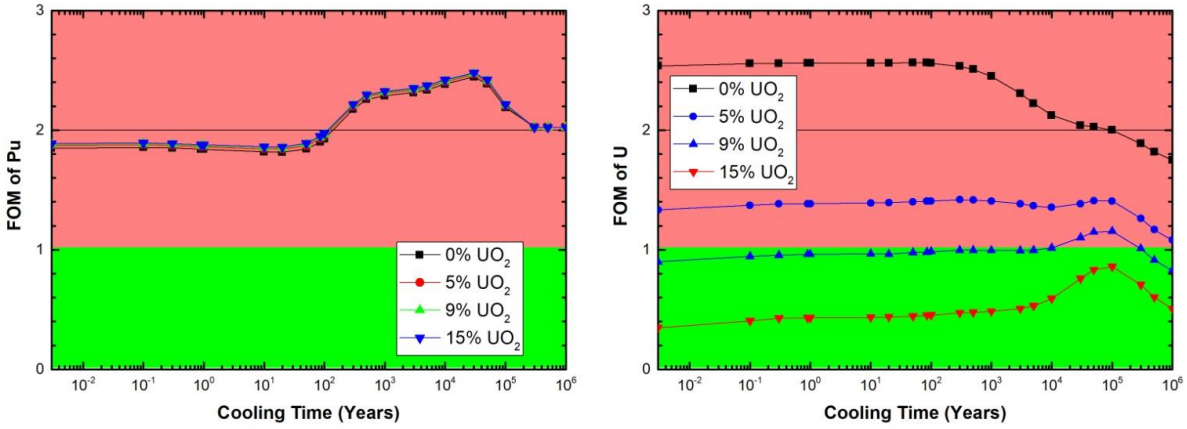

(a) (b)

Fig. 8. The FOMs of Pu and U reprocessed from Pu/Th/U fuel as function of cooling time for various Nat-U contents.

3.3 Uranium-based Fuel Cycles

Three different types of uranium-based fuel cycles were investigated and compared with the Pu/Th fuel cycle. These fuels are: Low-Enriched-Uranium (LEU), LEU mixed with thorium (U/Th), and re-enriched Reprocessed Uranium (Rep-U).

The FOM of plutonium reprocessed from these fuels is plotted in Fig. 9, along with that of Pu from Pu/Th for comparison. The Pu from U/Th was relatively less attractive than that reprocessed from LEU. This is due to the higher decay heat in U/Th, caused by the higher wt% of Pu-238 (Fig. 10). The higher wt% of Pu-238 in U/Th can be attributed to the higher enrichment of U/Th (higher wt% of U-235 and U-236) compared with LEU. These isotopes capture neutrons to form U-237 which decays to Np-237. Np-237 captures another neutron to form Np-238 which undergoes a beta decay to Pu-238.

Therefore, using LEU or U/Th would result in a more attractive Pu compared with that of Pu/Th but will eliminate the problem of U-233, which has the highest FOM. In addition to that, it will eliminate the threat of using the Reg-Pu in the fresh fuel for weapons as discussed before.

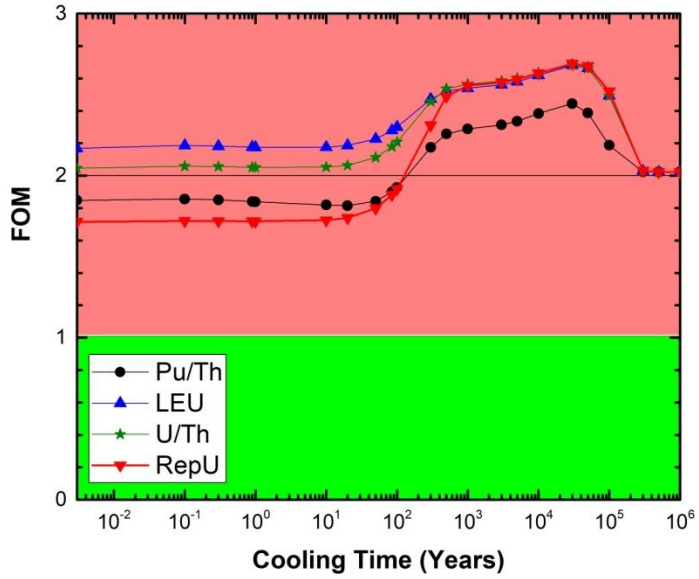

Fig. 9. FOM of Pu reprocessed from different uranium-based fuels as function of the cooling time.

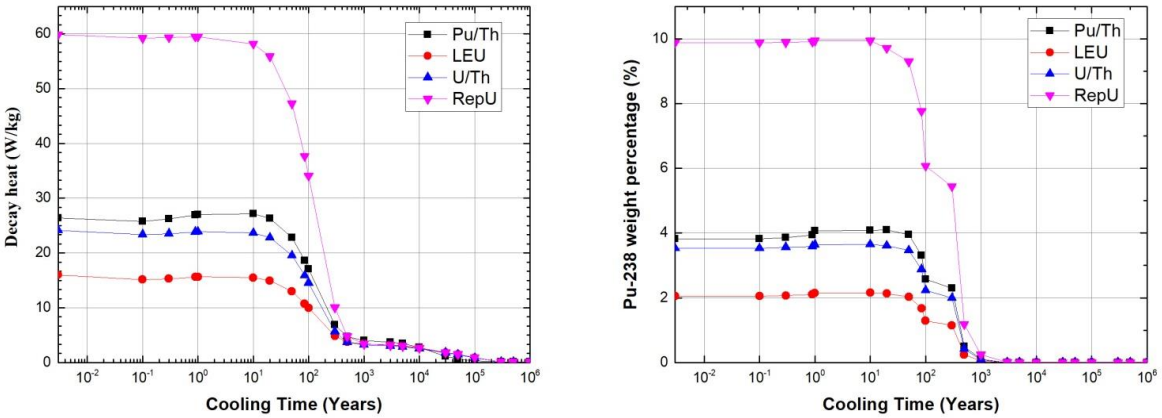

(a) (b)

Fig. 10. Decay heat (left) and wt.% of Pu-238 (right) in the reprocessed Pu from different uranium-based fuels.

The FOM of Pu generated from the spent fuel of Rep-U was the lowest FOM of Pu from all studied fuel cycles, as shown in Fig. 9, for the first 100 years. This will have both the advantage of reducing the preference of Pu in the spent fuel as well as eliminating the threat of using the Reg-Pu in the fresh fuel. Comparing the Pu in Pu/Th and Rep-U showed that the FOM reduced mainly as a result of the higher decay heat due to the higher weight percentage of Pu-238 in the reprocessed uranium (Fig. 10), which is in turn due to the higher U-236 content in the reprocessed uranium (Table 3).

3.4 Comparison of different fuel cycles

Table 5 summarizes the above-mentioned results by giving the FOM of both Pu and U, for fresh and for the first 100 years of spent fuel of all the studied fuel cycles. The different fuel cycles can be compared based on the maximum FOM of each fuel cycle (last column of Table 5). Using this criterion, the Reprocessed Uranium (Rep-U) is the most proliferation resistant fuel cycle, followed by LEU/Th, Pu/Th/U and LEU. The least proliferation resistant fuel cycle is Pu/Th.

This approach may ignore the fact that a specific fuel cycle could impose a higher proliferation risk if a highly attractive materials exist in both the fresh fuel and in the spent fuel, compared with a fuel cycle which only contains highly attractive material in the spent fuel. Therefore, another method is proposed here which can assess the proliferation resistance of both fresh and spent fuel.

In the proposed approach, the attractiveness of the whole cycle is represented by four letters according to the attractiveness of: Pu in fresh fuel; Pu in spent fuel; U in fresh fuel; and U in spent fuel. These letters are: “H” for high attractiveness (FOM >2); “M” for medium attractiveness (2 > FOM > 1); “L” for low attractiveness (1 > FOM > 0) and “VL” for very low attractiveness (FOM < 0).

For example, for Pu/Th fuel cycle, Pu in fresh and spent fuel has high and medium attractiveness respectively, while uranium in fresh and spent fuel would be N/A (no uranium in the fresh fuel) and high attractiveness respectively. Therefore, the Pu/Th can be described as (H-M-N/A-H).

As this qualitative description is not easy to interpret, and to ease the comparison between the different fuel cycles, a numerical system was proposed such that the numbers 0, 1, 2, and 3 were assigned to VL or N/A, L, M and H respectively. Hence for Pu/Th, the (H-M-N/A-H) would be (3+1+0+3) which is equal to 8. Note that this number is not simply the addition of the different FOMs of each material, but it is a number which can indicate how the whole fuel cycle (fresh and spent fuel) may impose a proliferation risk.

The application of this method and the resulting rank for each fuel cycle is shown in Table 5. The most proliferation resistant fuel cycle, for the first 100 years, was the Reprocessed Uranium (Rep-U), followed by LEU, then by U/Th. U/Th fuel has U-233 in the spent fuel with a FOM less than 1.0 but it is still in the "low" attractiveness category according to Table 1. This caused the total rank of U/Th to be higher than that of LEU.

Theoretically speaking, U/Th is less proliferation resistant than LEU but practically, both will have almost the same attractiveness for weapons; The choice between them can be based on other aspects (like cost, better resource utilization and the radiotoxicity of the spent fuel).

The Pu/Th/U fuel with 9% of Nat-U (optimized value) comes next in the ranking. Pu/Th/U can be in the same rank as the U/Th fuel cycle if 20% of Nat-U were added, but this decreases the destruction of the Pu in the fresh fuel and hence, increases the radiotoxicity of the spent fuel. The lowest-ranked fuel cycle, the one with the least proliferation resistance, was the proposed Pu/Th fuel cycle.

Table 5. FOM, attractiveness of Pu and U for the different fuel cycles proposed.

Fuel Cycle	Pu				U				Num. Rank	Max. FOM
	Fresh fuel		Spent fuel		Fresh fuel		Spent fuel			
	FOM	Atr.	FOM	Atr.	FOM	Atr.	FOM	Atr.		
Rep-U (9.55% U-235)	N/A	N/A	1.74	M	< 0	VL	N/A	N/A	2	1.74
LEU (9.0% U-235)	N/A	N/A	2.19	H	< 0	VL	N/A	N/A	3	2.19
U/Th (19.75% U-235)	N/A	N/A	2.08	H	1.0	L	0.33	L	5	2.08
Pu-Th-U (20% Nat-U)	2.13	H	1.85	M	< 0	VL	< 0	VL	5	2.13
Pu-Th-U (9% Nat-U)	2.13	H	1.85	M	< 0	VL	0.95	L	6	2.13
Pu/Th	2.13	H	1.81	M	N/A	N/A	2.56	H	8	2.56

3.5 Lattice Calculations

3.5.1 Effect of Adding Uranium to Pu/Th on the Reactivity and Exit Burnup

The effects of adding Nat-U at the expense of Th, on the reactivity of the fresh fuel and on the exit burnup of Pu/Th were investigated and discussed in this section. It was expected that adding Nat-U would increase the reactivity, given that Nat-U has 0.711 wt% of fissile isotope U-235. On the contrary, Nat-U reduced the reactivity as shown in Fig. 11(a).

The relative discrepancies between the four factors of Pu/Th/U and Pu/Th were calculated and plotted in Fig. 11 (b) Positive values mean that the corresponding factor is higher in Pu/Th/U than in Pu/Th and vice versa.

No significant change in the thermal utilization factor or fast fission factor is observed. The number of fission neutrons emitted per absorption (η) linearly increases with the amount of Nat-U content. This is due to existence of the fissile isotope U-235 at the expense of the fertile thorium. On the other hand, the resonance escape probability decreases with increasing the Nat-U content.

The range of the resonance absorption in U-238 extends to a higher neutron energy [23]. Accordingly, adding the Nat-U to Pu/Th decreases the reactivity of the fresh fuel due to the increase in the resonance absorption.

The exit burnup of Pu/Th/U, represented as a percentage of that of the nominal fuel, is demonstrated in Fig. 11 (c). The exit burnup decreases with increasing Nat-U content till 6 % when it starts to increase again. Adding 20% of Nat-U gives the same exit burnup as the nominal fuel. Although the reactivity of the fresh fuel decreases with adding Nat-U, the exit burnup shows a different behaviour. This is because of the competing effects of resonance absorption and the number of neutrons emitted per absorption *(η)*. At EOC, the Pu/Th/U would have larger amounts of the fissile isotopes U-235, Pu-239 and Pu-241 compared with Pu/Th, while U-233 would decrease in Pu/Th/U (due to the reduction of Th-232 content). The fission cross sections of U-235, Pu-239 and Pu-241 are higher than that of U-233 while the number of neutrons emitted per fission (ν) is higher for Pu-239 and Pu-241 compared with U-233 [24].

Accordingly, at the same burnup, η will increase with increasing the content of Nat-U. At small amounts of Nat-U, resonance absorption is the predominant effect, causing the reduction in the exit burnup. With larger amounts of Nat-U, more Pu-239 and Pu-241 will exist at EOC, causing an increase in the value of η and hence the burnup.

As mentioned before, adding 9% of Nat-U was chosen as the optimal value to render the uranium in the spent fuel unattractive. This will decrease the exit burnup by about 10% which can be compensated for by increasing the wt% of PuO_2 to 15.1% and 12.08% in the inner and outer rings respectively, or by increasing the amount of Nat-U to 20%. The last option has the advantage of decreasing the FOM of uranium to a value less than zero, but at

the expense of the reduction in the destruction ratio of the Pu from 42% to 40% of the initial plutonium content (Fig. 11 (d)).

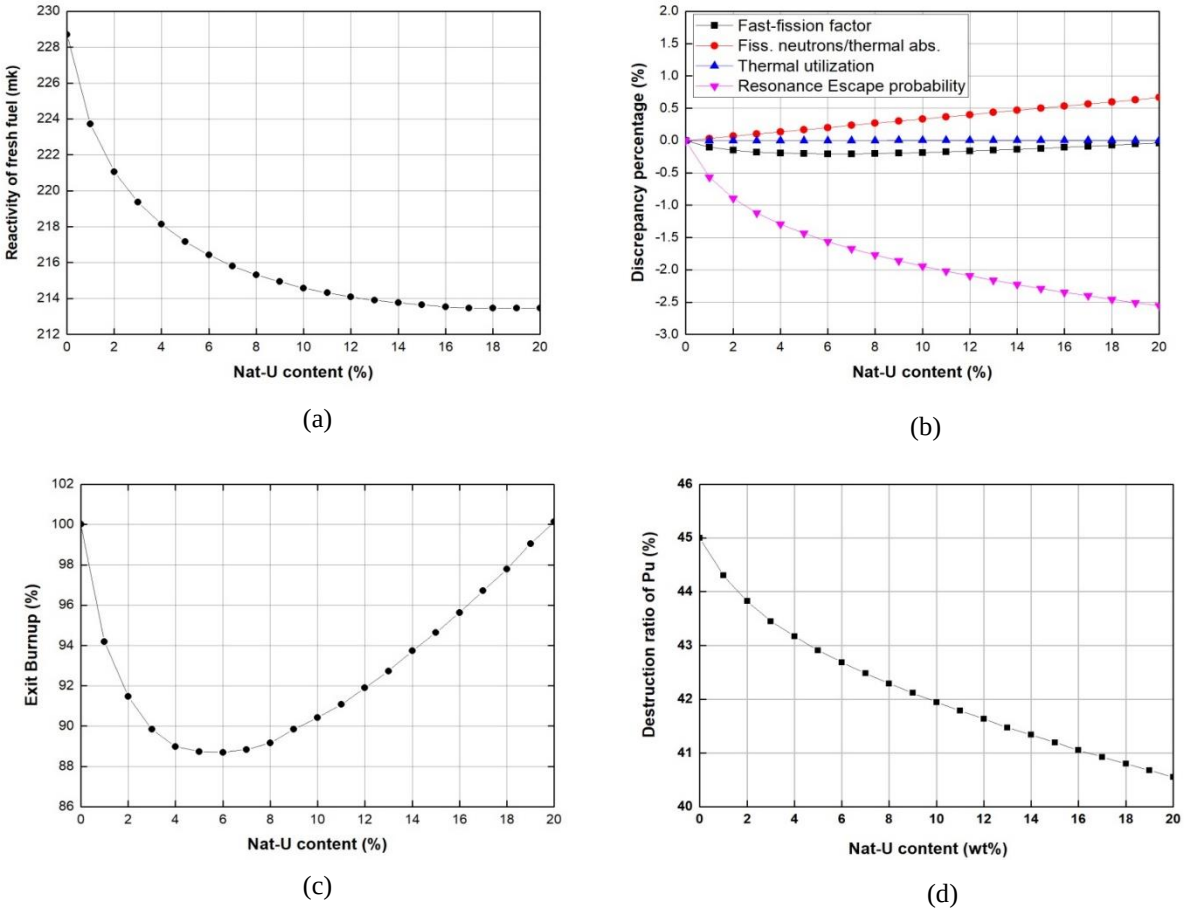

Fig. 11. (a) Reactivity of fresh fuel, (b) discrepancy of four-factors, (c) exit burnup and (d) destruction ratio of Pu of Pu/Th/U fuel as function of Nat-U content.

3.5.2 Reactivity Feedback Coefficients

The reactivity feedback coefficients for all proposed fuel cycles were calculated using equation (2) and are presented in this section in Table 6. The reactivity coefficients of all proposed fuels have the same sign which implies that all fuel cycles would behave in a similar way under transient conditions.

Voiding the inner coolant decreases the reactivity for all fuel cycles. Inner coolant contributes to the moderation. Therefore, voiding the inner coolant hardens the neutron spectrum, which causes an increase in the resonance absorptions. The fast fissions would increase the reactivity, but the reduction in reactivity due to resonance absorptions has a stronger effect.

Pu/Th/U fuel has the most negative value of ICVR. Adding Nat-U to Pu/Th increases the resonance absorptions due to the existence of U-238. Increasing the value of ICVR could be useful in the shutdown of the reactor in case of accidents.

Rep-U has a higher negative value of ICVR compared with LEU. This is because of the higher resonance absorptions in Rep-U due to the existence of U-234 and U-236 in larger quantities compared with that in LEU, given that U-234 and U-236 have higher capture cross sections than U-238 [24].

The combined effect of voiding the inner and outer coolant is dominated by the effect of voiding the inner coolant only, due to the low nominal density of the outer coolant.

Regarding FTC and MTC, no significant difference was found between the different fuel cycles. The reactivity decreases with increasing the fuel temperature due to the Doppler effect. It increases with the temperature of the moderator due to the increase in the thermal utilization. The absorptions of neutrons in the moderator decreases with increasing the moderator temperature [25-26].

Table 6. Reactivity feedback coefficients for various fuel cycles

Fuel Cycle	ICVR (mk)	OCVR (mk)	TCVR (mk)	FTC (pcm/K)	MTC (pcm/K)
Pu/Th	-20.66	4.84	-13.51	-1.1	2.0
Pu-Th-U (9% Nat-U)	-25.22	5.18	-17.13	-1.3	2.1
Rep-U (9.55% U-235)	-16.24	3.85	-11.54	-0.8	1.6
LEU (9.0% U-235)	-12.83	3.34	-9.65	-0.6	1.6
U/Th (19.75% U-235)	-20.02	3.36	-16.90	-1.0	1.8

4. Conclusion

The material attractiveness of Pu/Th fuel, proposed for the Canadian concept of Super-Critical Water Reactors, was evaluated using the Figure-of-Merit methodology proposed by Bathke et al. The plutonium produced in Pu/Th fuel cycle was found to be less attractive for weapons than the reactor-grade plutonium. This was true for the first 100 years after the discharge from the reactor. After 100 years, and due to the decay of Pu-238, the FOM of Pu increased making Pu highly attractive for weapons. In addition to Pu, the uranium bred in the spent fuel was highly attractive with a FOM value of 2.6.

The material attractiveness of LEU, U/Th, RepU and Pu/Th/U was investigated as well. The Pu reprocessed from LEU and U/Th was more attractive than that from Pu/Th, but the highly attractive U-233 was not produced in these two fuel cycles.

The Pu from RepU was the least attractive Pu from all the studied fuel cycles for the first 100 years after discharge. Regarding Pu/Th/U fuel, the optimal amount of Nat-U, added to Pu/Th to render the uranium unattractive, was found to be 9%.

A ranking system to compare the attractiveness of the various fuel cycle, which takes into account the attractiveness of the fresh fuel as well, was proposed. RepU was found to be the most proliferation resistant fuel cycle, for the first 100 years of decay, due to its high content of heat-producing Pu-238. LEU and U/Th came next, followed by Pu/Th/U (which can be on the same rank as LEU and U/Th by adding more uranium). Pu/Th/U has the advantage of destruction of the stockpile of Pu and the reduction of the toxicity of the spent fuel. The least proliferation resistant fuel cycle was the nominal Pu/Th one, due to the existence of highly attractive materials in both the fresh and spent fuel.

Adding Nat-U to Pu/Th decreased the initial reactivity of fresh fuel due to the resonance absorption in U-238. The exit burnup decreased at the beginning with adding Nat-U, then it started to increase again. 20% of Nat-U was found to give the same burnup as Pu/Th. The optimal value of 9% of Nat-U decreased the exit burnup by 10% which can be compensated by increasing the wt.% of PuO_2 from 15% to 15.1% and from 12% to 12.08% in the inner and outer rings respectively.

Investigation of the reactivity coefficients of the studied fuel cycled showed that all fuels have the same sign of reactivity feedback. Regarding CVR, the Pu/Th/U will have the most negative value which will help to bring the core to a safe state faster in case of an accident. The fuel and moderator temperature coefficients did not show significant differences between the fuels studied.

The present study may assist the designers in choosing the best fuel cycle. However, this study shows that all fuel cycles are suitable for the PT-SCWR, and the choice may be based on other criteria. For example, Pu/Th can be used in states which do not pose proliferation risks (like nuclear weapons states), while another more proliferation resistant fuel cycle may be used in other states.

5. Acknowledgments

The authors would like to thank Dr. Jeremy Pencer, for his valuable comments and suggestions. This work was partly funded by the University Network of Excellence in

Nuclear Engineering (UNENE), Canada and by the Natural Sciences and Engineering Research Council of Canada (NSERC), under grant no. RGPIN-2020-06897.

6. References

[1] US DOE, A technology roadmap for generation IV nuclear energy systems, https://www.gen-4.org/gif/jcms/c_40481/technology-roadmap (2002).

[2] J. Pencer, A. Colton, Progression of the lattice physics concept for the Canadian supercritical water reactor, in: 34th Annual Conference of the Canadian Nuclear Society, Toronto, Canada, June 9-12, 2013.

[3] INTERNATIONAL ATOMIC ENERGY AGENCY, Guidance for the Application of an Assessment Methodology for Innovative Nuclear Energy Systems, IAEA-TECDOC-1575 Rev.1, IAEA, Vienna (2009). https://www.iaea.org/publications/8158/guidance-for-the-application-of-an-assessment-methodology-for-innovative-nuclear-energy-systems.

[4] Generation IV International Forum, Evaluation methodology for proliferation resistance and physical protection of Generation IV nuclear energy systems, Rev. 6, (2011).

[5] W.S. Charlton, R.F. Lebouf, C. Gariazzo, D.G. Ford, C. Beard, S. Landsberger, M. Whitaker, Proliferation resistance assessment methodology for nuclear fuel cycles, Nucl. Technol. 157 (2007) 143–156. https://doi.org/10.13182/NT07-A3809.

[6] T. Aoki, H. Sagara, C.Y. Han, Material attractiveness evaluation of inert matrix fuel for nuclear security and non-proliferation, Ann. Nucl. Energy. 126 (2019) 427–433. https://doi.org/10.1016/j.anucene.2018.10.063.

[7] Y. Kimura, M. Saito, H. Sagara, Evaluation of Proliferation Resistance of Plutonium Based on Decay Heat, J. Nucl. Sci. Technol. 48 (2011) 715–723. https://doi.org/10.1080/18811248.2011.9711754.

[8] C.G. Bathke, B.B. Ebbinghaus, B.A. Collins, B.W. Sleaford, K.R. Hase, M. Robel, R.K. Wallace, K.S. Bradley, J.R. Ireland, G.D. Jarvinen, M.W. Johnson, A.W.

Prichard, B.W. Smith, The attractiveness of materials in advanced nuclear fuel cycles for various proliferation and theft scenarios, Nucl. Technol. 179 (2012) 5–30. https://doi.org/10.13182/NT10-203.

[9] Y. Kimura, M. Saito, H. Sagara, C.Y. Han, Evaluation of proliferation resistance of plutonium based on spontaneous fission neutron emission rate, Ann. Nucl. Energy. 46 (2012) 152–159. https://doi.org/10.1016/j.anucene.2012.03.032.

[10] INTERNATIONAL ATOMIC ENERGY AGENCY, IAEA Safeguards Glossary, International Nuclear Verification Series No. 3, IAEA, Vienna (2003).

[11] W. Peiman, I. Pioro, K. Gabriel, Thermal-Hydraulic and Neutronic Analysis of a Reentrant Fuel-Channel Design for Pressure-Channel Supercritical Water-Cooled Reactors, J. Nucl. Eng. Radiat. Sci. 1 (2015). https://doi.org/10.1115/1.4026393

[12] R. Ibrahim, A. Buijs, J. Luxat, A simplified core model of the SCWR, in: 39th Annual Conference of the Canadian Nuclear Society and 43rd Annual CNS/CAN Student Conference, Ottawa, Canada, June 23-29, 2019.

[13] C.H.M. Breeders, G. Kessler, Fuel cycle options for the production and utilization of denatured plutonium, Nucl. Sci. Eng. 156 (2007) 1–23. https://doi.org/10.13182/nse07-a2681.

[14] Rearden, B.T., Jessee, M.A., 2018. SCALE Code System, Oak Ridge National Laboratory. ORNL/TM-2005/39, Version 6.2.3.

[15] Goorley, J.T., James, M.R., Booth, T.E., Brown, F.B., Bull, J.S., Cox, L.J., Durkee Jr, J.W., Elson, J.S., Fensin, M.L., Forster III, R.A. and Hendricks, J.S. Initial MCNP6 release overview-MCNP6 version 1.0 (No. LA-UR-13-22934). Los Alamos National Lab.(LANL), Los Alamos, NM (United States). https://doi.org/10.2172/1086758.

[16] C. Lloyd, B. Goddard, Proliferation resistant plutonium: An updated analysis, Nucl. Eng. Des. 330 (2018) 297–302. https://doi.org/10.1016/j.nucengdes.2018.02.012.

[17] H.R. Trellue, C.G. Bathke, P. Sadasivan, Neutronics and material attractiveness for PWR thorium systems using monte carlo techniques, Prog. Nucl. Energy. 53 (2011) 698–707. https://doi.org/10.1016/j.pnucene.2011.04.007.

[18] C.G. Bathke, R.K. Wallace, K.R. Hase, B.W. Sleaford, B.B. Ebbinghaus, B.W. Collins, K.S. Bradley, A.W. Prichard, B.W. Smith, An assessment of the attractiveness of material associated with thorium/uranium and uranium closed fuel cycles from a safeguards perspective, in: Annual Meeting of the Institute of Nuclear Materials Management (INMM), Baltimore, United States, July 11-15, (2010).

[19] C. Lloyd, B. Goddard, R. Witherspoon, The effects of U-232 on enrichment and material attractiveness over time, Nucl. Eng. Des. 352 (2019) 1–6. https://doi.org/10.1016/j.nucengdes.2019.110175.

[20] R. Moir, U232 nonproliferation features, Lawrence Livermore National Lab.(LLNL), (2010), LLNL-TR-438648.

[21] J. Kang, F.N. von Hippel, U-232 and the proliferation-resistance of U-233 in spent fuel, Sci. Glob. Secur. 9 (2001) 1–32. https://doi.org/10.1080/08929880108426485.

[22] A. Kuperman, Plutonium for Energy?: Explaining the Global Decline of MOX : a Policy Research Project of the LBJ School of Public Affairs, University of Texas at Austin, Nuclear Proliferation Prevention Project, 2018.

[23] Nuclear Data Center at KAERI, Table of Nuclides. http://atom.kaeri.re.kr/.

[24] A.L. Nichols, M. Verpelli, D.L. Aldama, Handbook of nuclear data for safeguards: database extensions, August 2008, IAEA.

[25] A. Moghrabi, D.R. Novog, Investigation Of Reactor Physics Phenomena In The Canadian Pressure Tube Supercritical-Water Reactor, CNL Nucl. Rev. 5 (2016) 253–268. https://doi.org/10.12943/CNR.2016.00031.

[26] E.M. Glanfield, Lattice Physics Calculations for Alternative Fuels for the Canadian SCWR, MA.Sc thesis, McMaster University, 2017.

Chapter 7 Conclusions and Future Work

The Canadian concept of Super Critical Water Reactor, which is one of the GEN-IV reactor systems is known as PT-SCWR. It uses a mixture of reactor-grade plutonium and thorium as a fuel, in a once-through cycle. The motivation beyond using Pu/Th was preserving the limited uranium ore and, hence, enhancing the sustainability of nuclear energy, which is one goal of the Gen-IV nuclear system.

Using a mixture of Pu/Th in the whole core is a unique feature of PT-SCWR as no other reactor is running solely on this fuel. But in fact, using Pu/Th as fuel is accompanied by different challenges. As the safety of using this new fuel in PT-SCWR was the subject of numerous research, the implication of using Pu/Th on the long-term waste management in Canada, and the risk associated with proliferation are needed to be assessed as well. The reasons for that are associated with the goals of GEN-IV. Reduction of the burden of long-term management is another goal that falls under the umbrella of sustainability and increasing the proliferation resistance is a crucial goal of GEN-IV given that PT-SCWR is a power-generating rector and, therefore, it is expected to be promoted commercially. These are the main research areas of this thesis. The summary and conclusion of each part are given in the next sections.

7.1 Implication of Pu/Th on the DGR design and criticality safety

The Canadian's plan for long-term waste management is to package the spent fuel into suitable canisters and store them in an underground deep geological repository, excavated in suitable stable rock formations, with the ability to retrieve the spent fuel if needed. As the fleet of nuclear reactors in Canada is of CANDU type, the Canadian's design of DGR was done assuming that the spent fuels are low-burnup CANDU bundles. A previous study showed that the high burnup spent fuel, from European Pressurized Reactor (EPR), can be stored in the Canadian DGR with some modification in the design, but the total DGR size for both are comparable.

By proposing the PT-SCWR as a once-through fuel cycle, the spent Pu/Th fuels are assumed to go to the DGR for final disposal. The implications of this scenario on the design of the Canadian DGR and the criticality safety were the subject of Chapter 4 (paper #1). Pu/Th fuel has higher decay heat than uranium and it is expected that it would need a larger repository.

The Canadian's DGR is a network of underground horizontal tunnels where the canisters, containing the spent fuel, are stored inside boreholes drilled vertically inside each tunnel. The distance between the canisters and between different tunnels, which determine the size of the DGR, should be chosen such that the thermal criterion for the design of DGR is not violated. The thermal criterion is that the maximum temperature of the bentonite in contact with the canister should be less than 100 °C. As a safety margin, the maximum temperature was chosen to be 90 °C in this work, giving 10 °C.

The thermal analysis of the repository was performed using the computer code CODE-BRIGHT, which is used before for the thermal analysis of the Canadian and Swedish DGR. The whole repository is divided into repeated unit cells. A unit cell is considered as a representation for the whole repository using the appropriate boundary conditions.

The geometry of the unit cell is modeled in CODR-BRIGHT. The thermal load of the canister, as a function of cooling time, is needed as an input.

The thermal power of the canisters depends on the number of channels inside the canister and their decay heat. To get the decay heat, as a function of colling time, after discharge from the reactor, the unit cell of PT-SCWR was modeled using SCALE/TRITON for the burnup calculations. At the end of the life of the channel inside the reactor, the decay heat as a function of cooling time was estimated using SCALR/ORIGEN.

The minimum canister spacing was estimated for different scenarios. The investigated cases involved different cooling times, between 60 and 150 years after discharge from the reactor, and different numbers of channels per canister, three, four, and five channels per canister. For comparison, the size of the repository if uranium-oxide fuel was used in PT-SCWR instead of Pu/Th was calculated as well.

It was found that switching to Pu/Th fuel will increase the size of the repository between three to four times compared with uranium oxide fuel. The conclusions for different cases for Pu/Th fuel are:

- For the same initial power of the canister, but using more channels per canister, a larger canister spacing will be required, but the overall size of the repository will be reduced. Using four or five channels per canister would reduce the size of the repository by 9 % or 16 % compared with using three channels per canister. This will, however, require longer cooling times. For five channels per canister and a cooling time of 110 years, the size of the repository will be 3.6 times larger than that of uranium fuel.
- For the same cooling time, using fewer channels per canister would decrease the size of the repository (due to the reduced initial power of the canister), but the reduction in the size of the repository will require increased cost for the extra canisters needed and extra excavation costs (134 and 101 boreholes are needed for three and four channels per canister respectively).

Correlations between the minimum canister spacing and the initial power of the canister (cooling time) were proposed, by fitting the data of simulation, for three, four, and five channels per canister. Also, it was found that two canisters with the same initial power, but different rates of power decay, will not give the same required minimum canister spacing. This is the reason that each case had to be modeled individually.

As the Pu/Th canister would be stored in the storage area before the final underground disposal, the criticality safety should be evaluated. this was done using the computer code MCNP, assuming fresh fuel and water-filled canisters. this represents the most reactive conditions. The effective neutron multiplication factor was found to be $0.84327 \pm 1.3\times10^{-4}$ and $0.85811 \pm 1.3\times10^{-4}$for Pu/Th and uranium fuel, which are both less than the criticality safety limit of 0.95, without taking any fuel burnup credit.

A quantitative estimate and optimization of the Canadian DRG size, when Pu/Th spent fuel is stored, is the main accomplishment of this study. Alongside excluding the hazardous of criticality accidents for spent fuel from PT-SCWR.

7.2 Occupational and public safety

As Pu/Th will contain ^{232}U which is a hard gamma emitter, the implications on the occupational safety of workers in DGR were worth to be assessed.

A comparison between the Pu/Th and other fuel cycles, namely, LEU/Th (two LEU/Th fuels with different enrichments and different UO_2/ThO_2 ratios), and the regular LEU was also made. The enrichment of ^{235}U in LEU/Th and LEU was adjusted to give the same exit burnup of the proposed Pu/Th fuel, namely 60 GWd per ton of heavy metals (THM).

The gamma and neutron source terms were estimated using SCALE/ORIGEN. These source terms were used inside MCNP in a fixed-source simulation to calculate the dose rate at different distances from a fuel channel and a canister holding four channels per canister in case of Pu/Th and twelve channels per canister for uranium-based fuel.

For the first 100 years, the gamma source term was almost the same for all studied fuels. This is because, for the first 100 years, the main contribution to the gamma is the fission products. Although the gamma emissions were almost the same for all fuels after 50 years of decay, the gamma dose rate to the workers from exposure to Pu/Th fuel was 8% higher than that of LEU, and hence 13% thicker shielding was found to be needed. This is due to the hard gammas emitted from ^{208}Tl and ^{244}Cm.

Comparing LEU/Th with LEU, it was found that a 5% higher gamma dose resulted from U/Th due to high-energy gammas from ^{208}Tl. Around 10% thicker shielding will be needed. In addition to the higher occupational dose for LEU/Th fuel, it did not show any better utilization of the uranium ore as more uranium will be needed given the higher enrichment needed for LEU/Th fuel cycle.

The neutron dose rate of the Pu/Th fuel is the highest dose rate of all fuels studied.

In addition to the occupational doses, the effect of storing Pu/Th on the post-closure safety of the DGR was investigated by estimating the peak dose rate to the public in case of a simultaneous failure of several canisters.

It was found that the peak dose rate to the public will be 75% higher in the case of Pu/Th fuel than in uranium-based fuel. The root cause of that is the higher yield of the ^{129}I per fission from plutonium compared with that from uranium.

It is worth to emphasize that using Pu/Th will not cause the public's peak dose rate to exceed the recommended limit of 0.3mSv/a, but it will increase the dose to the public, and this increased dose has to be justified against the ALARA principle.

A novel contribution to the knowledge from this study was: 1) the estimation of the occupational and public dose rate when Pu/Th is stored inside the DGR; 2) using LEU/Th fuel instead of LEU did not show any improvement in the occupational dose rate or the utilization of the uranium ore; and Finally, Pu/Th can still be safely stored inside the DGR.

As the occupational dose is one of the metrics which can be used to compare different fuel cycles, the results of this study can help the decision makers in choosing the optimal fuel cycle for the Gen-IV PT-SCWR.

7.3 Assessment of proliferation resistance

PT-SCWR is a commercial concept, and it is expected that Canada will try to sell it to other countries, therefore, proliferation risk must be carefully investigated. Giving another country fresh fuel with is made from plutonium, even if it is reactor-grade, but it is still a potentially explosive material [70], poses a challenge from the proliferation point of view.

In addition to that, the spent fuel of Pu/Th will contain ^{233}U which is also a material that can be used to construct nuclear weapons.

Assessment of the proliferation resistance of Pu/Th fuel and comparison with other fuels was the goal of this study. The attractiveness of Pu/Th for weapons usage was evaluated using the Figure-of-Merit (FOM) methodology. It was compared to the attractiveness of other fuel cycles namely, Low Enriched Uranium (LEU), LEU/Th, Re-enriched Reprocessed Uranium (RepU), and Pu/Th/U. The neutronic properties of the investigated fuels were checked as well.

The isotopic vector, heat content, and gamma source term of each nuclear material were calculated, as a function of cooling time, using SCALE/ORIGEN. The bare critical mass and dose rate, which are needed as part of FOM, were estimated using MCNP.

The plutonium produced in Pu/Th fuel cycle was found to be less attractive for weapons than the reactor-grade plutonium. This was true for the first 100 years after the discharge from the reactor. After 100 years, and due to the decay of ^{238}Pu, the FOM of Pu, from the spent fuel of Pu/Th, increased making it highly attractive for weapons. In addition to Pu, the uranium bred in the spent fuel was found to be highly attractive for weapons.

The Pu reprocessed from LEU and LEU/Th was more attractive than that from Pu/Th, but the highly attractive ^{233}U was not produced in these two fuel cycles. The Pu from RepU was the least attractive Pu of all the studied fuel cycles for the first 100 years after discharge. Regarding Pu/Th/U fuel, the optimal amount of Nat-U, added to Pu/Th to render the uranium unattractive, was found to be 9%.

A ranking system to compare the attractiveness of the various fuel cycle, which considers the attractiveness of the fresh fuel as well spent fuel, is a major contribution of this work.

According to this ranking system, RepU was found to be the most proliferation-resistant fuel cycle, for the first 100 years of decay, due to its high content of heat-producing ^{238}Pu. LEU and LEU/Th came next, followed by Pu/Th/U (which can be on the same rank as LEU and LEU/Th by adding more uranium). Pu/Th/U has the advantage of the destruction of the stockpile of Pu and the reduction of the toxicity of the spent fuel.

The least proliferation-resistant fuel cycle was the nominal Pu/Th one, due to the existence of highly attractive materials in both the fresh and spent fuel.

Adding Nat-U to Pu/Th decreased the initial reactivity of fresh fuel due to the resonance absorption in ^{238}U. The exit burnup decreased at the beginning with adding Nat-U, then it started to increase again. 20% of Nat-U was found to give the same burnup as Pu/Th. The optimal value of 9% of Nat-U decreased the exit burnup by 10% which can be compensated by increasing the wt.% of PuO^2 from 15% to 15.1% and from 12% to 12.08% in the inner and outer rings respectively.

Investigation of the reactivity coefficients of the studied fuel cycles showed that all fuels have the same sign of reactivity feedback. Regarding CVR, the Pu/Th/U will have the most negative value which will help to bring the core to a safe state faster in case of an accident. The fuel and moderator temperature coefficients did not show significant differences between the fuels studied.

7.4 Conclusions and recommendations for future work

In this section, the author mentioned the conclusions of the analysis done in this thesis and recommendations for future work.

As everything has pros and cons, using Pu/Th in PT-SCWR will increase sustainability by reducing the amount of uranium ore mined. This is true as there are stockpiles of Pu from weapons and from reprocessing of the spent fuel from current reactors. But this is not a panacea for sustainability, as, to get plutonium, uranium has to be burned first inside the reactor.

According to the results of this thesis, Pu/Th will increase the size of the repository, and hence the cost, by three to four times. Pu/Th will cause an increase in the radiological doses to the workers and the public, but it will not exceed the regulatory limits. Pu/Th is a very attractive material for weapons especially as fresh fuel and, hence, poses a proliferation risk.

As part of this thesis, other fuel cycles were studied as an alternative to Pu/Th and LEU. Using LEU/Th did not show any surplus behavior compared with LEU. During the proliferation analysis, another fuel cycle was proposed, which is reprocessed uranium (RepU). It showed a better proliferation resistance and sustainability (by reduction of the new uranium ore and reduction of decay heat of spent fuel compared to Pu/Th).

RepU needs to be enriched and can have its technical challenges as well. Therefore, a recommendation for future work is to investigate the safety and feasibility of using RepU in the PT-SCWR. A complete analysis of the costs for each fuel cycle can also help in choosing the optimal fuel cycle, especially economy is one goal of GEN-IV.

Another proposed fuel was Pu/Th/U. it helped in increasing the proliferation resistance by eliminating the proliferation risk of ^{233}U, but the risk associated with the fresh fuel would still exist. Using natural or depleted uranium mixed with Pu/Th should be investigated from a safety point of view.

Finally, this study shows that all fuel cycles are suitable for the PT-SCWR, and the choice may be based on other criteria. For example, Pu/Th can be used in states which do not pose proliferation risks (like nuclear weapons states), while another more proliferation-resistant fuel cycle may be used in other states.

It is worth repeating that all the above analyses were done assuming a once-through fuel cycle. All the results would change in case of a closed fuel cycle. Investigating the feasibility of a closed fuel cycle is also a recommendation for the future. This can help in sustainability by extracting the ^{233}U from Pu/Th. In this case, a detailed plan should exist that defines clearly how many cycles should be run using Pu and then switch to ^{233}U/Th. This is another study.

Switching to a close cycle is a political decision as well. As Canada has no interest in reprocessing, it might be hard to switch to a closed cycle. The prospects and challenges associated with the closed cycle may be worth some study as well.

References

[1] INTERNATIONAL ATOMIC ENERGY AGENCY, "Nuclear Power Reactors in the World," IAEA, Vienna, Reference Data Series No. 2, 2019.

[2] S. Goldberg and R. Rosner, "Nuclear reactors: Generation to generation", Cambridge: American academy of arts and sciences, 2011.

[3] J. G. Marques, "Review of Generation-III/III+ Fission Reactors," *Nuclear Energy Encyclopedia*. pp. 231–254, Aug. 12, 2011, doi: https://doi.org/10.1002/9781118043493.ch22 .

[4] U. S. DoE, "A technology roadmap for generation IV nuclear energy systems," 2002, Accessed: July., 20, 2022. [Online]. Available: https://www.gen-4.org/gif/jcms/c_40481/technology-roadmap

[5] https://www.intechopen.com/chapters/40422 (accessed Jun. 20, 2022).

[6] Y. Oka, S. Koshizuka, Y. Ishiwatari, and A. Yamaji, *Super light water reactors and super fast reactors: supercritical-pressure light water cooled reactors.* New York: Springer Science+Business Media, 2010. https://doi.org/10.1007/978-1-4419-6035-1 .

[7] M. Yetisir *et al.*, "Canadian supercritical water-cooled reactor core concept and safety features," *CNL Nucl. Rev.*, vol. 5, no. 2, pp. 189–202, 2016.

[8] L. K. H. Leung and A. Nava-Dominguez, "Thermal-Hydraulics Program in Support of Canadian SCWR Concept Development," *J. Nucl. Eng. Radiat. Sci.*, vol. 4, no. 1, Dec. 2017, doi: https://doi.org/10.1115/1.4037807 .

[9] J. Li and M. Yetisir, "Systematic approach to the development of the Canadian SCWR reactor for design optimization," Canada, 2012. [Online]. Available: http://inis.iaea.org/search/search.aspx?orig_q=RN:49101504 .

[10] M. Yetisir, J. Pencer, M. McDonald, M. Gaudet, J. Licht, and R. Duffey, "The Supersafe© Reactor: A Small Modular Pressure Tube SCWR," *AECL Nucl. Rev.*, vol. 1, no. 2, pp. 13–18, Dec. 2012, doi: https://doi.org/10.12943/ANR.2012.00014 .

[11] Nuclear Waste Management Organization, "Choosing a Way Forward: The Future Management of Canada's Used Nuclear Fuel: Executive Summary Draft Study Report," Nuclear Waste Management Organization, Toronto, Canada, 2005.

[12] C. G. Bathke *et al.*, "The attractiveness of materials in advanced nuclear fuel cycles for various proliferation and theft scenarios," *Nucl. Technol.*, vol. 179, no. 1, pp. 5–30, 2012, doi: https://doi.org/10.13182/NT10-203 .

[13] N. Tsoulfanidis and S. Landsberger, *Measurement and detection of radiation*, 5th ed. CRC press, 2021.

[14] G. F. Knoll, *Radiation detection and measurement*, 4th ed. John Wiley & Sons, 2010.

[15] H. Wollersheim. (2020). Particle and Radiation Detectors: Advances & Applications [PDF document]. Available: https://web-docs.gsi.de/~wolle/TELEKOLLEG/KERN/LECTURE/Wollersheim/2020/86-Interaction-Particle.pdf

[16] H. Wollersheim. (2020). Interaction of gamma rays with matter [PDF document]. Available: https://web-docs.gsi.de/~wolle/TELEKOLLEG/KERN/LECTURE/Wollersheim/2020/42-GammaInteraction.pdf

[17] INTERNATIONAL ATOMIC ENERGY AGENCY, "Handbook on Photonuclear Data for Applications Cross-sections and Spectra," IAEA, Vienna, IAEA-TECDOC-1178, 2000.

[18] S. Grdanovska, "Characterization of radiation damage to a novel photonic crystal sensor," Ph.D. dissertation, University of Maryland, 2015.

[19] J. J. Duderstadt and L. J. Hamilton, *Nuclear reactor analysis*. Wiley, 1976.

[20] https://astronuclphysics.info/JadRadFyzika3.htm (accessed Jun. 18, 2022).

[21] W. M. Stacey, *Nuclear reactor physics*, 3rd ed. John Wiley & Sons, 2018.

[22] J. R. Lamarsh and A. J. Baratta, *Introduction to nuclear engineering*, 3rd ed. Upper Saddle River, NJ: Prentice hall, 2001.

[23] JANIS (Java-based Nuclear Data Information Software); The JEFF-3.1.1 Nuclear Data Library.

[24] https://www.nuclear-power.com/neutron-cross-section (accessed May2,2022)

[25] R. W. Bauer, J. D. Anderson, S. M. Grimes, D. A. Knapp, and V. A. Madsen, "Application of a Simple Ramsauer Model for Neutron Total Cross Sections," *Nucl. Sci. Eng.*, vol. 130, no. 3, pp. 348–360, 1998, doi: https://doi.org/10.13182/NSE98-A2011

[26] D. G. Cacuci, "Lattice Physics Computations," *in Handbook of Nuclear Engineering*, vol. 2. D. Knott and A. Yamamoto, Eds. Springer Science & Business Media, 2010.

[27] B. Rouben (2011). Fundamental Reactor-Physics Concepts. in CANDU Reactor Physics Course.

[28] D. Rozon, *Introduction to nuclear reactor kinetics*. Polytechnic International Press Montréal, Canada, 1998.

[29] J. R. Askew, F. J. Fayers, and P. B. Kemshell, "General description of the lattice code WIMS," *Journal of the British Nuclear Energy Society*, vol. 5, pp. 564 – 585, Oct. 1966.

[30] G. Marleau, A. Hébert, and R. Roy, "A user guide for DRAGON Version 4," I*nstitut de génie nucléaire, Départment de génie physique, École Polytechnique de Montréal, Montréal*, 2011.

[31] D. Knott, B. H. Fossen, M. Edenius, "CASMO-4, A Fuel Assembly Burnup Program, Methodology," *STUDSVIK/SOA-95/2, Studsvik of America, Inc.*, 1995.

[32] E. Varin, A. Hébert, R. Roy and J. Koclas, "A User Guide for DONJON Version 3.01," *Institut de génie nucléaire, Département de génie physique, École Polytechnique de Montréal, Montréal*, 2005.

[33] T. Downar, Y. Xu and V. Seker, *PARCS v3.0 U.S. NRC Core Neutronic Simulator User Manual.* University of Michigan. MI., 2013. [Online]. Available: https://www.nrc.gov/docs/ML1016/ML101610098.pdf

[34] N. Tsoulfanidis, *The nuclear fuel cycle*. La Grange Park, Illinois: American Nuclear Society, 2013.

[35] https://www.ibm.com/cloud/learn/monte-carlo-simulation (accessed Mar. 20, 2022).

[36] D. G. Cacuci, "General Principles of Neutron Transport," *in Handbook of Nuclear Engineering,* vol. 1. A. K. Prinja and E. W. Larsen, Eds. Springer Science & Business Media, 2010.

[37] M. B. Chadwick *et al.*, "ENDF/B-VII. 0: next generation evaluated nuclear data library for nuclear science and technology," *Nucl. data sheets*, vol. 107, no. 12, pp. 2931–3060, 2006.

[38] A. Koning *et al.*, "The jeff-3.1 nuclear data library-jeff report 21," Organization for Economic Co-Operation and Development, 2006.

[39] K. Shibata *et al.*, "Japanese evaluated nuclear data library version 3 revision-3: JENDL-3.3," *J. Nucl. Sci. Technol.*, vol. 39, no. 11, pp. 1125–1136, 2002.

[40] R. E. MacFarlane and D. W. Muir, "The NJOY nuclear data processing system version 91," Los Alamos National Lab., NM, Rep. no.LA-12740-M, 1994.

[41] P. Mohanakrishnan, O. P. Singh, and K. Umasankari, *Physics of nuclear reactors*. Academic Press, 2021.

[42] ICRP Publication 103, "The 2007 Recommendations of the International Commission on Radiological Protection," *Ann. ICRP* ., vol. 37, no. 2-4, pp. 1-332, 2007.

[43] https://www.nrc.gov/materials/fuel-cycle-fac/stages-fuel-cycle.html (accessed July 20, 2022).

[44] B. Mason and C. B. Moore, "Principles of geochemistry," 1985.

[45] https://www.world-nuclear.org/information-library/nuclear-fuel-cycle/conversion-enrichment-and-fabrication/conversion-and-deconversion.aspx (accessed Jun. 20, 2022).

[46] https://web.evs.anl.gov/uranium/faq/uf6properties/faq8.cfm (accessed Jun. 10, 2022).

[47] https://www.world-nuclear.org/information-library/nuclear-fuel-cycle/conversion-enrichment-and-fabrication/fuel-fabrication.aspx (accessed Jun. 20, 2022).

[48] H. Feiveson, Z. Mian, M. V. Ramana, and F. von Hippel, "Spent Fuel from Nuclear Power Reactors: An Overview of a New Study by the International Panel on Fissile Materials," *Int. Panel Fissile Mater.*, pp. 1–21, 2011. Available: https://fissilematerials.org/library/ipfm-spent-fuel-overview-june-2011.pdf

[49] INTERNATIONAL ATOMIC ENERGY AGENCY, "Status and Advances in MOX Fuel Technology," IAEA, Vienna, Technical Reports Series No. 415, 2003.

[50] Swedish Nuclear Fuel and Waste Management Co., "Long-term safety for KBS-3 repositories at Forsmark and Laxemar - a first evaluation Main Report of the SR-Can project," Sweden, TR-06-09, 2006. [Online]. Available: http://www.skb.se/upload/publications/pdf/TR-06-09webb.pdf

[51] J. LEE, D. CHO, H. CHOI, and J. CHOI, "Concept of a Korean Reference Disposal System for Spent Fuels," *J. Nucl. Sci. Technol.*, vol. 44, no. 12, pp. 1565–1573, 2007, doi: https://doi.org/10.1080/18811248.2007.9711407

[52] Nuclear Waste Management Organization, "Ensuring Safety: Multiple-Barrier System," NWMO, Toronto, Canada, 2015.

[53] SNC-Lavalin, "APM Conceptual Design and Cost Estimate Update Deep Geological Repository Design Report Crystalline Rock Environment Copper Used Fuel Container," SLN report No. 020606-6100-REPT-0001, Toronto, Canada, 2011.

[54] P. Sellin, "Buffer and backfill process report for the safety assessment SR-Can," Swedish Nuclear Fuel and Waste Management Co., Sweden, 2006.

[55] Nuclear Waste Management Organization, "Deep Geological Repository Conceptual Design Report Crystalline / Sedimentary Rock Environment," NWMO, Toronto, Canada, Rep. no. APM-REP-00440-0015 R001, 2016.

[56] ICRP Publication 122, "Radiological Protection in Geological Disposal of Long-lived Solid Radioactive Waste," *Ann. ICRP*, vol. 42, no. 3, pp. 1–57, Jun. 2013, doi: https://doi.org/10.1016/j.icrp.2013.01.001

[57] INTERNATIONAL ATOMIC ENERGY AGENCY, "Geological Disposal Facilities for Radioactive Waste," IAEA, Vienna, Safety Standards Series No. SSG-14, 2011.

[58] Nuclear Waste Management Organization, "Postclosure Safety Assessment of a Used Fuel Repository in Crystalline Rock," NWMO, Toronto, Canada, Rep. no. TR-2017-02, 2017.

[59] Nuclear Waste Management Organization, "Postclosure Safety Assessment of a Used Fuel Repository in Sedimentary Crystalline Rock," NWMO, Toronto, Canada, Rep. no. TR-2018-08, 2018.

[60] INTERNATIONAL ATOMIC ENERGY AGENCY, "Proliferation Resistance Fundamentals for Future Nuclear Energy Systems," IAEA, Vienna, IAEA STR-332, December 2002.

[61] H. D. Bengelsdorf, "Technological opportunities to increase the proliferation resistance of global civilian nuclear power systems," *Small Mediu. Sized React. Status Prospect.*, p. 155, 2002.

[62] Proliferation Resistance and Physical Protection Evaluation Methodology Working Group, "Evaluation Methodology for Proliferation Resistance and Physical Protection of Generation IV Nuclear Energy Systems," GIF/PRPPWG/2011/003, Sep. 2011.Available: https://www.gen-4.org/gif/upload/docs/application/pdf/2013-09/gif_prppem_rev6_final.pdf .

[63] INTERNATIONAL ATOMIC ENERGY AGENCY, "Guidance for the application of an assessment methodology for innovative nuclear energy systems INPRO manual - Overview of the methodology Vol 1 of 9 of the final report of phase 1 of the International Project on Innovative Nuclear Reactors and Fuel Cycles (INPRO)," IAEA, Vienna, 2008. [Online]. Available: http://www-pub.iaea.org/MTCD/publications/PDF/TE_1575_CD/PDF/TE_1575_vol1_2008.pdf.

[64] M. Å. Lindell, S. Grape, A. Håkansson, and S. J. Svärd, "Assessment of proliferation resistances of aqueous reprocessing techniques using the TOPS methodology," *Ann. Nucl. Energy*, vol. 62, pp. 390–397, 2013.

[65] INTERNATIONAL ATOMIC ENERGY AGENCY, "Guidance for the application of an assessment methodology for innovative nuclear energy systems INPRO manual - Proliferation resistance Vol 5 of the final report of phase 1 of the International Project on Innovative Nuclear Reactors and Fuel Cycles (INPRO)," IAEA, Vienna, 2008. [Online]. Available: http://www-pub.iaea.org/MTCD/publications/PDF/TE_1575_CD/PDF/TE_1575_vol5_2008.pdf

[66] T. Aoki, H. Sagara, and C. Y. Han, "Material attractiveness evaluation of inert matrix fuel for nuclear security and non-proliferation," *Ann. Nucl. Energy*, vol. 126, pp. 427–433, 2019, doi: https://doi.org/10.1016/j.anucene.2018.10.063

[67] Y. KIMURA, M. SAITO, and H. SAGARA, "Evaluation of Proliferation Resistance of Plutonium Based on Decay Heat," *J. Nucl. Sci. Technol.*, vol. 48, no. 5, pp. 715 – 7 23, 2011, doi: https://doi.org/10.1080/18811248.2011.9711754

[68] INTERNATIONAL ATOMIC ENERGY AGENCY, "IAEA Safeguards Glossary," IAEA, Vienna, Nuclear Verification Series No. 3, 2003.

[69] T. Ault, S. Krahn, and A. Croff, "Comparing the environmental impacts of uranium- and thorium-based fuel cycles with different recycle options," *Prog. Nucl. Energy*, vol. 100, pp. 114–134, 2017, doi: https://doi.org/10.1016/j.pnucene.2017.05.010

[70] [1] J. C. MARK, F. V. O. N. HIPPEL, and E. LYMAN, "Explosive Properties of Reactor-Grade Plutonium," *Sci. \& Glob. Secur.*, vol. 17, no. 2–3, pp. 170–185, 2009,. doi: https://doi.org/10.1080/08929880903368690